Metabolic engineering of the ethylmalonyl-CoA pathway in *M. extorquens* AM1 for 1-butanol production

Bo Hu

A dissertation

Submitted in partial fulfillment of the

Requirements for the degree of

Doctor of Philosophy

University of Washington

2014

Reading Committee:

Mary Lidstrom, Chair

François Baneyx

James Carothers

Program Authorized to Offer Degree:

Chemical Engineering

Contents

University of Washington

Abstract

Metabolic engineering of the ethylmalonyl-CoA pathway in *M. extorquens* AM1 for 1-butanol production

Bo Hu
Chair of the Supervisory Committee:
Professor Mary Lidstrom
Department of Chemical Engineering

M. extorquens AM1 has several advantages as a potential platform strain for industrial production of valuable chemicals, such as the capability of using an inexpensive carbon feedstock, clarified central metabolism, and availability of genetic tools. However, several fundamental questions involving how metabolic pathways are regulated and how they function as a system remained unsolved, which impedes progress in the metabolic engineering of *M. extorquens* AM1. This work is a compilation of efforts aiming to address initial issues related to the metabolic engineering of *M. extorquens* AM1 and establish a synthetic 1-butanol pathway as a proof of principle case. First, we investigated and characterized the effect of a *tetR*-type regulator (CcrR) on the expression of *ccr*, a critical gene of the EMC pathway, a key target for metabolic engineering. Furthermore, to demonstrate the potential of *M. extorquens* AM1 as a future industrial microorganism, a 1-butanol synthesis pathway was established in *M. extorquens*

AM1 by diverting part of the native crotonyl-CoA flux from the EMC pathway to 1-butanol production. Engineered strains demonstrated different 1-butanol production using ethylamine as a substrate, and optimization was carried out. Finally, adaptive laboratory evolution was used as a tool to develop *M. extorquens* AM1 for high 1-butanol tolerance. We applied a serial transfer method to isolate two mutants that demonstrated improved 1-butanol tolerance compared to the parent strain. Whole genome sequencing of evolved strains revealed mutations that may be responsible for the observed phenotype. Our success in producing 1-butanol from the engineered *M. extorquens* AM1 opens the possibility for using methylotrophs for bulk chemical production. In addition, the collected information from this research will provide useful guidance for metabolic engineering of *M. extorquens* AM1 as an industrial platform in the future.

Acknowledgements

I would like to give acknowledgment to financial support through the Department of Energy (DE-SC0006871). I would like to thank the members of the Lidstrom lab both past and present for their valuable guidance and advice throughout the course of this work. Special thanks are in order to David Beck, Mila Chistoserdova, Marina G. Kalyuzhnaya, Song Yang, Elizabeth Skovron, Yanfen Fu, Cecilia Martinez Gomez, Nate Good and all members of my committee. I would also like to thank my parents for their unconditional love and support. Finally, I would like to thank my advisor Mary Lidstrom for her support during these past six years. I am extremely grateful and honored to be her graduate student. I appreciate for her knowledge and insightful discussions and valuable suggestions that keep my Ph.D. experience stimulating.

List of Tables

List of Figures

Chapter 1 Background

1.1 *Methylobacterium extorquens* AM1

Methylotrophic bacteria are a diverse group of microorganisms that utilize reduced carbon compounds containing no carbon-carbon bonds such as methane, methanol and methylamine as the sole carbon and energy source [1]. With the rising threat of climate change caused by greenhouse gases, methylotrophs have received much attention due to their importance in global C_1 cycling. These bacteria are widespread in the natural environment and have been isolated from a variety of terrestrial habitats including plants, soils and sediments. Some methylotrophic bacteria, such as *Methylobacterium extorquens*, *Methylococcus capsulatus*, and *Methylosinus trichosporium*, can readily grow under laboratory conditions [2]. Physiological and biochemical studies of these laboratory-cultivated strains not only elucidate enzymatic reactions and pathways involved in the methylotrophic mechanism, but also provide valuable insights into genetic manipulation of metabolic pathways for producing useful chemicals from methanol and methane.

Known as *Pseudomonas* AM1 for 'Airborne Methylotroph #1' when isolated in the 1960s, *Methylobacterium extorquens* AM1 is the best studied methylotroph to date.[3] It is a pink-pigmented facultative methylotrophic α-proteobacterium capable of using both C_1 compounds (such as methanol and methylamine) as well as multiple-carbon compounds (such as ethylamine and succinate) for carbon assimilation and energy synthesis. *M. extorquens* AM1 belongs to the group of *Methylobacterium* species that can be found abundantly in the plant phyllosphere, where they are able to capture methanol released from pectin degradation during plant growth [4].

The practical significance of *M. extorquens* AM1, such as the biosynthesis of amino acids and single cell protein and bioconversion of methanol into products with economic value has brought it into prominence since the 1960s [5]. However, for some time it was not deeply studied owing to our poor understanding of methylotrophic bacteria and lack of genetic tools for metabolic engineering compared to model microorganisms like *E. coli* and *S. cerevisiae*. Recently, the whole genome sequence and in depth biochemical study of *M. extorquens* AM1 has shed light on mapping the central metabolic network and enabled initial systems biology approaches to explore its genetic responses to environmental changes [6,7]. Detailed knowledge of the central carbon metabolism acquired through the physiological and biochemical studies of *M. extorquens* AM1 is useful for any further biotechnological application of this organism.

1.2 Methylotrophic Metabolism in *Methylobacterium extorquens* AM1

M. extorquens AM1 was the model organism used to delineate the serine cycle for C_1 assimilation into central metabolism. The central methylotrophic metabolism of *M. extorquens* AM1 is composed of several functional steps, or modules as they are often termed (Figure 1.1).

In the first module, methanol is oxidized to formaldehyde via primary oxidation by methanol dehydrogenase, a quinoprotein with a prosthetic group pyrroloquinoline quinone (PQQ) as the catalytic center [8]. Two different types of methanol dehydrogenase are present in *M. extorquens* AM1: MxaF-MDH and XoxF-MDH, which use calcium and rare earth elements like lanthanum, cerium and praseodymium as cofactors, respectively [9]. While MxaF-MDH is one of the most highly expressed gene and accounts for the majority of methanol dehydrogenase activity in methanol-grown cells, XoxF-MDH positively regulates the expression of MxaF-MDH and is capable of rescuing cells deleted for *mxaF* in the presence of rare earth elements [10,11].

Formaldehyde is transferred from the periplasm into the cell and condensed with the C_1 carrier coenzyme tetrahydromethanopterin (H_4MPT), a folate analog that had long been thought to be unique to methanogenic archaea [12]. The resulting product methylene-H_4MPT is further oxidized to formate through reactions in common with methanogenesis, catalyzed by a set of enzymes (MtdA/B, Mch, FhcABCD). Formate is one of the main branch points for methylotrophic metabolism [13]. Multiple formate dehydrogenases have been identified in the genome of *M. extorquens* AM1. Fdh1, Fdh2, or Fdh3 can be deleted without phenotype, but Fdh4 is necessary for normal growth on C_1 compounds [14]. Part of the formate is oxidized to CO_2, producing energy and reducing equivalents essential for cell anabolism. The other portion of formate is converted to formyl-tetrahydrofolate (H_4F), which is further reduced through three enzymatic reactions (FtfL, MtdA, and Fch) to methylene-H_4F, the entry metabolite to the serine cycle. Accumulation of formaldehyde caused by environmental perturbation is detrimental for cell growth on C_1 compounds, so the carbon flux distribution between assimilation and oxidation is elaborately regulated by small molecules like methenyl-dH_4MPT in order to rapidly respond and remove intracellular formaldehyde [15].

The serine cycle is a unique assimilation pathway in methylotrophs that generates two C_3 molecules from 3 molecules of methylene-H_4F and 3 molecules of CO_2. The initial step is condensing glycine with methylene-H4F to produce serine catalyzed by serine hydroxymethyltransferase (GlyA), a characteristic enzyme of the serine cycle. Serine is subsequently converted to a series of C_3 and C_4 intermediates including phosphoglycerate, phosphoenolpyruvate, oxaloacetate and malate, which are important precursors involved in common metabolic pathways such as the tricarboxylic acid cycle, gluconeogenesis, the pentose-phosphate pathway and the Entner-Doudoroff pathway [16]. Some of the malate is used for

regenerating the initial acceptor glycine by cleavage of malyl-CoA to glyoxylate and acetyl-CoA. Acetyl-CoA generated by the serine cycle is recycled by the ethylmalonyl-CoA pathway (the EMC pathway), which converts one molecular of acetyl-CoA to two molecules of glyoxylate for reincorporation into the serine cycle, and also for replenishment of precursors removed for biosynthesis [17].

Several enzymes of the TCA cycle also participate in the operation of the serine cycle and ethylmalonyl-CoA pathway, and these show high activities during growth on C_1 compounds. However, the TCA cycle is not complete during growth on C_1 compounds, and only a small portion of the total flux flows through parts of the TCA cycle. The α-ketoglutarate dehydrogenase is not active under these conditions, and the α-ketoglutarate generated by the TCA cycle is mainly used for biomass synthesis [18]. Only a tiny percentage of CO_2 release was attributed to the TCA cycle in cells grown on methanol, suggesting it is not involved in energy generation [19].

1.3 Growth on C_2 Compounds in *M. extorquens*

M. extorquens AM1 is able to grow on C_2 compounds like ethylamine and ethanol whose assimilation does not require the participation of C_1 transfer steps. An incomplete and partially reversed serine cycle possesses low level carbon flux in order to synthesize important metabolites such as phosphoglycerate and phosphoenolpyruvate. But unlike in C_1 assimilation, the serine cycle only plays a minor role in C_2 assimilation of *M. extorquens* AM1, which heavily depends on the EMC pathway and the TCA cycle (Figure 1.2). Two-carbon substrates are first oxidized to acetaldehyde and then to acetate by a set of dehydrogenases [20]. Acetate is converted to acetyl-CoA as the entry point into central carbon metabolism.

Both the EMC pathway and the TCA cycle are capable of incorporating acetyl-CoA. However, it has been suggested that the TCA cycle is mainly responsible for the generation of reducing equivalents and the EMC pathway replenishes metabolites that either leave the cycle for biosynthetic purposes or are consumed by the TCA cycle [19]. In the TCA cycle, acetyl-CoA is condensed with oxaloacetate to form the six-carbon compound citrate, which is subsequently decarboxylated to succinyl-CoA by losing two carboxyl groups as CO_2. Succinyl-CoA is converted to malate by reactions shared with the EMC pathway, and malate is used for oxaloacetate regeneration via a reaction catalyzed by malate dehydrogenase. The reactions of the EMC pathway in C_2 assimilation are the same as in C_1 assimilation. All EMC intermediates including crotonyl-CoA can be detected in cells grown on C_2 compounds. Acetyl-CoA is converted to glyoxylate via the EMC pathway, which is used to synthesize important biomass precursors such as glycine and serine. Since glyoxylate is not required for keeping serine cycle maintenance, it is condensed with acetyl-CoA to generate malate by malate lyase in an opposite manner relative to the methylotrophic growth condition [19].

1.4 Ethylmalonyl-CoA Pathway

1.4.1 Metabolic reactions involved in the ethylmalonyl-CoA pathway

To close the serine cycle requires conversion of acetyl-CoA to glyoxylate, but the majority of serine cycle methylotrophs do not contain the key enzymes of the classic glyoxylate shunt such as isocitrate lyase. The growth of *M. extorquens* AM1 on C_2 compounds also requires the conversion of acetyl-CoA to C_3/C_4 intermediates, which cannot be fulfilled by the TCA cycle alone in bacteria lacking isocitrate lyase. The question of how *M. extorquens* AM1 metabolizes acetyl-CoA to glyoxylate remained unanswered for over 35 years after the first description of the serine cycle. Genome analysis enabled the identification of candidate enzymes involved in this

pathway, but the whole pathway was not completely clarified until the discovery of several unique enzymes catalyzing the interconversion of C_4/C_5 compounds including ethylmalonyl-CoA. Thus this alternative pathway was called the ethylmalonyl-CoA pathway (EMC pathway).

The EMC pathway starts with the conversion of acetyl-CoA to crotonyl-CoA via three enzymes that are similar to those involved in biosynthesis of poly-3-hydroxybutyrate or oxidation of fatty acids: beta-ketothiolase (PhaA), acetoacetyl-CoA reductase (PhaB) and crotonase (CroR), here interlinked with the PHB cycle via the reactions catalyzed by PhaA and PhaB (14). Although another key PHB enzyme, PhaC does not participate in the operation of the EMC pathway, a null mutant exhibits growth defects on C_1 and C_2 compounds. One key enzyme of the EMC pathway is crotonyl-CoA carboxylase/reductase (Ccr), which catalyzes an ATP-independent reductive carboxylation of crotonyl-CoA to (S)-ethylmalonyl-CoA (15). This is followed by the conversion of (S)-ethylmalonyl-CoA to (R)-ethylmalonyl-CoA and then to (S)-methylsuccinyl-CoA by ethylmalonyl-CoA epimerase and ethylmalonyl-CoA mutase (Epi and Ecm). The methylsuccinyl-CoA is oxidized to mesaconyl-CoA via a methylsuccinyl-CoA dehydrogenase (Msd). The unique reactions catalyzed by Ccr, Epi, Ecm and Msd constitute the characteristic part of the EMC pathway. Mesaconyl-CoA is converted to methylmalyl-CoA by mesaconyl-CoA hydratase (Mcd) and one molecule of this C5 compound is cleaved into one molecule of glyoxylate and one molecule of propionyl-CoA, catalyzed by the same lyases that cleave malyl-CoA to glyoxylate and acetyl-CoA (MclA1 and MclA2). The later part of the EMC involves carboxylation of propionyl-CoA to methylmalonyl-CoA, isomerization of methylmalonyl-CoA to succinyl-CoA and then to malate by reactions from the TCA cycle. One highlight of the EMC pathway is the occurrence of 2 net carboxylation steps, which

assimilate two molecules of CO_2 and result in carbon products that are half derived from methylene H_4F and half from CO_2.

1.4.2 Function of the ethylmalonyl-CoA pathway in methylotrophic growth

During C_1 assimilation, the ethylmalonyl-CoA pathway is mainly used to regenerate glyoxylate for reincorporation into the serine cycle and the balanced equation is as follows: acetyl-CoA + $2CO_2$ = 2 glyoxylate + H^+ + CoASH. In vivo metabolic flux analysis of methanol-grown *M. extorquens* AM1 demonstrated that the amount of glyoxylate released from the cleavage of mesaconyl-CoA was almost identical with the replenishment of the glyoxylate pool from propionyl-CoA, suggesting the EMC pathway only plays a minor role of C_3/C_4 intermediate synthesis [17].

Mutants in the EMC pathway genes grow normally on compounds with more than 2 carbons, such as succinate [21]. In keeping with this finding, most EMC pathway genes are upregulated in cells grown with methanol compared to succinate, with exceptions being the genes coding for enzymes also involved in other parts of metabolism, such as *phaA*, *phaB* and *sdhABCD* (encoding succinate dehydrogenase). However, multiple expression patterns were observed in a substrate-switching experiment in which succinate was replaced with methanol as the sole carbon source [7]. In that case, some EMC pathway genes increased expression initially, then dropped expression later, others decreased expression initially, then increased later, and others either showed little response, increased steadily throughout the transition, or dropped steadily throughout the transition. This study indicates that multiple regulatory systems may exist for tuning expression of the EMC pathway genes when cells grow on different substrates.

The specific activities of EMC enzymes showed a similar pattern with transcriptomic studies of the corresponding EMC genes. Compared with succinate-grown cells, enzymes involved in PHB synthesis, β-ketothiolase and acetoacetyl-CoA reductase showed lower activities in cells grown with methanol, consistent with the observation that succinate-grown cells contain higher levels of PHB than methanol-grown cells [22]. However, other EMC enzymes of the ethylmalonyl-CoA pathway were generally up-regulated in methanol-grown cells, suggesting a high carbon flux through this reaction sequence in methylotrophic cells compared to cells grown on succinate [23]. All specific activities of EMC enzymes were above the hypothetical minimal value calculated from relative flux distribution of methylotrophic growth (Peyraud et al. 2009), suggesting that the whole EMC pathway is not a limiting factor for cell growth on methanol and is able to maintain constant metabolic flux through all intermediates.

The majority of the acetyl-CoA released from the serine cycle was recycled by the EMC pathway (about 10% of total carbon flux). All metabolites of the EMC pathway can be detected in methanol-grown cells except for acetoacetyl-CoA and crotonyl-CoA, which have small pool sizes. The EMC pathway involves two NADPH-consuming steps at the reduction of acetoacetyl-CoA and the carboxylation of crotonyl-CoA, and thus contributes to about 25% of the total NADPH demand. One of the major NADPH-generating steps is oxidation of methylene-H_4MPT catalyzed by MtdA/MtdB, which has been found to be a control point of C_1 assimilation. Therefore, this pathway can potentially play the role of a redox-balancing mechanism and the alteration of intracellular reducing power could affect the metabolic flux through the EMC pathway.

1.4.3 Function of the ethylmalonyl-CoA pathway in C_2 assimilation

During C_2 assimilation, the EMC pathway is primarily used to replenish metabolites that either leave the TCA cycle for biosynthetic purposes or are consumed by the TCA cycle [19]. Acetyl-CoA derived from C_2 substrates are converted into important C_3/C_4 precursors such as succinate and malate. The balanced equation is 3 acetyl-CoA + 2 CO_2 = malate + succinate.

In cells grown on C_2 compounds, genes specific to the EMC pathway were generally induced by about 2-fold compared with succinate-grown cells except for *mcd* and *epm*, which were down-regulated, suggesting that a multiplex regulatory mechanism exists for the EMC pathway [20]. Proteome analysis from *M. extorquens* AM1 grown on acetate and methanol showed that most enzymes of the EMC pathway were detected at a similar abundance during growth on acetate relative to methanol [24]. However, the specific activities of most EMC enzymes were lower in acetate-growth cells than methanol-grown cells [23]. The low enzyme activity should be sufficient to support cell growth given the slower growth rate on C_2 compounds. This conclusion was supported by the metabolic flux analysis that EMC pathway fluxes normalized to the respective carbon uptake rates were identical in cells grown on methanol and acetate. Despite the fact that in C_2 assimilation acetyl-CoA is the entry metabolite for anabolism and the EMC pathway replaces the serine cycle as the central assimilatory pathway, it undertakes the same extent of metabolic flux relative to C_1 assimilation [19].

1.4.4 Biotechnological potential of the ethylmalonyl-CoA pathway

Unlike the serine cycle, the ethylmalonyl-CoA pathway is a non-cyclic pathway that does not require replenishment of acceptor molecules. Thus any unique intermediate of the pathway can in principle be used as a starting point to synthesize a value-added product. The EMC pathway involves unusual metabolites, such as crotonyl-CoA, ethylmalonyl-CoA,

methylsuccinyl-CoA, and mesaconyl-CoA, which are of interest for the production of valuable compounds including biofuels in *M. extorquens* AM1. For example, removal of the CoA moiety of those CoA derivatives could lead to the production of stereochemically defined acids, most of which are commercially unavailable [25]. Recent research has reported that expressing thioesterase in *M. extorquens* AM1 led to production of mesaconic and methylsuccinic acid during growth on methanol [26]. Ethylmalonyl-CoA and methylmalonyl-CoA are commonly used extender units for polyketide biosynthesis. The direct carboxylation of crotonyl-CoA to ethylmalonyl-CoA by Ccr without addition of ATP offers a unique advantage of generating ethylmalonyl-CoA and methylmalonyl-CoA through the EMC pathway. These two metabolites can potentially be converted to carboxylates and lactones by modified polyketide synthases [27]. Finally, 1-butanol can be generated from crotonyl-CoA. 1-butanol emerges as a promising target compound for engineered *M. extorquens* AM1 because a significant percentage of the total carbon flux for assimilation naturally flows through crotonyl-CoA via the native EMC pathway. Thus, the addition of only two extra steps could divert this naturally high flux to produce 1-butanol. If productivities similar to those for *E. coli* and *Clostridium* could be obtained, it should be cheaper to produce 1-butanol from methanol than glucose, due to the difference in price. Regardless of economic feasibility, 1-butanol production could serve as a proof of principle for manipulating the metabolic network in *M. extorquens* AM1, especially in terms of diverting flux from interesting EMC intermediates to value-added products. In addition, it could be realistic to produce 1-butanol from natural gas in the future via methane-utilizing bacteria, which would be even more economically attractive given the low price of natural gas.

1.5 Biobased 1-Butanol Fuel

1.5.1 Advantages of biobutanol as a renewable alternative to gasoline.

There is an increasing interest in the production of biofuels from renewable resources due to the growing concerns about global warming and climatic change, insecurity of fossil fuel supply and rising crude oil price. Currently bioethanol dominates the US market of alternative liquid transportable fuels, but biobutanol offers a set of advantages over bioethanol that make it a more promising next generation fuel. 1-Butanol is less soluble in water than ethanol, reducing the possibility of contamination in groundwater and this trait also makes it feasible to use liquid-liquid extraction for 1-butanol recovery in industrial fermentation. Unlike ethanol, 1-butanol is compatible with current petro infrastructure and can be blended with gasoline in a high ratio [28,29]. This removes the need to build up many refineries, tanks and pipelines for 1-butanol transportation and storage. The energy density of 1-butanol is close to that of gasoline, so one gallon of gasoline blended with equal volume of 1-butanol produces nearly the same mileage as pure gasoline. Finally, butanol can be blended with gasoline in any concentration and ethanol can be blended up to 85%. Therefore, it has attracted attention in academia and industry to explore an economically favorable method for biobutanol production.

1.5.2 1-Butanol synthesis pathways in natural clostridia

Similar to bioethanol, biobutanol can be produced from a variety of conventional feedstocks such as sugar cane, sugar beet, corn, wheat, cassava and sorghum. In addition, biobutanol processes will be compatible with future biofuel feedstocks such as lignocellulosics from fast-growing energy crops (e.g. grasses) or agricultural byproducts (e.g. corn stalks) [30].

The biobutanol industry ceased after World War II due to the cheap price of gasoline, but regained attention after the first oil crisis in the 1970's. As a result, interest in progress on biobutanol, actually all biofuels, is tightly related to the oil price. For biobutanol, an oil price below $ 80/barrel could make it unattractive for government and companies. Traditionally, biobutanol was produced by the natural solventogenic microorganisms like *C. acetylbutylicum* via the so-called ABE fermentation (Acetone-Butanol-Ethanol fermentation). This anaerobic fermentation process uses starchy compounds such as molasses as substrate and generates acetone, butanol and ethanol in a ratio of 3-6-1. A well-operated industrial plant could produce as high as 20 g/L 1-butanol, but 13-15 g/L is a reasonable level for industry because high concentrations of 1-butanol generally inhibit cell growth [31].

The butanol biosynthesis route in clostridium has been thoroughly described in previous studies. Sugars were catabolized to pyruvate via the Embden-Meyerhof-Parnas pathway and pyruvate is decarboxylated to acetyl-CoA as the starting point for a five-step coenzyme A-mediated pathway [32]. The first three steps are similar to that of the EMC pathway: two acetyl-CoA are condensed into acetoacetyl-CoA whose oxo-group is reduced and dehydrated into a carbon-carbon double bond, forming crotonyl-CoA. Crotonyl-CoA is hydrogenated into butyryl-CoA by a butyryl-CoA dehydrogenase coupled with an electron transferring protein (Bcd and EtfAB). The last step is the reduction of butyryl-CoA to butanol by a bifunctional aldehyde/alcohol dehydrogenase (AdhE2). The CoA-dependent pathway requires sufficient supply of reducing power as it consumes three molecular of NADH for one molecular of butanol .

Metabolic engineering of clostridium for improved butanol production has achieved limited success with increasing knowledge of physiology. Whole genome sequencing of model

organisms like *Clostridium acetobutylicum* ATCC8244 provides a comprehensive understanding of metabolic pathways involved in carbon assimilation and redox balance during acidogenesis and solventogenesis. Transcriptome and proteome analysis related to various physiological aspects such as sporulation, solventogenesis or butanol stress help identify important control points in fermentation pathways [33–35]. Although gene deletion and chromosomal integrations for both fundamental investigations and practical applications remain a difficult task for clostridium, there are some recent advances in developing effective genetic tools such as Clostran (a Group II intron directed mutagenesis system for *Clostridium*) and integration vectors [36,37]. However, engineering *C. acetobutylicum* to improve butanol production is still a challenging task because of the lack of information regarding regulatory mechanism determining the organism's life cycle and the inherent complexity of genetically modifying these organisms.

1.5.3 Metabolic engineering approaches to produce biobutanol

The disadvantages of clostridia for use in industrial fermentations push forward metabolic engineering approaches to construct butanol synthesis pathways in heterologous microorganisms with broad substrate ranges and high solvent tolerance. Reconstruction of the CoA-dependent pathway from *Clostridium* in recombinant heterotrophs is one of the initial attempts. Enzymatic kinetics for each step of the clostridial pathway has been studied in order to select enzyme components that normally work in the biosynthetic rather than the degradative direction. A typical synthesized CoA-dependent pathway is composed of building blocks from multiple microorganisms. Successful examples include *E. coli* , *S. cerevisiae, Lactobacillus brevis, Pseudomonas putida,* and cyanobacteria, which demonstrate a variety of butanol productivity from a wide range of carbon sources [38–41]. The preliminary butanol titers are significantly lower than that of clostridium. But combined with other strategies to enhance the

supply of NADH and acetyl-CoA, it has been reported that 1-butanol production with a high titer of 30g/L can be achieved using *E. coli* in flasks with constitutive product removal [42].

Another popular pathway for 1-butanol synthesis is the keto-acid pathway, which involves part of an amino acid biosynthesis pathway and the last two steps in the Ehrlich pathway for 2-keto acid degradation. Amino acid biosynthesis pathways produce various 2-keto acids with different carbon numbers, which can be converted to aldehydes by broad-substrate-range 2-keto-acid decarboxylases (KDCs) and then to alcohols by alcohol dehydrogenases (ADHs). Using this method, a series of alcohols can be produced from different precursors, such as isobutanol, 3-methyl-butanol, 3-methyl-1-pentanol, *etc.* 1-Butanol comes from 2-ketobutyrate, which goes through keto acid chain elongation to 2-ketovalarate, then is decarboxylated and reduced into 1-butanol. The existing *E. coli* metabolic pathways can be genetically modified to increase the production of the specific 2-keto acid so that the desired alcohol could be produced. The substrate selectivity of the promiscuous 2-keto-acid decarboxylases can also be engineered in order to drive the carbon flux toward the target alcohol [43].

The coenzyme-A dependent pathway follows the chemistry of beta-oxidation in the reverse direction and many organisms including *E. coli* have similar fatty acid beta-oxidation pathways that could break fatty acids into acetyl-CoA. A functional reversed beta-oxidation pathway for butanol production was constructed in *E. coli* by manipulation of global regulators, expression of termination enzymes and elimination of branch pathways. The engineered strain is able to produce 1.9g/L butanol from glucose [44,45].

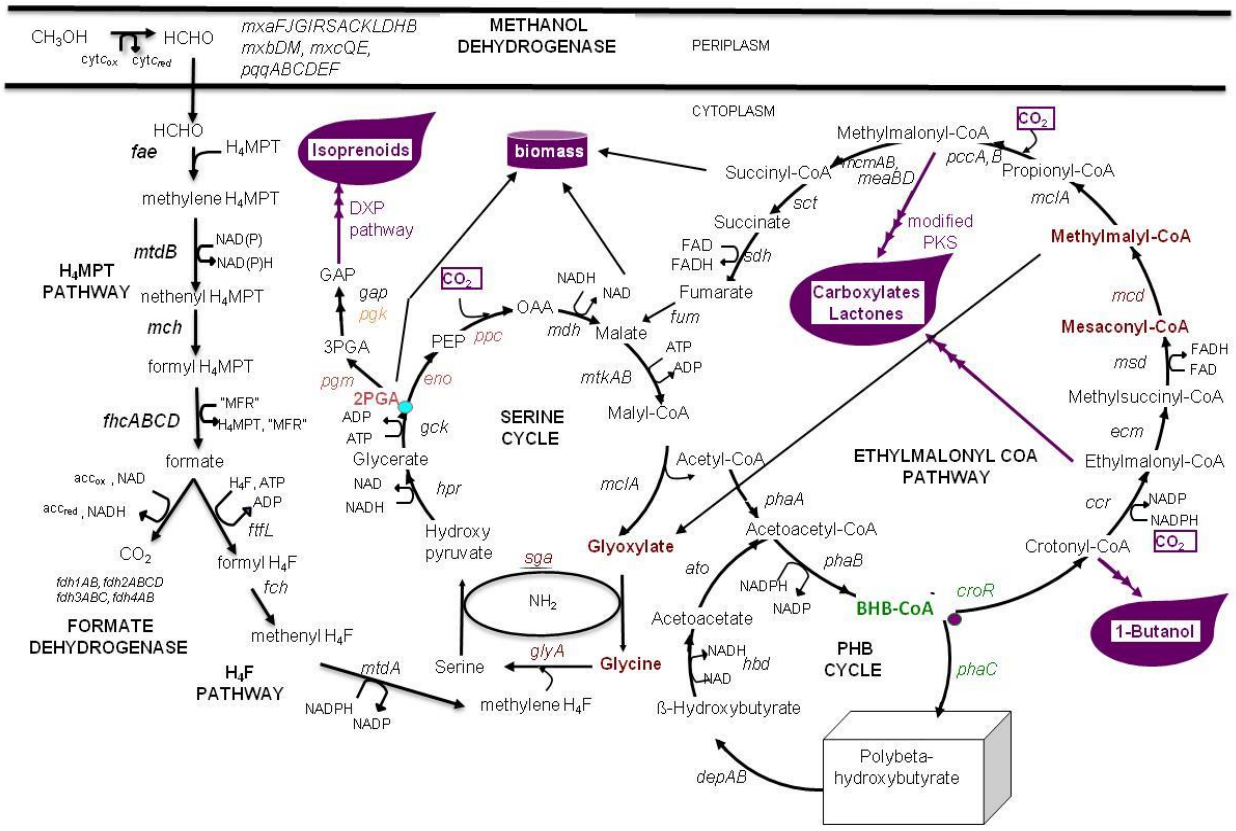

Figure 1.1: Methylotrophic metabolism in *M. extorquens* AM1.

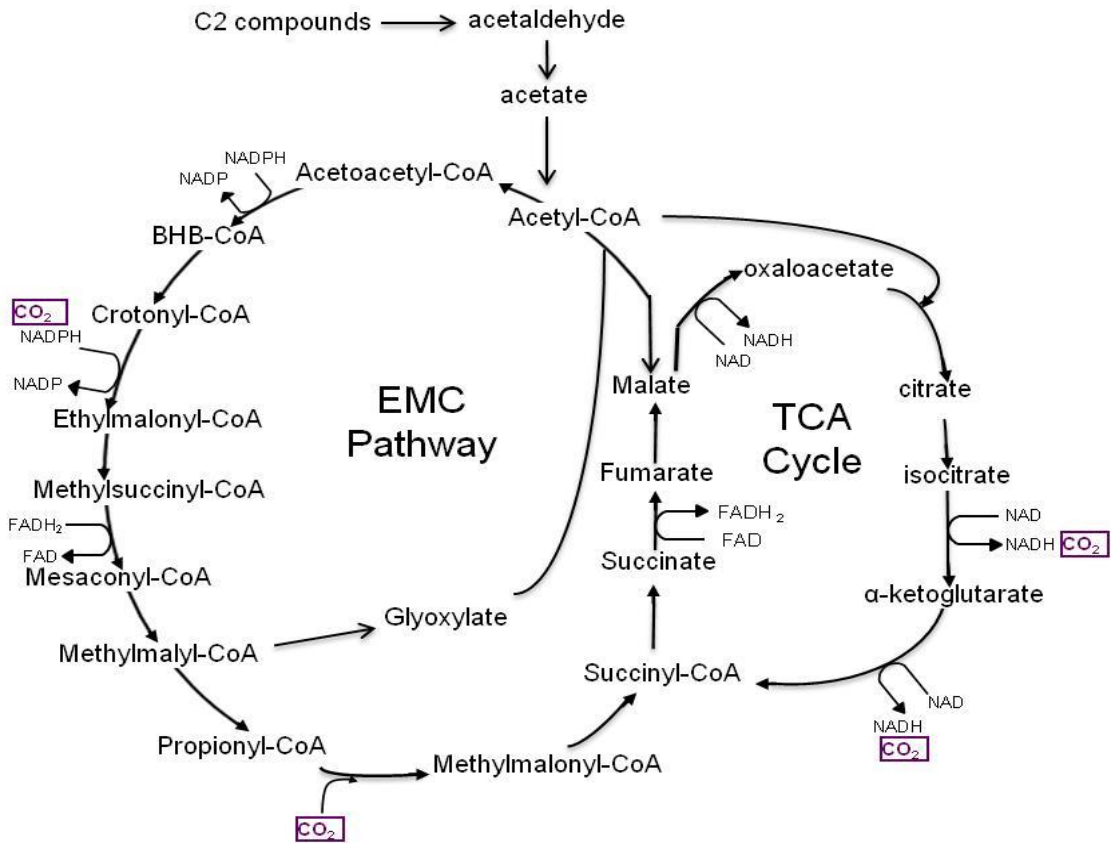

Figure 1.2: The central metabolism of *M. extorquens* AM1 during growth on C_2 compounds.

Chapter 2 : Identification and characterization of a TetR-type regulator activating the transcription of a gene of the ethylmalonyl-CoA pathway

2.1 Introduction

Methylobacterium extorquens AM1 is a facultative methylotroph capable of using C_1 compounds such as methanol, C_2 compounds like ethylamine and multiple carbon compounds such as succinate as sole carbon and energy sources. This α-proteobacterium has served as a model organism for research on C_1 and C_2 metabolism for over 50 years [1] and has been considered a promising biotechnological platform due to the relatively inexpensive substrates and high flux through intermediates of biotechnology or commercial interest that are involved in C_1 and C_2 assimilation [25]. The complete assimilatory pathway for both C_1 compounds and C_2 compounds in this bacterium has been shown to involve the ethylmalonyl-CoA pathway (EMC pathway; Figure 2.1), which regenerates glyoxylate from acetyl-CoA. Glyoxylate is, a key intermediate of the serine cycle during growth on C_1 compounds [46] and during growth on C_2 compounds, glyoxylate condenses with acetyl-CoA to generate malate [24].

In *M. extorquens* AM1, genes involved in methylotrophic pathways are often clustered in large operons [6,47]. However, the genes coding for the EMC enzymes are either not co-localized or are loosely clustered in opposite orientations (Figure 2.2), and thus, not co-transcribed. In addition, transcriptomic studies of *M. extorquens* AM1 growing on different substrates showed that the EMC pathway genes are expressed in multiple patterns. Mutants in EMC pathway genes grow normally on compounds with more than 2 carbons, such as succinate [48]. In keeping with this finding, most EMC pathway genes are upregulated in cells grown with methanol or ethylamine compared with succinate, with exceptions being the genes coding for enzymes also

involved in other parts of metabolism, such as the first enzymes of the EMC pathway, β-ketothiolase (*phaA*) and acetoacetyl-CoA reductase (*phaB*), which overlaps with the PHB synthesis pathway, and succinate dehydrogenase (*sdhABCD*), which overlaps with the TCA cycle (Figure 2.1; [20,49]). However, multiple expression patterns were observed in, a substrate-switching experiment in which methanol was added to replace succinate as the sole carbon source [7]. In that case, some EMC pathway genes increased expression initially, then dropped expression later, others decreased expression initially, then increased later, and others either showed little response, increased steadily throughout the transition, or dropped steadily throughout the transition. These studies indicate that multiple regulatory systems may exist for tuning expression of the EMC pathway genes when cells grow on different substrates. Therefore, an investigation of EMC pathway regulators is needed to enhance our understanding of how this key assimilatory pathway is controlled, as well as to generate valuable information for metabolic engineering of the EMC pathway.

To date, no known regulator of expression for any of the EMC pathway genes has been identified. Because the EMC pathway intermediates are of interest for the engineering of valuable chemicals, it is important to obtain a more complete understanding of how this pathway is regulated in order to manipulate flux through the EMC pathway intermediates. In this study, we identify the first known regulator of one of the EMC pathway genes, *ccr*, and show that this TetR-type regulator (CcrR) directly binds a palindromic sequence upstream of the promoter controlling expression of *ccr*.

2.2 Materials and Methods

2.2.1 Bacterial strains, vectors and growth conditions

Escherichia coli strains Top 10 (Invitrogen), BL21 (DE3) (Novagen, Madison, Wis.), and S17-1 were cultivated at 37ºC in Luria-Bertani medium. *M. extorquens* AM1 was routinely cultured in the minimal medium described previously [49]with one of the following substrates: succinate (20mM), methanol (125mM), or ethylamine (20 mM). Growth of mutants with ethylamine was tested in liquid culture with or without glyoxylate (1mM). Antibiotics were supplied at concentrations as follows: tetracycline (Tet) 10 μg/ml, kanamycin (Km), 50 μg/ml, ampicillin (Amp), 100 μg/ml and rifamycin (Rf), 50 μg/ml.

Growth curve assessments were carried out in biological triplicates. Tested strains were grown in tubes of 3 ml minimal medium at 30°C to late log phase, subcultured (0.5 ml) into 50 ml of minimal medium in 250-ml flasks containing the appropriate carbon source and antibiotics, then inoculated at 30 °C on shakers at 200 rpm.

The following cloning vectors were used: pCR2.1 (Invitrogen, CA) for cloning PCR products, pCM62 and pCM80 [50] as expression vectors, pET24a, pET21b, pET15b (Invitrogen) for protein expression, pCM130 [50] for promoter fusion construction, pCM 184 [51] as an allelic exchange suicide vector for gene deletion and pRK2013 [52] as a helper plasmid for matings.

Triparental or biparental matings between *E. coli* and *M. extorquens* AM1were performed overnight on nutrient agar at 30 ºC. Cells were then washed with sterile minimal medium and plated on selective medium with succinate. Rifamycin was used for *E. coli* counter-selection. Kanamycin-resistant transconjugants obtained on succinate medium containing rifamycin were screened for tetracycline sensitivity to identify potential null mutants.

2.2.2 Mutant generation

Insertion mutants were generated using the allelic exchange method as described previously. For the *ccrR* mutant, 0.6kb fragments upstream and downstream of gene were PCR amplified using primer listed in Table 2.2. The amplified products were subcloned into *Eco*RI-*Kpn*I site and *Sac*II-*Sac*I site of pCM184 respectively. For the *arsR* mutant, 0.6kb fragments upstream and downstream of gene were PCR amplified using primer listed in Table 2.2. The amplified products were subcloned into *Bag*II-*Kpn*I site and *Apa*I-*Sac*I site of pCM184 respectively. The constructs were transformed into *E.coli* S-17 cell for triparental mating with wild type *M. extorquens* AM1 and pRK 2013 helper cell.

All mutations were confirmed by diagnostic PCR. The Km marker was deleted by using Cre-mediated recombination as described previously [51]. To overexpress the ArsR type regulator in *M. extorquens* AM1, the gene was first PCR amplified and further cloned into pCR2.1. The fragment between *Kpn*I and *Eco*RI was further moved into pCM80, which uses the *mxaF* promoter to promote expression in *M. extorquens* AM1.

2.2.3 Construction of promoter fusions

The primers listed in Table 2.2 were used for the amplification of putative promoter regions of a varying size upstream of *phaB, mcl, katA-ccr, katA, meaB* and *ecm*. The primers were specifically designed to create restriction sites at both end of the fragment which were cloned into the pCM130 vector. The resulting promoter fusion vectors were transferred into wild type *M. extorquens* AM1 and *ccrR* mutant via conjugation, and expression of the putative promoter was determined by measuring catechol 2,3-dioxygenase activity.

2.2.4 RNA extraction and RT-PCR

50 ml of methanol-grown cultures of *M. extorquens* AM1 were grown in 250ml flasks till OD_{600} of 0.8-1.0. The biomass was collected by centrifugation at 5,000 rpm at 4 ºC for 10 min. Total mRNA was extracted from cell pellet using the RNeasy Mini kit (Qiagen), followed by DNase I digestion (Ambion). The harvested RNA was quatified by Nanodrop spectrophotometer. Reverse transcription-PCR (RT-PCR) was carried out using the iScript One-Step RT-PCR kit (BIO-RAD) in a 30 μl reaction mixture containing 10 ng of RNA template. To completely eliminate DNA contamination, multiple DNase I treatments were conducted.

2.2.5 Enzymatic assays

M. extorquens AM1 cells grown with methanol were harvested at an OD_{600} of 0.8-1.0 and then resuspended in 1 ml of 0.1 M potassium phosphate buffer (pH 7.5). Crude cell extracts were obtained by passing cells through a French pressure cell at 1.2×10^8 Pa, clarification by 15 min centrifugation at 15,000× g at 4 ºC. A standard spectrophotometric assay for Ccr activity was performed at 30°C as described [53] except that 2 mM NADPH was used and Ccr activity was measured by following the production of NADPH at 340 nm using an extinction coefficient of 6.2 mM^{-1} cm^{-1}. Acetoacetyl-CoA reductase (PhaB) was measured using a continuous photometric assay. The reaction mixture contained 100 mM Phosphate buffer pH 7.5, 0.5 mM NADPH, 0.5 mM acetoacetyl-CoA and appropriate amounts of cell extract, PhaA activity was measured by following the consumption of NADPH at 340 nm using an extinction coefficient of 6.2 mM^{-1} cm^{-1}. For promoter fusion assays, catechol dioxygenase (XylE) was assayed as described [54]. Quantitative assays for XylE were conducted in a 1.5 ml cuvette (pavelength 1 cm) at 30 ºC in a total volume of 1 ml containing the following: 0.1 M Phosphate buffer (pH 7.5); 0.1 mM catechol; and appropriate amounts of cell-free extract. XylE activity was calculated as the

absorbance change at 375nm and one mU of XylE activity corresponds to 1 nmol produced catechol 2-hydroxymuconic semialdehyde min^{-1} per mg protein (Extinction coefficient ε375 = 33 mM^{-1} cm^{-1}). Qualitative Protein concentrations were determined by the BCA assay using bovine serum albumin as a standard (Thermo Scientific, MA).

2.2.6 Expression and purification of CcrR

The *ccrR* gene was first amplified by PCR and cloned into the *Nde*I-*Xho*I sites of pET24a and pET21b to create C-terminal His-tag fused protein. The N-terminal His-tag fused protein was created by cloning *ccrR* gene into the *Nde*I-*Xho*I sites of pET15b. *E. coli* cells harboring pET24a::*ccrR* were grown in 8 L of LB medium with 100 μg/ml of ampicillin to an OD 600 of 0.5 to 0.8 and then were induced by 1 mM IPTG for 16 hr at 220 rpm shaking speed. Clarified crude cells were resuspended in 20 ml of buffer A (50 mM Tris pH 7.8, 5 mM imidazole, 10% glycerol). Crude cell extracts were obtained by two passages through a French pressure cell at 1.2×10^8 Pa, followed by 30 min centrifugation at 15,000× g at 4 ºC. The soluble fraction was filtered by Millipore 0.45μm filter. The protein solution was then used for His-tagged purification using Ni-NTA superflow resin as per manufacturer instructions (Qiagen, CA). His-Tagged CcrR was separated by FPLC (ÄKTAprime plus, GE Healthcare life science, Sweden) using the following method: Add 5 ml of the 50% Ni-NTA slurry to 20ml protein solution and mixed gently by shaker for 1 hr at 4 ºC. Load protein-resin mixture carefully into an empty column. The column was washed using 4 column volumes of Buffer B (50 mM Tris pH 7.8, 200 mM NaCl, 5 mM imidazole, 10% glycerol). His-tagged CcrR was eluted by using an imidazole gradient of 50-500 mM at a flow rate of 1 ml/min. Purified protein was desalted by PD-10 columns (GE healthcare) using the following steps: Equilibrium column with desalting butter (50 mM Tris pH 7.8, 12% glycerol) and load 2.5 ml protein solution. The sample enters the packed

bed completely before addition of 3.5 desalting buffer for elution. To increase protein concentration, the aliquot was centrifuged through Amicon Ultra-15 Centrifugal Filter (Millipore) at 5,000 rpm for 10 min. All purified protein were verified by 15% SDS PAGE gel electrophoresis and stored at -80 ºC. Qualitative Protein concentrations were determined by the BCA assay using bovine serum albumin as a standard (Thermo Scientific, MA).

2.2.7 Gel retardation assays

Putative promoter regions of about 400 bp were amplified by PCR. Gel-purified PCR products were ^{32}P-labelled with DNA 5'-End Labeling System (Promega, WI) according to the manufacturer instructions in which the dephosphorylation step was neglected. To prepare samples for gel retardation assays of *katA-ccr* promoter fragments, a series of regions upstream of *katA* were amplified by PCR. The mutated *ccr* promoter region in which the putative CcrR binding site was replaced with a non-palindromic sequence was synthesized by Genscript, Inc., NJ to prepare probes for assays. Labeled DNA fragments were incubated with varying concentrations of purified CcrR in binding buffer [5 mM Tris-HCl (pH7.5), 50mM NaCl, 1mM MgCl, 0.5mM dithiothreitol, 0.5mM EDTA, 4% glycerol, 0.05 μg/ml poly(dI-dC)] for 30 min at room temperature and the reaction was stopped by adding 2μl of 0.5M EDTA. The samples were separated by Novex 6% retardation gel electrophoresis (Invitrogen, CA) in 0.5 ×TBE and at 200 V. The gels were dried using gel drier (MODEL 583, Bio-Rad, CA) and exposed to phosphor screens (PerkinElmer, MA) for 2-6 hr. The images were analyzed using Geliance 600 Image Analysis software (PerkinElmer).

2.3 Results

2.3.1 Effects of mutations in predicted regulatory genes on the capacity to assimilate C1 and C_2 compounds

Two genes (GeneID: 7990213&7990204) potentially encoding tetR-type and arsR-type regulators are located near the EMC pathway genes *ccr* and *ecm* in the genome of *M. extorquens* AM1, but their function for metabolic network has not been discovered yet. The microarray results of several mutants (Table 2.1) demonstrate that expression level of tetR-type regulator shows similar pattern with that of many genes on EMC pathway, while expression level of arsR-regulator performs in the opposite way. This information indicates that tetR-type regulator may acts as an enhancer controlling genes on EMC pathway and arsR-regulator could be an inhibitor. Following experiments were carried out to verify this hypothesis.

To assess the influence of these genes on C_1 and C_2 metabolism in *M. extorquens* AM1, an insertion mutant in each gene was constructed via allelic exchange. The mutant strain deficient in the ArsR-type regulator showed no growth defect when grown with C_1 or C_2 compounds. To test the possibility that this regulator might have a negative effect on gene expression, an overexpression construct was generated and tested for growth with the same substrates. No effect on growth was observed compared to the wild-type. However, the mutant deficient in the TetR-type regulator, here designated CcrR, exhibited decreased growth on methanol and ethylamine (Figure 2.3). It was found that the CcrR mutant strain grew more poorly on ethylamine, with a doubling time of 21 h compared to a doubling time of 9 h for the wild type. In addition, the final OD_{600} of the *ccr* mutant strain was similar to the wild-type strain after growth on methanol, but was only about half that of the final OD_{600} for the wild-type strain when grown with ethylamine (Figure 2.3). The addition of glyoxylate partially facilitated the assimilation of

ethylamine, further proving that CcrR is more like a regulator of EMC pathway. Further studies focused on CcrR.

2.3.2 Effects of the *ccrR* mutation on promoter activities of EMC genes

The activities of promoter regions of five EMC genes (*mclA*, *meaB*, *ecm*, *phaB*, *ccr*) in wild-type *M. extorquens* AM1 and the *ccrR* mutant were investigated by using a reporter vector carrying a promoterless *xylE* gene. The length and location of promoter region fragments tested were based on sequence analysis, and included the 300-400 bp sequence upstream of *mcl*, *meaB*, *phaB*, *ccr* and the 700bp sequence upstream of *ecm*. Since 180 bp separate *ccr* and *katA* (a catalase-encoding gene, for which mutants have no observable phenotype; [55]), it was possible that these two genes are cotranscribed. Therefore, the 400bp sequence upstream of *katA* was also tested. PCR-amplified promoter regions were ligated into pCM130 and transformed into wild-type *M. extorquens* AM1 and the *ccrR* mutant strain, and then assayed for XylE activity. The results are summarized in Table 2.3.

The data revealed that the region upstream of *ccr* does not appear to contain a promoter but the region upstream of *katA* did show promoter activity, supporting the hypothesis that the two genes are cotranscribed. Activity of the promoter fusions for *mclA*, *meaB*, *phaB*, and *ecm* were not significantly affected by the loss of *ccrR*, while the promoter activities of *katA*-*ccr* were reduced ~2-fold but not eliminated in the absence of *ccrR*. This data suggest that ccrR has a positive effect on the promoter region of *katA*-*ccr*, but does not regulate the expression of other EMC genes in this test.

In order to further assess the possibility that *katA* and *ccr* are cotranscribed, RT-PCR assays were performed across the intergenic region of *ccr* and *katA*. Although the transcriptional

orientation of ecm is opposite to that of ccr and katA, the intergenic region of *katA* and *ecm* was also checked by RT-PCR in case of a cotranscription event between *ecm* and *katA* driven by promoters downstream of ecm. A RT-PCR band of the correct size was obtained for the intergenic region, while no product was obtained upstream of the *katA* region, which is the region between *katA* and *ecm* (Figure 2.4). These data suggest that *ccr* and *katA* are cotranscribed from the promoter region upstream of *katA*.

2.3.3 Influence of CcrR on Ccr and PhaB activity

Since the CcrR mutant showed decreased expression from the *katA-ccr* promoter, the activity of Ccr was tested in the *ccrR* mutant and compared to wild-type cells grown with methanol. In the *ccrR* mutant, Ccr activity was about 40% of the wild-type level (from 220 ± 3.7 mu/mg to 102 ± 10.2 mu/mg, measurements are done in three biological replicates). This result is consistent with the ~2-fold decrease in the *ccr* promoter activity seen for the *ccrR* mutant strain.

The activity of PhaB was also tested in the *ccrR* mutant in case that CcrR has an indirect regulation on PhaB. The PhaB activity in the ccrR mutant is not significantly different with that of wild type (173 ± 15.2 mu/mg versus 183 ± 13.1 mu/mg), which is in accordance with the results of promoter fusion reporter suggesting the expression of PhaB is irrelevant to the presence of CcrR.

2.3.4 CcrR binds to the *katA-ccr* promoter region

To characterize the *katA-ccr* promoter binding activity of CcrR, a recombinant CcrR with six-histidine residues was constructed and overexpressed in *E. coli*. An induction period of 16 hrs yielded decent amounts of both N-terminal and C-terminal His-tagged CcrR, and the optimal incubation temperature was determined to be 30 ºC (Figure 2.5). N-terminal CcrR-His_6 was then

purified on a nickel-nitrilotriacetic acid resin column and the purity was confirmed by Coomassie Blue staining of SDS-polycarylamide gels (Figure 2.6). CcrR-His_6 at >95% purity by SDS-PAGE analysis was used to examine binding to the promoter region upstream of *katA-ccr* using a gel retardation assay. The purified CcrR-His_6 specifically bound the *katA-ccr* promoter region, as demonstrated both by direct binding and by competition with the unlabeled *katA-ccr* promoter region. In the gel retardation assays, illustrated in Figure 2.7, incubation of CcrR-His_6 with radiolabeled *katA-ccr* promoter produced two shifted bands of slower migration through the gel than free *katA-ccr* promoter probes. The region upstream of *phaB* was used as a control, since it is not likely to bind to CcrR according to the promoter fusion assay. No shifted bands were observed in this control. Furthermore, the shifted bands were enhanced by addition of increasing amounts of the His-tagged protein to the assay mixtures but could be eliminated upon addition of a 10-fold excess of unlabeled *katA-ccr* promoter region. These results suggested that CcrR-His_6 specifically recognizes the *katA-ccr* promoter region.

2.3.5 CcrR binds to a palindromic sequence upstream of the *katA-ccr* promoter region

In order to narrow down the length of sequence containing the exact location of the CcrR binding site, a nested set of DNA fragments for the postulated *katA-ccr* promoter region were PCR amplified to obtain a series of DNA fragments of 400bp, 300bp, 200bp and 100bp upstream of the translational start for *katA*. Gel electrophoresis mobility shift assays with these fragments showed that only the 400 bp fragment was shifted in the presence of CcrR (Figure 2.8A). These fragments were also used in the promoter fusion assays as described previously. No XylE activities were detected in either the wild-type or *ccrR* mutant except when the 400bp region was tested (Table 2.4), indicating that the region 300-400 bp upstream of the *katA* translational start site is necessary for expression of the *katA-ccr* promoter.

Since CcrR shows homology to the TetR-type regulator family, the pattern of interactions between CcrR and the *katA-ccr* promoter is likely to share some similarity with the common binding pattern of the TetR-type family. A typical TetR DNA-binding system consists of a symmetric TetR dimer and a palindromic operator in which two identical monomers bind the same DNA sequence on the main strand and the complementary strand respectively [56]. Therefore, the *katA-ccr* promoter region was screened for palindromes using mEmboss (http://emboss.open-bio.org/pipermail/emboss/2007-July/003051.html). A single palindrome sequence was identified (CGCGCCTTGAGGCGCG) from nucleotides -334 to -321 with respect to the *katA* translational start site. To test the role of this palindrome sequence as a CcrR binding site, a synthesized *katA-ccr* promoter region was introduced in which the palindrome was changed to the non-palindromic sequence, CCATATGTGGTATTGG. No shifted bands were observed using this sequence (Figure 2.8B), whereas the natural CcrR-binding sequence showed a clear shifted band. These results suggest that this palindrome sequence from -334 to -321 is the CcrR binding site. The regions upstream of other EMC pathway genes were screened for the presence of this palindrome sequence, but no similar sequences were identified.

2.4 Discussion

During C1 assimilation in *M. extorquens* AM1, the EMC pathway is an important adjunct to the serine cycle, generating glyoxylate from acetyl-CoA (Figure 2.1). As a first step towards understanding genetic control of the genes of this pathway, we have investigated two potential regulators, an ArsR-family homolog and a TetR-family homolog that are located near two of the key genes of the EMC pathway, *ccr* and *ecm*. Our results show that although the ArsR-family regulator does not appear to be involved in regulation of the EMC pathway, the TetR-family homolog designated CcrR is involved in positive regulation of expression of *ccr*, which encodes

the crotonyl CoA reductase/carboxylase, a key enzyme of the EMC pathway. CcrR is not only important for normal transcriptional expression of *ccr* and normal activity levels of Ccr, its absence results in poor growth on compounds for which Ccr is a required enzyme. The latter result suggests that a two-fold drop in the activity of Ccr results in limiting flux through this step of the EMC pathway.

The *ccr* gene is cotranscribed with a gene predicted to encode a catalase (*katA*). Mutations in *katA* do not affect growth on C_1 or C_2 compounds and strains lacking *katA* retain catalase activity [55]. In keeping with this finding, the genome annotation for *M. extorquens* AM1 lists two other putative catalase genes [47]. However, none of the enzymes of the EMC pathway or the other enzymes involved in C_1 or C_2 metabolism is known to generate hydrogen peroxide. Transcriptomics show that *katA* is induced during the transition from succinate to methanol in a pattern similar to *ccr* [7] yet the role of KatA in C_1 or C_2 metabolism, if any, remains unknown.

The TetR-type regulator is a broadly distributed regulatory family in the prokaryotes [56]. TetR family members are often involved in the regulation of genes related to environmental adaptation including utilization of diverse carbon sources [56]. CcrR contains signatures of a typical TetR regulator such as the helix-turn-helix motif and a palindromic binding site. However,, it also displays some unusual characteristics. Unlike the majority of members of the TetR family, CcrR functions as an activator rather than a repressor. However, a few TetR-type activators have been reported, including PsrA in *Pseudomonas syringae* pv. tomato Strain DC3000 [57], LuxR in *V. harveyi* [58], VceR in *Vibrio* cholera 569B [59] and AtrA in *Streptomyces griseus* [60]. Like CcrR, AtrA is not essential for expression and modulates expression about 2-fold. Most TetR-family regulators are also autoregulators, controlling their own expression.

However, the mutant and gel retardation results showed that like a few other TetR-family regulators [61–63], CcrR is not an autoregulator.

In this work, we have shown that CcrR stimulates expression of the *katA-ccr* promoter on the order of two-fold but is not required for this expression. Since *ccr* is expressed at very low levels in cells grown on succinate [49], these results suggest the possibility of additional regulatory elements, possibly a repressor mechanism.

Homologs of the palindromic sequence that was indicated as the CcrR binding site were not found in the postulated promoter regions of other ECM genes, consistent with the other results in this study suggesting that CcrR is a specific regulator for the *katA-ccr* promoter. Since expression from the other EMC pathway genes changes depending on the growth conditions [7,49], more regulators are likely involved. The reasons why EMC pathway genes show different regulatory patterns are not clear. It may indicate that some intermediates of the EMC pathway are drawn off for different purposes, and therefore, require separate regulatory systems. Alternatively, the in vivo activity of different enzymes of the EMC pathway may be tuned in part through transcriptional regulation, to help regulate flux through each step of the pathway.

The identification of a specific activator protein regulating expression of one of the genes of the EMC pathway is a first step in understanding how the pathway as a whole is regulated. This work sets the stage for identifying additional regulatory elements, information that will be a key to manipulating the EMC pathway for biotechnological applications.

2.5 Tables and Figures

Table 2.1: Microarray gene expression results (fold change) for selected EMC genes, comparing *M. extorquens* AM1 mutants to wild type.

Mutants	mcl1	Sga 9	sga17	gcv1	mcl2	gcv2
ccr	-1.80	-3.05	1.38	-1.28	-4.68	-1.06
mcl	-1.01	1.67	-1.41	1.64	-1.71	1.2
phaB	-2.56	1.79	1.15	1.31	1.32	1.13
pcc	-3.33	-2.22	1.69	-1.38	-2.96	1.22
meaB	-3.63	-1.47	1.13	-1.95	-1.91	-1.79
TetR-regulator	1.36	-9.12	1.02	-2.74	-6.55	-2.18
ArsR-regulator	4.92	-1.14	1.26	-1.13	-2.15	-1.41

Table 2.2: List of oligonucleotides used in this study.

Purpose	Name	Sequence from 5' to 3'
CcrR mutant construction	CcrRuf	CTCGAATTCCGACTTCGCCTTGCGCTG
	CcrRur	GTGGGTACCTCGGCCGAAAGCTCGTC
	CcrRdf	CGGCCGCGGTATTCAGATCCGACTTC
	CcrRdr	GCCGAGCTCGTGGGCGTTGCCCGAG
ArsR mutant construction	ArsRuf	GCCAGATCTTGCGCGGGGCCAGCTCG
	ArsRur	CAGGTACCTCATGATTTATCCATATG
	ArsRdf	CGCGGGCCCCGTAATCGCCCACGGATG
	ArsRdr	CACGAGCTCATGCGTGGCACGATAGGC
ArsR overexpression	ArsRf	ATGAGGCCCCTGTTTCACCCCGCGAT
	ArsRr	TTACGAAGCCCGCGCCGCGTAGGCG
PhaB promoter phusion test	PphaBf	GCTGAATTCCCGCGACGCTAAGAAG
	PphaBr	TATAAGCTTTAGTTTCCTCCGTGATC
Mcl promoter phusion test	Pmclf	GTAGAATTCGGTCAGCCGCGAGCAG
	Pmclr	GACAAGCTTCGGAAATCCTCCGTTCT
Mea promoter phusion test	PmeaBf	CTCGAATTCGAGGAAACGCCCCACCG
	PmeaBr	CTCAAGCTTGCCGTCTGCTCATCACG
KatA phusion test	PkatAf	GCGGAATTCGCTTGACCTCGGCGACGC
	PkatAr	GCGAAGCTTCGCATGTCTCTCCGTGTC
kata-ccr phusion test	PkatA-ccr f	AACTGCAGTCGTGGCACTCCCTGTTG
	PkatA-ccr r	CGCGAATTCACGAGCCGAACTCCTTC
Ecm phusion test	Pecm f	ATAGAATTCCGCGCGGGTCGCGGGCGGTG
	Pecm r	ATAAAGCTTTCCCACTCGACTCCCTGTCCG
RT-PCR test for katA-ccr cotranscription	katA uf	TGCATCAGAACCGGCCCACG
	katA ur	GCTTGACCTCGGCGACGCTCG
	katA-ccr f	ATCTCGCCGAGCTCGTAAAGGTCCT
	katA-ccr r	ATGATCGCGCACTGGTTCAAGGTG
Promoter fusion test in binding site detection	Pccr400u	GCGGAATTCGCTTGACCTCGGCGACGC
	Pccr300u	GCGGAATTCGAAGCCGCTGCGTCGCGTC
	Pccr200u	GCGGAATTCGCCGGCTCCCGACACAAC
	Pccr100u	GCGGAATTCGCTCCAAGCTCGGCCTCAC
	Pccrd	GCGAAGCTTCGCATGTCTCTCCGTGTC

Table 2.3: XylE activities of putative promoter-*xylE* transcriptional fusions in wild type *M. extorquens* AM1 and the *ccrR* mutant grown on methanol.

Fusion	Activity of XylE (mU)[a]	
	Wild Type	CcrR- mutant
P_{mcl}::xylE	33.4±8.7	35.3±9.2
P_{ccr}::xylE	<3	<3
P_{meaB}::xylE	51.4±10.7	44.4±6.9
P_{katA}::xylE	54.2±5.6	24.1±6.8
P_{ecm}::xylE	211±5.2	221±3.6
P_{phaB}::xylE	51.2±10.8	46.6±11.1

[a] Activity determinations were carried out in triplicate

Table 2.4: XylE activity of transcriptional *xylE* fusions of native and mutated *katA-ccr* promoters in wild-type *M. extorquens* AM1 and *ccrR* mutant grown on methanol.

Fusion	XylE activity (mU)[a]	
	Wild Type	CcrR- mutant
$P_{katA\text{-}ccr}$::xylE	61.2±8.4	21.9±6.6
$P_{katA\text{-}ccr300}$::xylE	<3	<3
$P_{katA\text{-}ccr200}$::xylE	<3	<3
$P_{katA\text{-}ccr100}$::xylE	<3	<3
$P_{\text{mutated } katA\text{-}ccr}$::xylE	58.4±3.4	26.2±10.7

[a] Activity determinations were carried out in triplicate

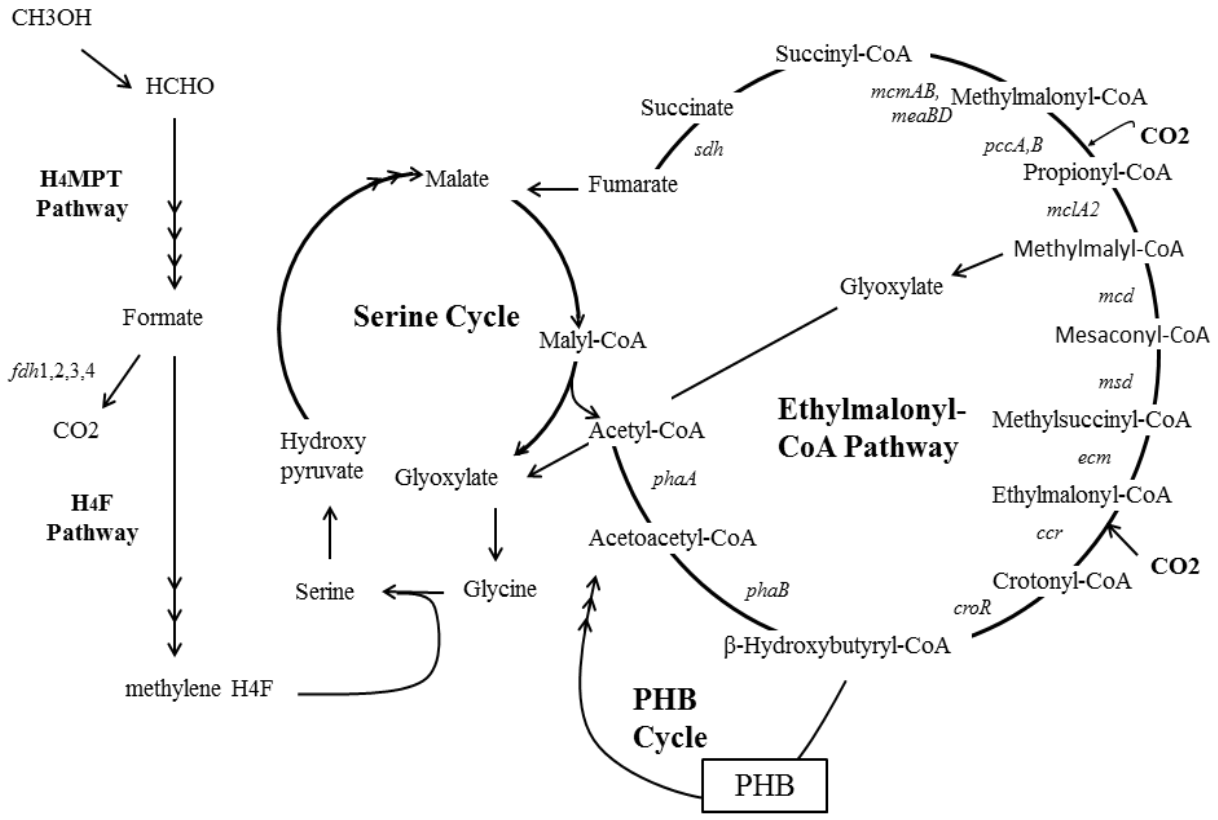

Figure 2.1: Methylotrophic metabolism in *M. extorquens AM1*. *PhaA*, β-ketothiolase; *PhaB*, acetoacetyl-CoA reductase; *CroR*, crotonase; *Ccr*, crotonyl-CoA carboxylase/reductase; *Ecm*, ethylmalonyl-CoA mutase; *Msd*, methylsuccinyl-CoA dehydrogenase; *Mcd*, mesaconyl-CoA hydratase; *MclA1/A2*, malyl-CoA/β-methylmalyl-CoA lyase; *Pcc*, propionyl-CoA carboxylase; *mcm*, methylmalonyl-CoA mutase; *mea*, methylmalonyl-CoA mutase; *Sdh*, succinate dehydrogenase; *fdh*, formate dehydrogenase.

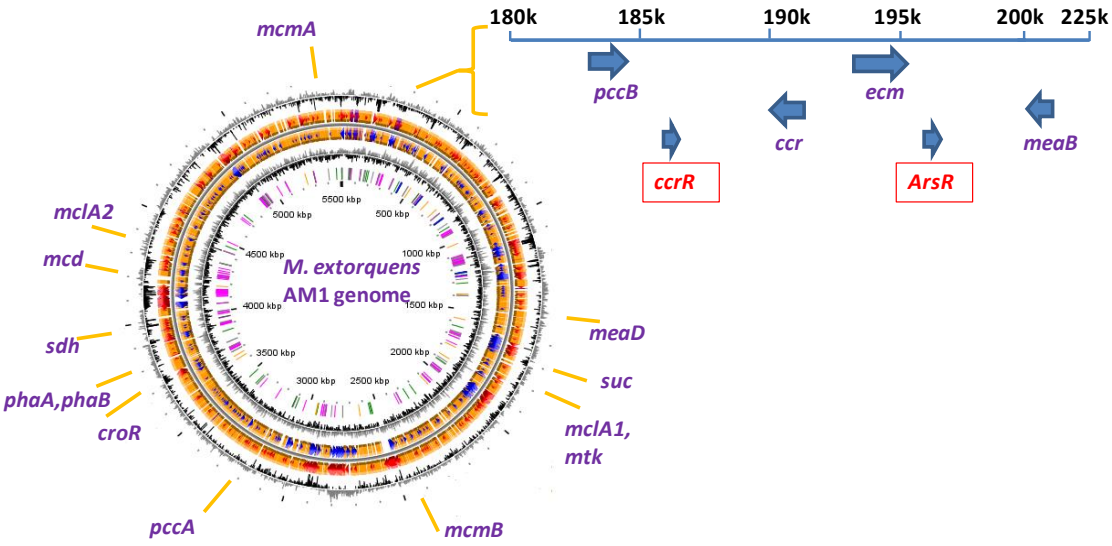

Figure 2.2: Genome-wide mapping of EMC genes.

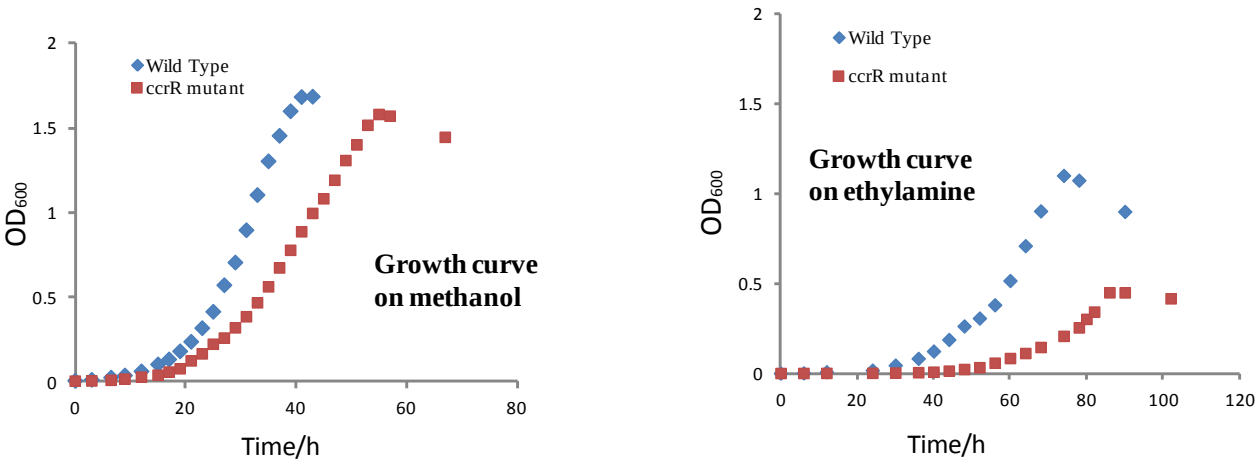

Figure 2.3: Growth curves of wild-type *M. extorquens* AM1 and the *ccrR* mutant grown on different substrates. (A) Growth with methanol; (B) growth with ethylamine. Graphs depict representative data from three biological replicates. The rate of growth varied by 8% between replicates.

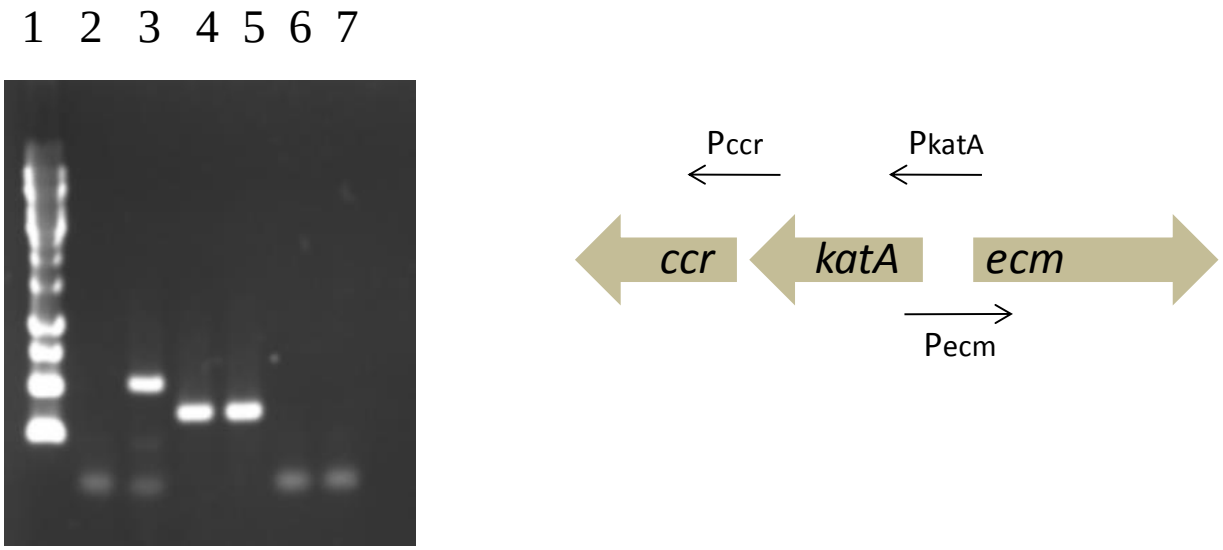

Figure 2.4: RT-PCR results for the intergenic region of *katA-ccr* and *ecm-katA*. Lane 1, DNA ladder; Lane 2, PCR results of *ecm-katA* region using cDNA as template; Lane 3, positive control of *ecm-katA* region using chromosomal DNA as template; Lane 4, PCR results of *katA-ccr* region using cDNA as template; Lane 5, positive control of *katA-ccr* region using chromosomal DNA as template; Lane 6, negative control of *ecm-katA* region using direct PCR without RT step; Lane 7, negative control of *katA-ccr* region using direct PCR without RT step

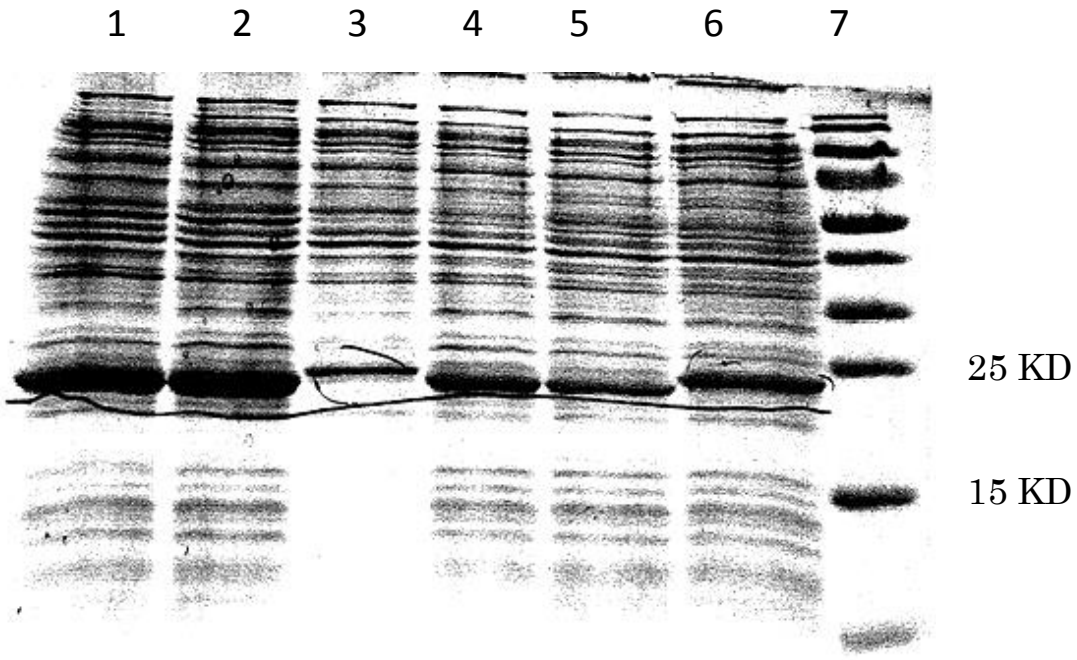

Figure 2.5: Expression of N-terminal and C-termimal His-tagged CcrR fusion protein in E.coli. All cultures were induced with IPTG and incubated for 16 hrs. Lane 1: crude extract of pET 24a :: *ccrR* (C-terminal, Kanamycin-resistent) incubated at 37 C; Lane 2: crude extract of pET 24a :: *ccrR* incubated at 30 C; Lane 3: crude extract of pET 21b :: *ccrR* (C-terminal, ampicilin-resistent) incubated at 37 C; Lane 4: crude extract of pET 21b :: *ccrR* (C-terminal, ampicilin-resistent) incubated at 30 C; Lane 5: crude extract of pET 15b :: *ccrR* (C-terminal) incubated at 37 C; Lane 6: crude extract of pET 15b :: *ccrR* incubated at 30 C; Lane 7: molecular weight marker.

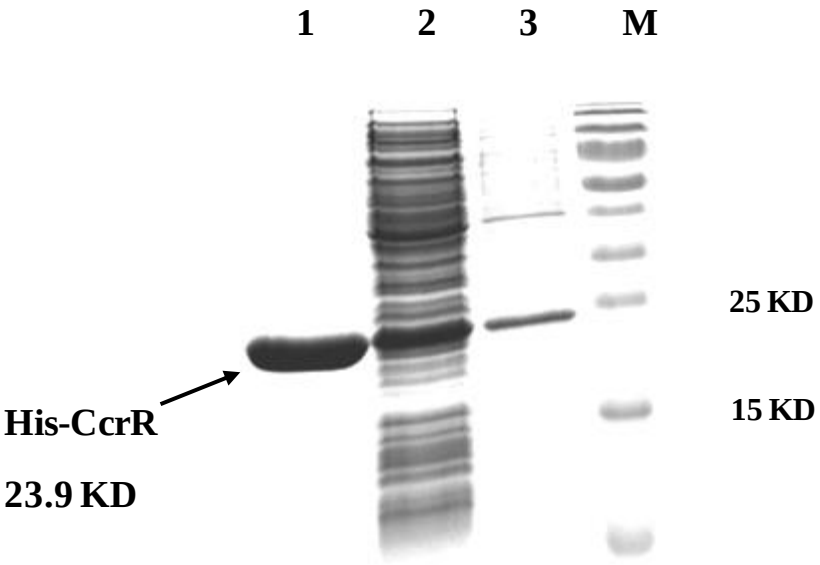

Figure 2.6: Purification of His-tagged CcrR from *E.coli*. Lane 1, the purified sample; Lane 2, soluble fraction of *E.coli* cells harboring pET 15b-ccrR; Lane 3, wash effluent during protein purification

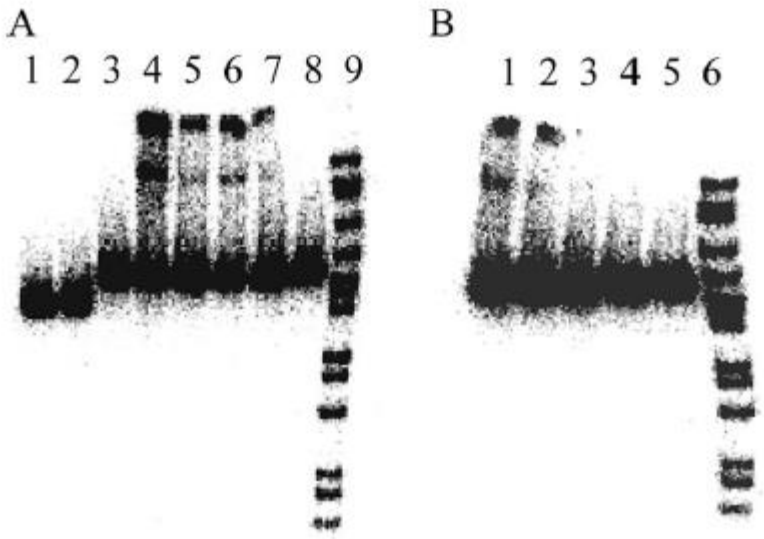

Figure 2.7: (A) Gel retardation assay for binding with purified CcrR. Lanes 1 and 2, P*phaB* fragment with 10 μg and 50 μg CcrR; lane 3, P*ccrR* fragment; lanes 4 to 7, decreasing concentrations of CcrR (100, 80, 50, and 20 μg of protein, respectively) with the P*katA-ccr* fragment; lane 8, no CcrR added with the P*katA-ccr* fragment; lane 9, DNA ladder. (B) Gel retardation assay for labeled P*ccr* competing with unlabeled P*ccr*. Lane 1, labeled P*ccr* with 25 μg CcrR; lanes 2 to 4, increasing concentrations of unlabeled P*ccr* (1, 10, and 50 times more than labeled P*ccr*, respectively); lane 5, no CcrR added; lane 6, marker.

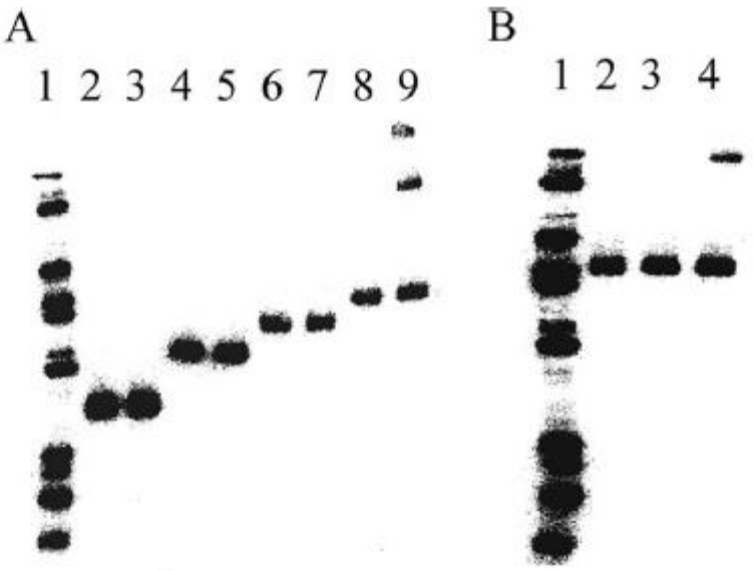

Figure 2.8: (A) Gel retardation assay for binding of *katA-ccr* subfragments with or without 50 μg purified CcrR. Lane 1, DNA ladder; lane 2, 100-bp *katA-ccr* fragment with no CcrR; lane 3, 100-bp *katA-ccr* fragment with CcrR; lane 4, 200-bp *katA-ccr* fragment with no CcrR; lane 5, 200-bp *katA-ccr* fragment with CcrR; lane 6, 300-bp *katA-ccr* fragment with no *katA-ccr* fragment and no CcrR; lane 7, 300-bp *katA-ccr* fragment with CcrR; lane 8, 400-bp *katA-ccr* fragment with no *katA-ccr* fragment and no CcrR; lane 9, 400-bp *katA-ccr* fragment with CcrR. (B) Gel retardation assay for binding of 50 μg purified CcrR with the mutated *katA-ccr* promoter region. Lane 1, DNA ladder; lane 2, control without CcrR; lane 3, CcrR plus the mutated *katA-ccr* promoter fragment; lane 4, CcrR plus the native *katA-ccr* promoter fragment.

Chapter 3 : Metabolic engineering of the ethylmalonyl-CoA pathway for 1-butanol production

3.1 Introduction

1-Butanol has been proposed to be a better alternative to ethanol as a replacement for gasoline because of its many advantages such as lower solubility in water, high compatibility with current petroleum infrastructure and high energy density [28,30]

Fermentative production of 1-butanol by clostridial species has a long history as the main industrial 1-butanol-producing process [28]. Although recent development of new genetic tools for solventogenic clostridia has led to evolved strains with a combination of desired traits [64,65], Industrial fermentation of clostridia still has several limitations such as formation of byproducts, spore formation and low cell density [66]. Therefore, there is growing interest on metabolically engineering alternative hosts for 1-butanol production. Recently, several groups have reported successful reconstruction of the butanol synthesis pathway of clostridia in non-native hosts, including *Escherichia coli* [38], *Saccharomyces cerevisiae* [39], *Pseudomonas putida*, *Bacillus subtilis* [41], and *Lactobacillus brevis* [67]. While starchy substrates or molasses are major carbon feedstocks for fermentative production of 1-butanol in clostridia or heterologous microorganisms, interest is growing in employing novel substrates that are economically competitive with petrochemical synthesis and at the same time are non-competitive with food for human consumption [29]. In the last few years, attention has focused on single carbon compounds such as methane and methanol as future alternative carbon feedstocks due to their relative abundances [68]. However, 1-butanol has not yet been reported to be produced by organisms capable of growing on methane (methanotrophs) or methanol (methylotrophs).

Methylobacterium extorquens AM1 is a facultative methylotrophic α-proteobacterium capable of using both one-carbon (C_1) compounds as well as multi-carbon compounds as sole carbon and energy sources. The potential practical significance of *M. extorquens* AM1 in biotechnology, such as the biosynthesis of amino acids and single cell protein and bioconversion of methanol into products with economic value has brought it into prominence since the 1960s [5]. As the most well understood methylotroph, *M. extorquens* AM1 is a potential platform for converting methanol to biofuels, building on the elucidation of pathways involved in C_1 and C_2 metabolism and development of tools for metabolic engineering. The ethylmalonyl-CoA pathway (EMC pathway, Figure 3.1), a central metabolic pathway in *M. extorquens* AM1, converts acetyl-CoA to glyoxylate for reincorporation into the serine cycle during C_1 assimilation and replenishes metabolites that either leave the cycle for biosynthetic purposes or are consumed by the TCA cycle during C_2 assimilation [19,46]. The EMC pathway involves unusual metabolites that are of interest for the production of valuable compounds, such as crotonyl-CoA, a key precursor of 1-butanol biosynthesis pathway in clostridia (Figure 3.1). Moreover, it has been shown that significant metabolic flux occurs through the EMC pathway during growth of *M. extorquens* AM1 on either C_1 or C_2 compounds, generating a stable supply of crotonyl-CoA as a direct precursor for 1-butanol production [16]. Therefore, in this work we describe the engineering of a modified CoA-dependent pathway in *M. extorquens* AM1 to produce 1-butanol.

3.2 Materials and Methods

3.2.1 Reagents

All chemicals including metabolite standards were purchased from Sigma-Aldrich (St. Louis, MO). Restriction enzymes, Phusion DNA polymerase, ligases and the Gibson Assembly Master Mix kits were supplied by New England Biolabs (Ipswich, MA). Media components

were purchased from commercial resources. The BCA kit for protein measurement was purchased from Thermo Scientific (Waltham, MA)

3.2.2 Strains, medium and growth condition

Strains used in this study are listed in Table 3.1. *Escherichia coli* strains Top 10 and S17-1 were cultivated at 37ºC in Luria-Bertani medium. *M. extorquens* AM1 was routinely cultured in the minimal medium (Hypho) described previously [49] with one of the following substrates: succinate (20 mM), methanol (125 mM), or ethylamine (20 mM). The 1-butanol production of engineered *M. extorquens* AM1 were also tested in the other two types of minimal medium whose recipes were reported in previous studies [69,70]. For triparental or biparental matings between *E. coli* and *M. extorquens* AM1, Difco nutrient broth supplemented with Difco BiTek agar (1.5% [wt/vol]) was used. Antibiotics were supplied at concentrations as follows: tetracycline (Tet) 20 μg/ml, kanamycin (Km), 50 μg/ml, ampicillin (Amp), 100 μg/ml and rifamycin (Rf), 50 μg/ml. 1mM of glyoxylate was used for tests for 1-butanol production from cells grown on methanol plus glyoxylate.

Growth curves and 1-butanol production assessments were carried out in biological triplicates. Tested *M. extorquens* AM1 strains were first grown in 3ml of minimal medium with 125 mM methanol and then subcultured (0.5 ml) from tubes into 75 ml of minimal medium in 250 ml flasks containing the appropriate carbon source, then inoculated at 30 °C on shakers at 200 rpm.

3.2.3 DNA manipulations

The protein sequences of butyryl-CoA dehydrogenase with an affiliated electron transfer flavoprotein (Bcd-etfAB), alcohol dehydrogenase (AdhE2) and NADH-dependent crotonyl-CoA reductase (Ter) were retrieved from GenBank with the following accession numbers: [Bcd-

etfAB: U17110.1, AdhE2: AF321779.1, Ter: AE017248.1]. Genes coding for these enzymes were synthesized into the vector pUC57 (Genescript, NJ, USA) with codon usage optimized for expression in *M. extorquens* AM1 in which codon usage frequency was calculated by counting codon frequency in a list of ORFs associated with the 129 highly expressed genes in both methanol-grown and succinate-grown *M. extorquens* AM1 cells. The gene encoding crotonase (*croR,* GeneID: 7993532) was cloned from *M. extorquens* AM1 genomic DNA. Standard restriction enzyme digestion and ligation techniques were used to construct plasmids except for the one used to create strain BHB9, which was constructed via Gibson Assembly. Genes were PCR amplified with Phusion polymerase and assembled into the *Xba*I-*Bam*HI and *Kpn*I-*Eco*RI restriction sites of plasmids with different promoter regions. Four promoters were tested, one high (*mxaF* promoter of pCM80; [71]), one low (*lac* promoter of pCM62; [50]), and two inbetween chosen based on published microarray data results(Pmeta1_3616 promoter of pAP775 and Pmeta1_002 promoter of pAP776; [7]). The expression vectors pAP775 and pAP776 were designed and constructed by replacing the *lac* promoter with the putative promoter region upstream of Gene meta1_3616 and Gene meta1_002, respectively. The relative expression of the promoters was PmxaF>> Pmeta1_3616 > Pmeta1_002 >Plac, based on relative microarray expression data. For plasmid construction of strain BHB9, the *croR* fragment was first amplified with the BH-GB-19 and BH-GB-20 primers and the spliced pHC61 vector fragments (with a *tac* promoter [72]) were PCR-amplified using BH-GB-21, BH-GB-22, BH-GB-37 and BH-GB-38 primers. The PCR products were DpnI digested and column-purified using Qiagen purification kit. All PCR products were then assembled together using Gibson Assembly Master Mix. The new construct was used as vector fragment to be assembled with the operon of

Pmeta1_3616::*adh*E2::*ter* using BH-GB-53 and BH-GB-54 primers and same assembling strategies. The oligonucleotides used are listed in Table 3.2.

3.2.4 Enzyme assays

10 ml of *M. extorquens* AM1 cells were harvested at mid-exponential phase (OD0.4-0.6) and then resuspended in the appropriate buffer as described below for each assay. Crude cell extracts were obtained by passing cells through a French pressure cell at 1.2×10^8 Pa. clarification by 15 min centrifugation at 15,000× g at 4 °C. Protein concentrations were determined by the BCA assay using bovine serum albumin as a standard according to the instructions of the supplier. All assays were conducted at 25 °C.

Trans-2-enoyl-CoA reductase (Ter) assay

A standard spectrophotometric assay for Ter activity was performed as described by monitoring the oxidation of NADH at 340 nm.[73] The assay mixture contained 0.5 mM crotonyl-CoA, 0.2 mM NADH in 0.1 M potassium phosphate buffer (pH 7.5). The reaction was initiated by addition of cell extracts.

Butanol dehydrogenase (AdhE2) assay

Butanol dehydrogenase activity was measured in the reverse direction as described by monitoring the increase in absorbance at 340 nm [74]. The assay mixture contained 19.6 mM butanol, 0.39 mM NAD+ and 78.5 mM semicarbazide hydrochloride in 68.8 mM Tris-HCl, pH 7.8. The reaction was initiated by addition of cell extracts.

Crotonase (CroR) assay

The CroR assay was conducted by monitoring the decrease of absorbance at 263 nm, corresponding to hydration of the double bond in crotonyl-CoA. The assay mixture contained

0.15 mM crotonyl-CoA in 0.1 M Tris-Hcl buffer, pH 7.6. The reaction was initiated by addition of crotonyl-CoA.

3.2.5 1-butanol quantification by GC-MS

10 ml of culture samples were centrifuged for 10 min at 5000 rpm. 2ml ethyl acetate was added to the supernatant. After the addition of 50 mg/L isobutanol as internal standard, the mixture was vortexed for 1 min and then centrifuged for 10 min at 5000 rpm to separate aqueous phase and ethyl acetate. The recovered ethyl acetate was analyzed by a HP 6890 gas chromatograph equipped with a Model 19091s-433 HP-5MS column (Agilent). Helium with 7.64 psi inlet pressure was used as carrier gas. 1ul of samples were analyzed with the following program: Set initial temperature at 50°C, ramped to 90°C at 10°C/min, ramped to 300°C at 45°C/min, maintained at 300°C for 1min. The injector temperature was maintained at 225°C. A standard curve was derived from measurements of 1-butanol aqueous solution. The ion source temperature was set to 250 °C. Mass spectra were collected at m/z 40 and m/z 56 with a 2.2 min solvent delay. The peaks were analyzed using Agilent data analysis software. Calibration curves were linear between 2 and 50 mg/L (Figure 3.2).

3.2.6 CoA derivative analysis by LC-MS

For *in vitro* demonstration of the synthetic pathway, cell extracts were prepared in the same way as for enzyme assays. The reaction mixture contained 0.7mM ^{13}C-labeled acetyl-CoA, 0.5 mM NADPH, 0.23 mM NADH and 0.1 mM Tris-Hcl buffer, pH7.5. The reaction was initiated by addition of cell extracts and quenched by 3x volume acetonitrile at 10s, 30s, or 5mins. The mixture was centrifuged for 10 min at 14000 rpm after incubation in -20 °C freezer for 1h. The supernatant was diluted with ddH_2O to 10% acetonitrile and frozen in liquid nitrogen before lyophilization. Each lyophilized sample was dissolved in 50 μl ddH_2O for LC-MS analysis.

For in vivo metabolites measurements, the samples for the determination of extracellular metabolites were collected from cultures when the cells had reached an OD600 of 0.5. 10ml of cell culture was filtered using a Millipore membrane (0.22 μm) and the membranes were then washed with 3-5 ml ice-cold quench buffer (21 mM ammonium formate, 0.17% (v:v) formic acid and 25% (v:v) ethanol). Cells were broken by passing through a French pressure cell at 1.2×10^8 Pa twice and the effluent was diluted by ddH_2O to the total volume of 30 ml. The mixture was then lyophilized to obtain LC-MS samples which were dissolved in 50 μl ddH_2O.

Both *in vitro* and *in vivo* metabolites were analyzed by a Waters Xevo LC–MS system consisting of an Acquity UPLC system and a Xevo triple-quadrupole mass spectrometer (Milford, MA). The LC conditions for the CSH-C18 column (130Å, 1.7 μm, 2.1 mm X 100 mm) are as follows: mobile phase A consisted of 25mM amonium acetate, 2% acetic acid (v:v) , 1% formic acid (v:v) in water, mobile phase B consisted of 2% acetic acid (v:v) , 1% formic acid (v:v) in acetonitrile. Initial A = 100%, set A = 80% at 2.5 min, A= 55% at 5 min, A= 5% at 6 min, A=100% at 7 min, A= 100% at 8 min. The flow rate is 0.3 ml/min. The MS was operated in the method described before [75] with minor modification. All data were analyzed using the Masslynx Quanlynx Applications Manager software.

3.3 Results

3.3.1 Construction of 1-butanol biosynthesis pathway

The essential enzymes for 1-butanol production are outlined in Figure 3.1, three of which (PhaA, PhaB and CroR) are already present in the ethylmalonyl-CoA pathway of *M. extorquens* AM1. In addition to these existing enzymes, heterologous enzymes were introduced to convert crotonyl-CoA to butanol [76,77]. Two alcohol dehydrogenase present in the *Clostridium acetobutylicum*: AdhE1 and AdhE2 [78]. Although engineered strains overexpressing either of the

homolog produced similar level of 1-butanol [41], AdhE2 was thought to be the more active homologue [79] and thus used in this study for the reduction of butyryl-CoA. A second enzyme was chose from either Bcd-etfAB from *Clostridium acetobutylicum* or Ter from *Treponema denticola* to catalyse the reduction of crotonyl-CoA to butyryl-CoA. The enzyme-coding genes were expressed in a polycistronic manner driven by promoters developed for overexpression in *M. extorquens* AM1. Four promoters were tested, ranging from high to low expression, including those for *mxaF, lac,* [71] and two chosen based on microarray data.

Engineered strains were tested for 1-butanol production using methanol or ethylamine as carbon source. Notably, no methanol-grown strains produced detectable 1-butanol. We hypothesized that the methanol dehydrogenase in *M. extorquens* AM1, a PQQ-dependent periplasmic alcohol dehydrogenase that can interconvert C_1-C_4 alcohols and aldehydes may interfere with net conversion of butyraldehyde to 1-butanol by catalysing the reverse reaction in the periplasm [80]. Therefore, we also tested 1-butanol production from a *mxaF* mutant growing on methylamine, which does not contain significant methanol dehydrogenase activity [81]. However, no 1-butanol was detected, suggesting that endogenous butanol dehydrogenase activity may not be an important factor. An alternative explanation is that the glyoxylate generated by the EMC pathway is essential for growth on methanol [20]. Tests for 1-butanol production from cells grown on methanol plus glyoxylate at a concentration known to rescue mutants in the EMC pathway for growth on methanol [48] did not result in detectable 1-butanol production, suggesting that lack of glyoxylate production was not a limiting factor.

Although the constructs tested were unable to produce 1-butanol during growth on methanol, three of the strains (BHB4, BHB7, and BHB8) produce detectable levels of 1-butanol during growth on ethylamine, with BHB7 showing the highest titer of 8.9 mg/L (Figure 3.3).

The three strains that generated detectable 1-butanol in ethylamine-grown cells, BHB4, BHB7 and BHB8 all contained Ter instead of the Bcd-etfAB cluster. The strain that generates the highest 1-butanol (BHB7) expresses the heterologous genes from a promoter of intermediate strength (Pmeta1_3616), suggesting that tuning of expression levels is critical for proper functioning of the 1-butanol production pathway.

3.3.2 Enzyme activities of heterologously expressed enzymes

Activities of the heterologous enzymes of the 1-butanol pathway were measured in extracts of cells grown on ethylamine. AdhE2 activity was measured in both directions and was successfully detected above the background activity present in wild type *M. extorquens* AM1 (Table 3.3). Attempts to measure a combined Bcd-etfAB activity were not successful using crude extract from cells that expressed *bcd-etfAB*. The lack of detectable activity may be due to the high oxygen sensitivity of the Bcd-etfAB assay, as in previous studies that have demonstrated the difficulties of obtaining reliable data for these activities in other engineered microbes [76] . This result is in keeping with the observations above that 1-butanol was not produced by these strains. Ter activities were measured in crude extracts of the engineered strains, and their levels were comparable to the levels of Ccr in extracts of wild type *M. extorquens* AM1 [23] .

3.3.3 *In vitro* isotopic tracing through reactions in the 1-butanol pathway

In order to assess overall function of the entire 1-butanol synthetic pathway, assays were carried out using cell extracts of ethylamine-grown wild type and BHB7 strains incubated with ^{13}C-labeled acetyl-CoA, NADPH and NADH, measuring accumulation of labeled intermediates over time. A set of parallel experiments were conducted in which reactions were incubated for 5s, 30s and 5min before quenching and mass spectrometry analysis. Through measurements of the ^{13}C isotopomer labeling patterns, we identified four of the five predicted

labelled intermediates (all except for crotonyl-CoA) in the 1-butanol producing pathway (Figure 3.4).

Labelled acetyl-CoA, acetoacetyl-CoA and 3-hydroxybutyryl-CoA were detected in similar amounts between wild type and the BHB7 strain during the time course. Crotonyl-CoA was not detected, even though the precursor to crotonyl-CoA, 3-hydroxybutyryl-CoA, and the downstream metabolite butyryl-CoA were both detected. Previous studies reported the difficulties of quantifying crotonyl-CoA in vivo because of the small pool size [20,46]. Small amounts of butyryl-CoA were detected in the assays of the wild type, but the amount was 13 to 43-fold higher in the BHB7 strain. This result is consistent with a previous report that a small amount of butyryl-CoA is detected in cellular extracts of *M. extorquens* AM1 grown on ethylamine [75]. The pathway for butyryl-CoA synthesis in wild type *M. extorquens* AM1 is not known. It could be a side product of the native reductive carboxylation reaction to form ethylmalonyl-CoA, or generated from isobutyryl-CoA via valine synthesis, or from metabolism of even-numbered fatty acids [82,83]. However, regardless of the source, the rate of butyryl-CoA synthesis in wild type is very low. The significant increase of labelled butyryl-CoA in strain BHB7 is consistent with the enzymatic function of Ter *in vitro* and shows that carbon flux to butyryl-CoA occurred via the 1-butanol synthetic pathway. In addition, accumulation of butyryl-CoA suggests that increasing the efficiency of AdhE2 might improve the system.

3.3.4 *In vivo* intermediates of the 1-butanol pathway

In order to identify potential bottlenecks of the 1-butanol pathway, we investigated *in vivo* intermediates by LC-MS. In these samples, four of five intermediates were detected in cell extracts of wild type and BHB7 strain, all except for acetoacetyl-CoA, which either has a small pool size or is not stable in sample pretreatment. The pool sizes of acetyl-CoA and 3-

hydroxybutyryl-CoA in BHB7 do not have significant differences compared to wild type, suggesting that upstream metabolic fluxes were not significantly affected by the introduction of the 1-butanol pathway (Figure 3.5). However, the pools of both crotonyl-CoA and butyryl-CoA are more than 10-fold lower in strain BHB7 than in the wild-type strain, presumably due to the depletion of crotonyl-CoA by Ter in the BHB7 strain. The result is expected since the accumulated butyryl-CoA could not be incorporated by central metabolic pathways in the wild type strain but can be removed by AdhE2 for 1-butanol synthesis in strain BHB7. These results suggest that an insufficient supply of crotonyl-CoA is a bottleneck for 1-butanol production, indicating this step as a target for further strain improvement.

3.3.5 Optimization of strain for 1-butanol production

One of the strategies available to adjust crotonyl-CoA supply is to decrease crotonyl-CoA flux through the EMC pathway. Ccr competes with Ter for crotonyl-CoA directly, but Ccr is essential for growth of *M. extorquens* in both C_1 and C_2 substrates [55]. Previously, we constructed a CcrR mutant which has half of the Ccr activity of the wild-type strain, but maintains the ability to grow on methanol and ethylamine, albeit at a lower growth rate [84]. The constructed plasmid that was successful in strain BHB7 was introduced into this CcrR mutant, which was tested for 1-butanol production on C_1 and C_2 compounds. However, this strain did not produce 1-butanol on methanol and a decreased amount of 1-butanol was detected from cells grown on ethylamine compared to wild-type, likely because the CcrR mutant grows more slowly on ethylamine compared to wild-type (Data not shown).

An alternative approach to increase total crotonyl-CoA supply is to overexpress crotonase. The gene encoding crotonase in *M. extorquens* AM1 (*croR*) was cloned under a modified *tac* promoter, which was then assembled with the 1-butanol operon (Pmeta1_3616::*adhE2*::*ter*) in

BHB7 to create a new strain, BHB9. A 3-fold increase of CroR activity was found in the extract of BHB9 compared to BHB7 (0.14 U/mg protein versus 0.05 U/mg protein, respectively; Figure 3.6). When growing on ethylamine, this strain produced 50% more 1-butanol (maximum 1-butanol titer = 13.6 mg/L) and no growth defect compared to BHB7. These results suggest that higher flux via CroR contributes to the increased production of 1-butanol. The 1-butanol mainly accumulated in exponential phase.

3.4 Discussion

Microorganism able to alternative carbon sources other than starchy compounds has huge potential for production of valuable chemicals and fuels from non-agricultural resources. Methylotrophs are of special interest due to their capability to use methanol as the sole carbon and energy source. Development of genetic engineering tools makes it possible to tune expression of genes in methylotrophic bacteria, as demonstrated in the biochemical studies of methylotrophy mechanism and production of dicarboxylic acid via exogenous thioesterases [11,15,26]. In this study, we successfully constructed a butanol pathway in *M. extorquens* AM1 by expression of native and heterologous genes. The engineered strain is able to produce up to 15 mg/L of butanol on ethylamine, comparable with the preliminary titers of engineered microorganism [39–41]. Previous studies have reported that tuning of expression levels was critical for proper functioning of the 1-butanol production pathway [40]. In this research, similar phenomena was observed as the strain that generates the highest 1-butanol (BHB7) expresses the heterologous genes from a promoter of intermediate strength. These results suggest optimization of pathway enzyme levels may contribute to further improvement of butanol production.

The slow enzymatic kinetics of clostridium Bcd-EtfAB complex has been previously identified as the bottleneck of butanol pathway [38]. The competition between heterologous

heterologously expressed Bcd-etfAB and native crotonyl-CoA carboxylase/reductase for crotonyl-CoA in engineered *M. extorquens* AM1 only aggravated this problem. Previous works have highlighted the difficulty associated with measuring the *in vitro* activity of Bcd–EtfAB as expressed in recombinant microorganisms [38,41]. Similarly, we were also unable to detect *in vitro* activity of Bcd–EtfAB strains. And the *in vivo* functionality of Bcd-EtfAB is also plausible considering Bcd-EtfAB is oxygen-sensitive and *M .extorquens AM1* is a strict aerobic bacteria. As a result, the unsuccessful expression of Bcd–EtfAB related butanol pathway in *M. extorquens* AM1 can be attributed to one of the reasons stated above. On the other hand, Ter has been demonstrated to outperform Clostridium Bcd–EtfAB complex by utilizing NADH as the direct reducing cofactor in effect forcing the reduction irreversible [42,85]. The reported Km value for Ter with respect to crotonyl-CoA is 2.7 μM, which is 100 times lower than that of the native Ccr (400 μM), and the Km value of a recombinant Ter in *E. coli* with respect to crotonyl-CoA is yet 5 times lower than that of Ccr [82,86] . The enzyme activities of expressed Ter in this study are also compatible with Ccr activities in ethylamine-grown cells. Therefore, Ter likely generates sufficient metabolic driving force toward the 1-butanol synthesis pathway, supported by the results showing that the Ter-containing strains generate detectable 1-butanol.

Growth on C_2 compounds is significantly different from growth on C_1 compounds, which likely underlies the difference in 1-butanol production. During growth on C_2 compounds, fewer steps are required for converting C_2 compounds into acetyl-CoA, and the proportion of total flux via the EMC pathway is higher than during C_1 growth. It has been suggested that the NADH pool is critical to drive 1-butanol synthesis due to the large NADH consumption by the 1-butanol production pathway [42]. Although neither of the NADH-linked formate dehydrogenases are essential for cell growth [14], a stoichiometric model suggests biomass synthesis is limited by

reducing power rather than ATP during growth on C_1 compounds, but not on C_2 compounds [19,87]. Moreover, during growth on two-carbon compounds, the level of NADH is 5 to 11- fold higher than on methanol [19]. One or more of these differences may be the reason why none of these constructs accumulated detectable amounts of 1-butanol during growth on methanol.

Two alcohol dehydrogenase present in the genome of clostridium acetobutylicum: AdhE1 and AdhE2 [78]. AdhE2 is thought to be the more active homologue and can only be purified and characterized under anoxic condition [79]. *In vitro* adhE2 activities were able to be measured under oxic conditions in this research, in accordance with previous reports. However, *in vitro* isotopic tracing showed accumulation of butyryl-CoA over the course of reaction time, suggesting that enzyme reaction catalysed by AdhE2 could be a rate-limiting step of butanol pathway. It has been shown in cyanobacteria that substitution of AdhE2 with oxygen insensitive butyryl-CoA reductase help improved butanol production [88]. Inconsistent growth of *M. extorquens* AM1 in oxygen limited environment implied the presence of intracellular oxygen during cell growth [89]. Therefore, similar strategies can be harnessed to improve butanol production in the future.

In summary, we reported metabolic engineering of the ethylmalonyl-CoA pathway in *M. extorquens* AM1 for 1-butanol production. The 1-butanol pathway contains part of the native ethylmalonyl-CoA pathway, a trans-enoyl-CoA reductase from *Treponema denticola* and alcohol dehydrogenase from *Clostridium acetobutylicum*. The engineered strains demonstrated various maximum 1-butanol titers from cells grown on ethylamine with the highest titer of 8.94 mg/L, which was further improved to 13.6 mg/L by overexpressing native crotonase. *In vitro* assays suggested that the enzymatic reaction catalyzed by AdhE2 is a rate-limiting step in 1-butanol synthesis. This study demonstrates that metabolic intermediates such as crotonyl-CoA can be used as substrates of a heterologous engineered pathway to produce value-added chemicals,

setting up the first example to develop *M. extorquens* AM1 into a platform for production of biofuels.

3.5 Tables and Figures

Table 3.1: *M. extorquens* strains and plasmids used in this study.

Strain	Plasmid/Genotype *	Reference
Wild Type	Rif derivative	27
BHB1	pCM66 (Plac:: bcd&etf-adhE2)	This study
BHB2	pCM80 (PmxaF:: bcd&etf-adhE2)	This study
BHB3	pAP775 (Pmeta1_3616 :: bcd&etf-adhE2)	This study
BHB4	pCM80 (PmaxF:: adhE2-ter)	This study
BHB5	pCM66 (Plac:: adhE2-ter)	This study
BHB6	pAP776 (Pmeta1_002:: adhE2-ter)	This study
BHB7	pAP775 (Pmeta1_3616 :: adhE2-ter)	This study
BHB8	pAP775 (Pmeta1_3616 :: ter-adhE2)	This study
BHB9	pHC61 (Pmtac:: croR:: Pmeta1_3616 :: adhE2-ter)	This study
Plasmids	Description	Reference
pCM66	M. extorquens expression vector (Plac, KmR)	25
pCM80	M. extorquens expression vector (PmxaF, TcR)	25
pAP775	M. extorquens expression vector (Pmeta1_3616, TcR)	E. Skovran
pAP776	M. extorquens expression vector (Pmeta1_002, TcR)	E. Skovran
pHC61	M. extorquens expression vector (Pmtac, KmR)	47

* Promoter Strength: PmxaF>Pmeta1_3616>Pmeta1_002>Plac

Table 3.2: Oligonucleotides used in this study

Name	Sequence 5'-3'
BH-GB-19	GGGCGGCGGCCGCGCCTAAATCGGATCCGGGCCCGCTAG
BH-GB-20	CGCGCAGTTCGGGCAACATATCTTAAGATCTTCCGTGCA
BH-GB-21	ATCGGATCCGGGCCCGCT
BH-GB-22	ATCTTAAGATCTTCCGTGCAGTTTAAGC
BH-GB-37	CATTATCGCGAGCCCATTTATACCCATATAAATCAGCATC
BH-GB-38	GATGCTGATTTATATGGGTATAAATGGGCTCGCGATAATG
BH-GB-47	TGTTATCCGCTCACAATTCC
BH-GB-48	ATTTCACACAGGAAACAGCT
BH-GB-53	GGATCAATTCGGCTTAAACTGCACGGAAGATC
BH-GB-54	GATCTTCCGTGCAGTTTAAGCCGAATTGATCC

Table 3.3: Enzymatic activities of Ter and AdhE2 in *M. extorquens* AM1 strains

Enzyme	**Strain**					
(nmol/min/mg)	**wild type**	**BHB4**	**BHB5**	**BHB6**	**BHB7**	**BHB8**
Ter	9.5 ± 3.3	59.1±19.8	41.5±13.6	52.1±12.2	62± 5.61	89.6± 22.3
AdhE2	17.5 ± 1.4	21.8±5.4	24.3 ± 3.2	28.2±11.8	31.3 ± 4.8	18.6±2.5

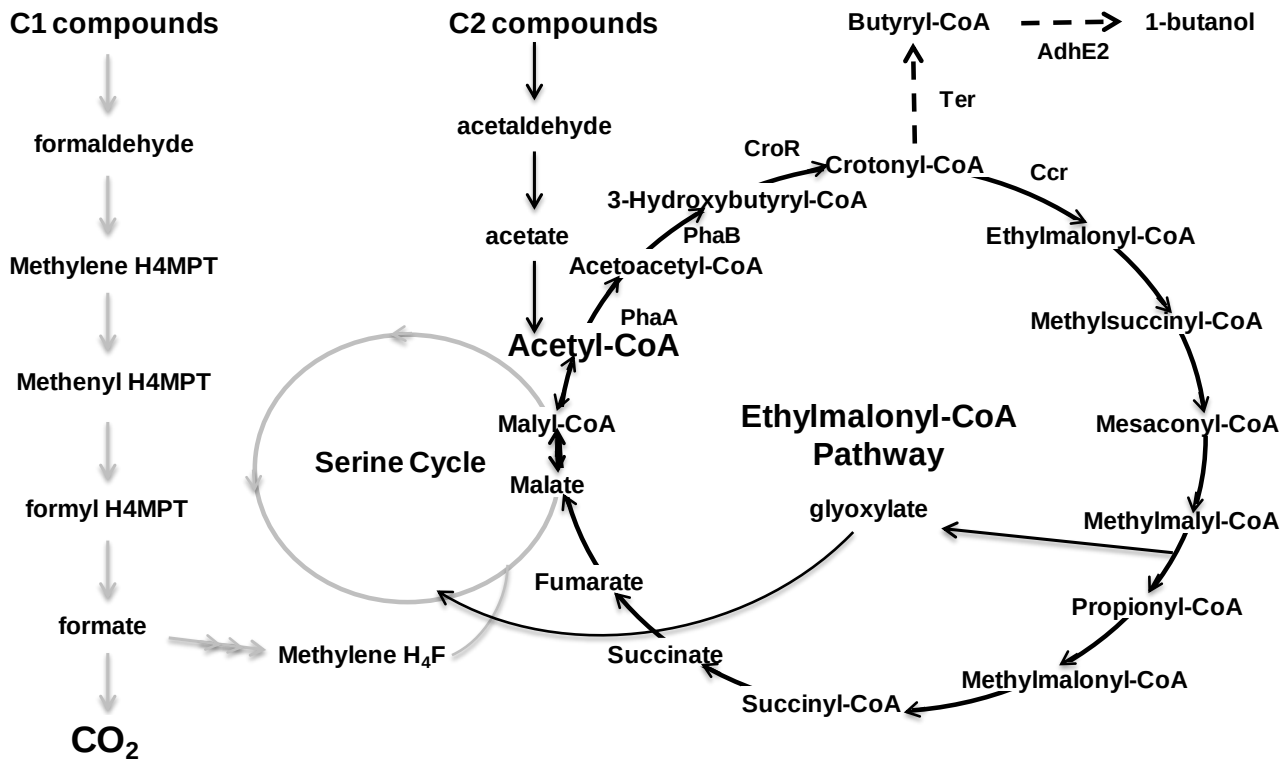

Figure 3.1: Ethylmalonyl-CoA pathway in *M. extorquens* showing intermediates for 1-butanol production. PhaA, β-ketothiolase; PhaB, acetoacetyl-CoA reductase; CroR, crotonase; Ccr, crotonyl-CoA carboxylase/reductase; Ter, trans-2-enoyl-CoA reductase; and AdhE2, bifunctional aldehyde/alcohol dehydrogenase. Gray lines represent methylotrophic pathways used exclusively in C_1 assimilation. Dashed lines represent the heterologous pathway for 1-butanol production.

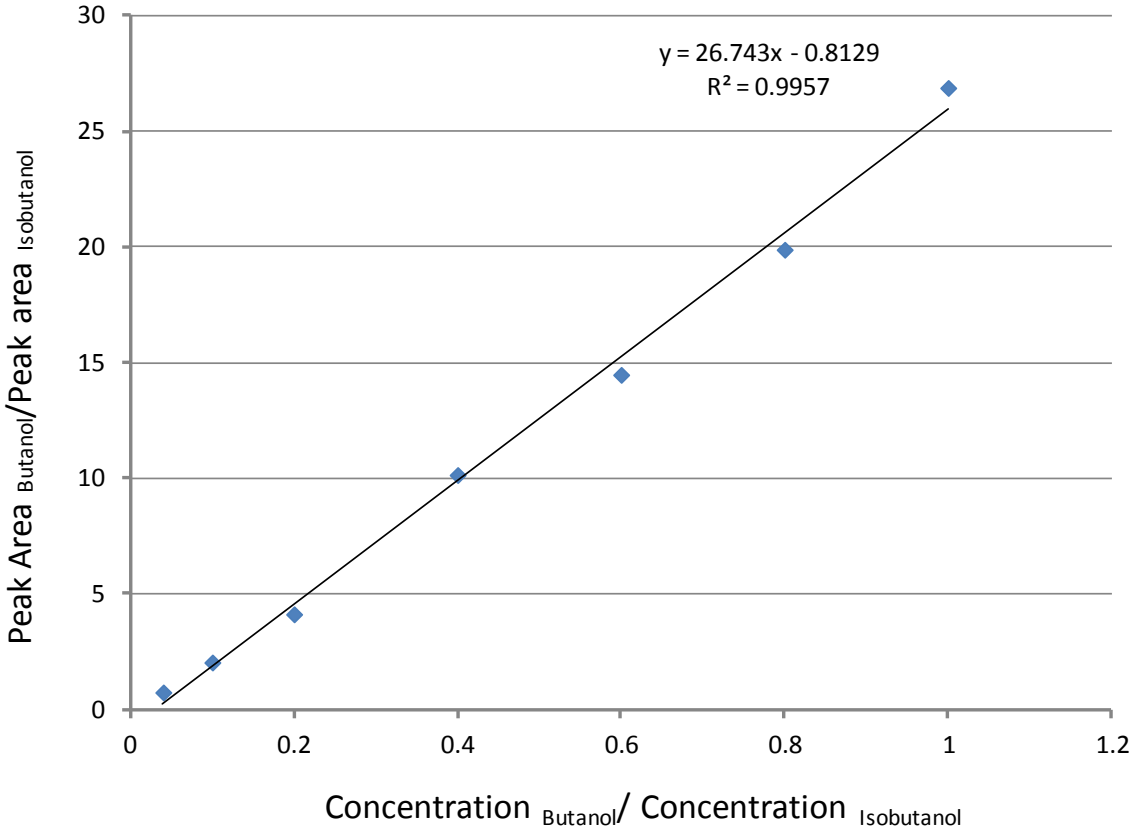

Figure 3.2: 1-butanol calibration curve obtained with GC-MS. Levels of standard Butanol dissolved in Hypho medium: 2mg/L, 5mg/L, 10mg/L, 20mg/L, 30mg/L, 40mg/L, 50mg/L. 50mg/L of isobutanol was used as internal standard.

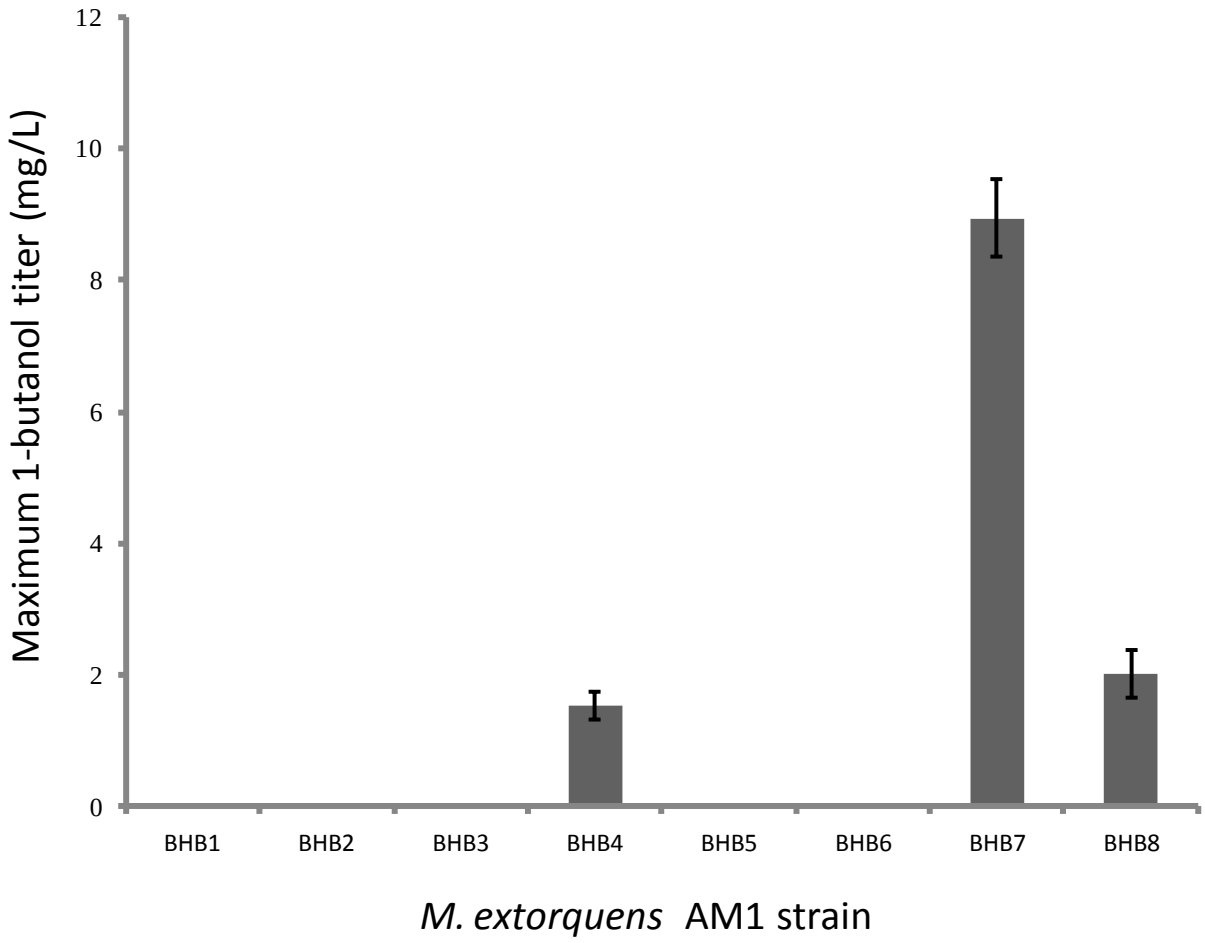

Figure 3.3: Maximum 1-butanol titer of engineered strains. Cells were grown in minimal medium with 20 mM ethylamine in shake flasks for 4 days. Error bars represent standard deviation of triplicate experiments.

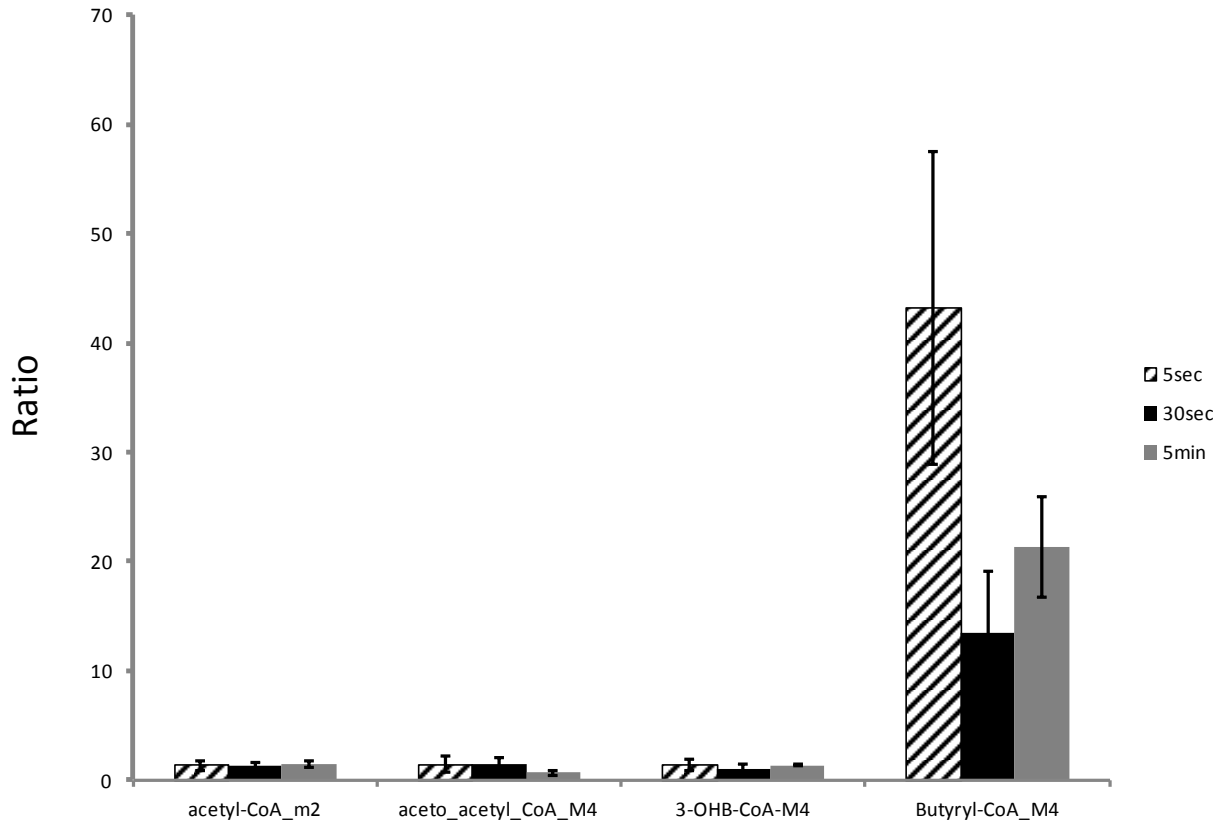

Figure 3.4: *In vitro* ^{13}C-based metabolic flux analysis of wild type and BHB7 strain. Results are ratios of values from BHB7 cell extracts compared to wild type values. The extracts of ethylamine-grown cells were fed with ^{13}C-labeled acetyl-CoA and radiolabeled metabolites were measured at different reaction times: 5 sec (stripe), 30 sec (black), 5 min (gray).

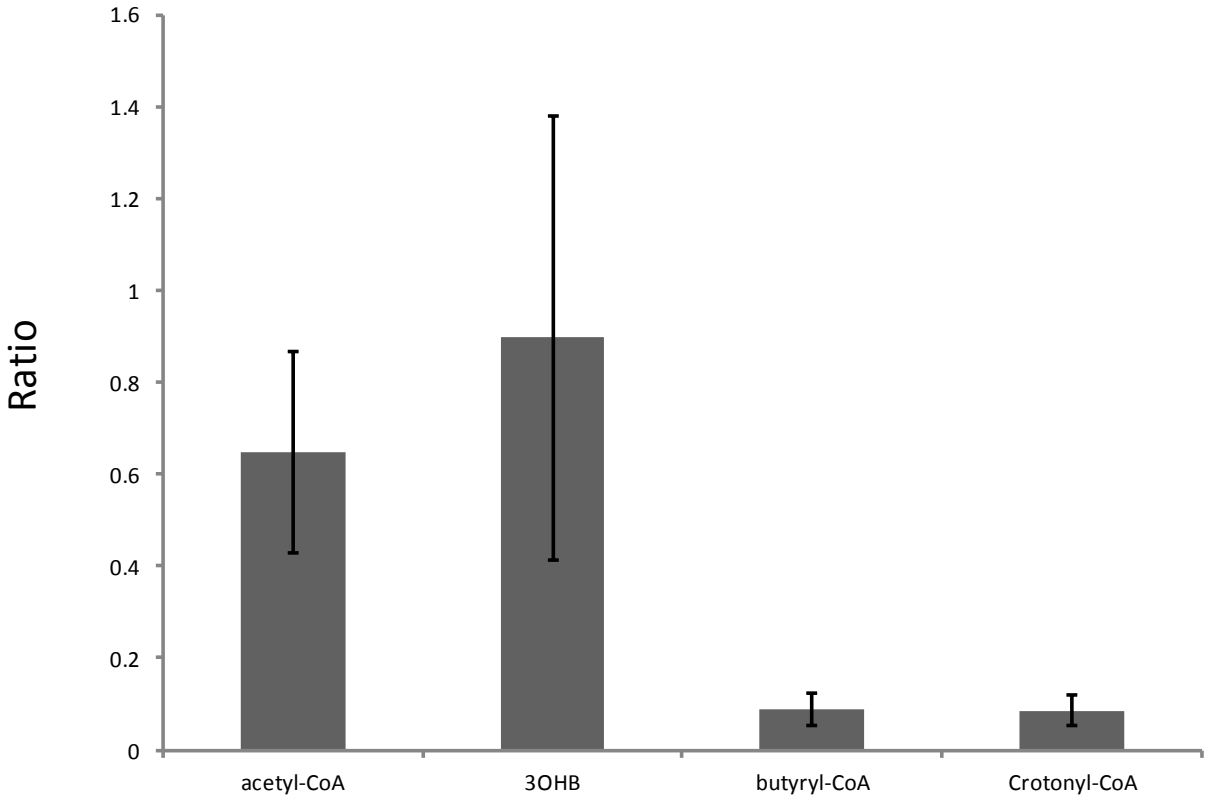

Figure 3.5: Comparison of *in vivo* 1-butanol pathway intermediates in wild type and strain BHB7 grown on ethylamine. Results are ratios of values from BHB7 compared to wild type values.

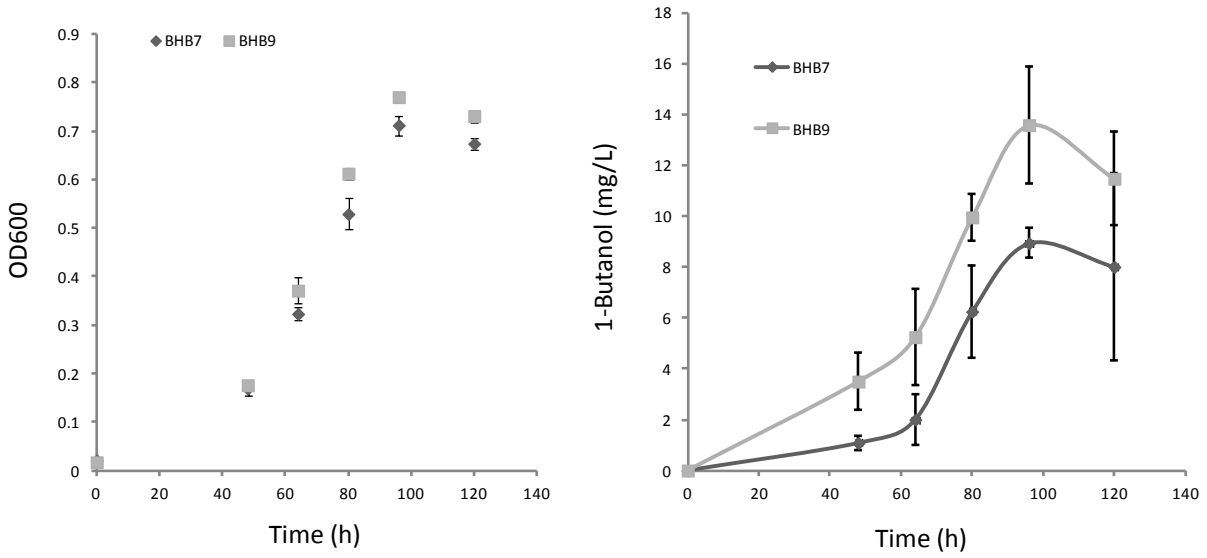

Figure 3.6: Effect of CroR overexpression on 1-butanol production. A) Growth of strain BHB7 (square) and BHB9 (diamond). B) 1-butanol production in culture of strain BHB7 (square) and BHB9 (diamond). All strains were inoculated in medium containing ethylamine (20 mM). Error bars represent standard deviation of triplicate experiments.

Chapter 4 : Adaptive laboratory evolution of *Methylobacterium extorquens* AM1 for 1-butanol tolerance

4.1 Introduction

Alcohols such as ethanol and 1-butanol are a major class of solvents that can be produced through biological fermentation [90]. Commercialized production of bio-alcohols requires a high concentration of products for economic efficiency. One of major roadblocks of the current fermentation is inhibited cell growth caused by the toxicity of alcohols to its producing strains. The high toxicity of solvents to cell growth is primarily ascribed to the chaotropic effects of the solvent and its interference with normal functions of membranes [91]. Under solvent stress, cells may respond by induction of the stress response system (heat-shock proteins), upregulation of detoxification mechanisms like transporters/efflux pumps, alteration of membrane structure and complex transcriptional and protein-level changes [92–94]. While the trend is that increased toxicity correlates with an increase in solvent hydrophobicity, the mechanism of toxicity varies with the length of the carbon backbone. In general, the toxicity of the alcohol correlates well with the octanol-water partition coefficient, Pow [95]. 1-butanol has a much higher Pow than ethanol (6.7 versus 0.48), which suggests 1-butanol should be more toxic to cells than ethanol. In fact, ethanologenic microorganisms such as *Zymomonas mobilis* is able to tolerate up to 16% (v/v) ethanol, while 1-butanol- producing bacterial strains such as clostridia rarely tolerate more than 2% 1-butanol [96]. In order to specifically analyze cell response to the stress caused by 1-butanol, several transcriptional studies have been conducted. The results indicate that 1-butanol exposure leads to a combination of several responses similar to solvent stress including cell envelope stress, oxidative stress, perturbation in respiratory systems, protein misfolding, acid stress and

induction of efflux systems [34,95,97]. However, in *E. coli*, the response networks of ethanol and 1-butanol are different, particularly in the regulation of genes responsible for proton motive force management. The complexity of cell responses to 1-butanol stress makes it unlikely to manipulate a single gene or a few genes as a cluster to improve cell tolerance to 1-butanol. Therefore, 1-butanol-tolerant derivatives of microorganisms are mainly developed through adaptive evolution or random mutagenesis [98].

One of the most popular methods to improve robustness of microbes is to cultivate them under clearly defined selective pressure for prolonged periods of time. When incremental stresses were applied to the culture, the strains adapted quickly to the changing environmental conditions and eventually evolved into more robust ones with regard to the selective pressure. This method is called experimental evolution or adaptive laboratory evolution (ALE) [99]. ALE has been used with great success to investigate the genetic mechanism of adaptation, as well as to study evolution of microorganisms. One example is the long term study of parallel *E. coli* adaption by Professor Lenski's research group in Michigan State University [100]. This approach was harnessed for a long time as a valuable method for industrial strain development, especially to enhance strain resistance to stress that commonly occurs in the industrial processing. Thanks to the development of new technologies including transcriptional profiling and massive next-generation DNA sequencing (NGS), the genetic basis of ALE was able to be analyzed at a genome scale [101]. Molecular changes acquired during adaptation such as single-nucleotide polymorphisms, insertions and deletions (indels), large genomic duplications, large deletions and transposable element insertions were uncovered by whole genome sequencing of ALE strains [102]. Thus phenotype-genotype correlations can be easily established to determine the genetic basis of

evolution, which can be used as a blueprint for rational design of industrial strains with desired traits.

Two common ALE techniques are employed to obtain evolved microbes: serial batch transfers and chemostat cultivation [103]. The former method involves sequential transfers of an aliquot of the culture from an old to a new batch culture with increased stress for an additional round of selection. Alternatively, continuous cultures in bioreactor vessels are applied. Each method has shortcomings. Cells grown in batch culture often suffered varying population density, fluctuating growth rate, insufficient nutrient supply and changing environmental conditions such as pH and dissolved oxygen (partial oxygen pressure, pO_2) [104]. In many cases, these factors may not be of great importance for evolution process but the simplicity of the experimental setup can prevent the implementation of complex environments for microbial selection experiments. Chemostat cultivation can precisely control the environmental parameters to maintain a stable population size and growth rate. But it often requires a complex experimental setup and high cost of operation. Both techniques have been applied to evolve strains for improved solvent tolerance.

In a recent study towards increased 1-butanol tolerance in *E. coli*, a large increase in solvent tolerance was rapidly achieved by combining laboratory evolution and genome shuffling of the evolved clones [105]. James Liao's research group in UCLA also reported an iso1-butanol-tolerant mutant isolated from serial transfers and five mutations (*acrA*, *gatY*, *tnaA*, *yhbJ*, and *marCRAB*) were identified to be primarily responsible for the increased iso1-butanol tolerance [106].

Methylotrophs and methanotrophs are vulnerable to solvent stress. *M. extorquens* AM1 showed inhibited growth in medium with 0.15% 1-butanol (v/v) and is unable to grow when the level of 1-butanol exceeds 0.25% (unpublished data). *Methylomicrobium alcaliphilum* 20Z and

Methylosinus trichosporium OB3b are even more sensitive, showing no growth with 0.1% 1-butanol during growth on methane. So far, only a few studies have reported the general stress response of methylotrophs and methanotrophs, such as the transcriptional analysis of *M. extorquens* AM1 to starvation and the effect of the PhyR regulon on the salt and ethanol tolerance of *M. extorquens* AM1 [107]. In this work, we applied a sequential transfer method to isolate mutated strains of *M. extorquens* AM1 tolerant to increased levels of 1-butanol. To understand the genotype–phenotype relationship of 1-butanol tolerance, we sequenced the whole genome of the evolved strain and aligned the reads with the published genome sequence. This research would not only test the approach of using ALE for strain improvement of *M. extorquens* AM1, but also provide valuable information to elucidate the genetic basis of solvent tolerance in *M. extorquens* AM1.

4.2 Methods and Materials

4.2.1 Strain, medium and growth condition

Escherichia coli strains Top 10 and S17-1 were cultivated at 37ºC in Luria-Bertani medium. *M. extorquens* AM1 wild type and 1-butanol-tolerant mutants were cultured in a minimal medium (hypho) [49] supplemented with 1.77 µg/L $CoCl_2$. One of the following substrates was used as carbon source: succinate (20 mM), methanol (125 mM), or ethylamine (20 mM). For triparental matings between *E. coli* and *M. extorquens* AM1, Difco nutrient broth supplemented with Difco BiTek agar (1.5% [wt/vol]) was used. Antibiotics were supplied at concentrations as follows: kanamycin (Km), 50 µg/ml, and rifamycin (Rf), 50 µg/ml.

4.2.2 Adaptive evolution of *M. extorquens* AM1

A sequential transfer method was used to isolate 1-butanol-tolerant mutants of *M. extorquens* AM1. *M. extorquens* AM1 was first streaked on the hypho methanol plate and a single colony was picked to inoculate 5 ml of liquid hypho methanol preculture. The preculture was then diluted into twenty 25ml plastic-cap tubes (1:100) containing 5 ml of hypho methanol medium and 0.15% 1-butanol (v/v). Cultures were inoculated at 30 ^{o}C for 72 h to late exponential phase and the culture of highest OD_{600} was selected as the seed culture for the next round of transfer. A series of transfers were conducted at the same concentration of 1-butanol (3-5 transfers). Then cultures were diluted and spread on solid medium to pick up single colonies for next round of inoculation, when the 1-butanol concentration in the medium was increased to 0.2%. The transfer process was continuously repeated with incremental 1-butanol concentration of 0.05% each time to the final concentration of 0.5%. 1-butanol-resistant mutants were stored in 10% DMSO at -80 ^{o}C.

4.2.3 1-butanol tolerance of selected mutants

Cultures of *M. extorquens* AM1 wild type and two 1-butanol-tolerant mutants (BHBT3 and BHBT5) were inoculated to middle exponential phase in 5 ml hypho methanol medium at 30 ^{o}C. Then 0.5ml of culture was distributed into 50 ml fresh hypho methanol medium in 250ml flasks containing appropriate amounts of 1-butanol. OD_{600} of the growing cultures was measured every 3-6 h for 72 h. For viable cell counting, cultures inoculated after 24 h were diluted with fresh hypho medium and spread on hypho methanol plates. Colonies formed after 3 days of incubation were counted (50-500 per plate). Triplicate experiments were performed for each individual condition.

4.2.4 Survival rates of *M. extorquens* AM1 under high 1-butanol pressure

Survival rates of mutated strains were assessed using the method described previously [108]. Single colonies of the mutated strain were inoculated in plastic tubes and subcultured into 250 ml flasks containing 50 ml hypho methanol medium. After 24 h of incubation, 0.5 ml of mid-log phase culture was mixed with 4.7 ml hypho methanol medium supplemented with 0.25 g 1-butanol (final 1-butanol concentration 50 g/L). The culture was then mixed and held for 30 min, which was followed by serial dilutions using fresh hypho medium. The diluted culture was spread onto hypho methanol plates and incubated at 30 ^{o}C for three days before counting colony numbers. A control experiment was set up using the same dilution procedure without the addition of 1-butanol. Cell survival rate was calculated as cfu per ml of buthanol-exposed culture divided by that of control culture.

4.2.5 Genomic DNA extraction and whole genome sequencing

The genomic DNA of BHBT3 and BHBT5 was extracted using a phenol/chloroform extraction protocol as described before [109]. Cells grown on methanol were harvested at mid-exponential phase and resuspended in 5 ml of lysis buffer (10mM NaCl, 20mM pH 8.0 Tris-HCl, 1mM EDTA and 2% (w/v) SDS). Cell lysates were incubated with 50 µl of 100mg/ml RNaseA and 250 µl of proteinase K overnight at 55^{o}C. The DNA was separated from protein and RNA by phenol/chloroform extraction and recovered via ethanol precipitation. The DNA samples for whole genome sequencing were dissolved in 400 µl TE buffer. Preparation of paired-end libraries and whole-genome sequencing was performed by Genewiz Inc. (Plainfield, NJ) using the Illumina-Miseq sequencing platform.

To detect changes between the sequenced strain and the butanol tolerant strains, the results of three independent analyses were combined. First, the raw reads were aligned to the

genome and processed using *breseq* version 0.19 [110]. Next, the raw reads were quality filtered using *Nesoni* version 0.122 (Nesoni, 2014). The filtered reads were assembled using *SPAdes* version 3.0 [111]. The assembled contigs were compared to the published sequence using in-house scripts based on processing the BLAST version 2.2.10 [112]. Finally, the filtered reads were aligned to the published scaffold with BWA version 0.7.5a-r405 [113] and the results were post-processed with SAMtools version 0.1.19-44428cd [114] for variant calling.

4.2.6 1-butanol measurement

The 1-butanol production of BHB10 was determined by GC-MS with the method described in Chapter 3.10 ml of culture samples were centrifuged for 10 min at 5000 rpm. 2ml ethyl acetate was added to the supernatant. After the addition of 50 mg/L isobutanol as internal standard, the mixture was vortexed for 1 min and then centrifuged for 10 min at 5000 rpm to separate aqueous phase and ethyl acetate. The recovered ethyl acetate was analyzed by a HP 6890 gas chromatograph equipped with a Model 19091s-433 HP-5MS column (Agilent) and an agilent 5973 single quadrupole mass spectrometer. Helium with 7.64 psi inlet pressure was used as carrier gas. 1µl of samples were analyzed with the following program: Set initial temperature at 50°C, ramped to 90°C at 10°C/min, ramped to 300°C at 45°C/min, maintained at 300°C for 1min. The injector temperature was maintained at 225°C. A standard curve was derived from measurements of 1-1-butanol aqueous solution (2 mg/L, 5mg/L, 10mg/L, 20mg/L, 30mg/L, 40mg/L, 50mg/L). The ion source temperature was set to 250 °C. Mass spectra were collected at m/z 40 and m/z 56 with a 2.2 min solvent delay. The peaks were analyzed using Agilent ChemStation software.

4.3 Results

4.3.1 Isolation of 1-butanol-tolerant mutants of *M. extorquens* AM1

A rifamycin resistant derivative of *M. extorquens* AM1 (wild type), which has been cultivated in Mary Lidstrom's lab for over 30 years, was selected as the parent strain for the evolution experiments [115]. The wild type strain was initially inoculated in hypho methanol medium containing 0.15% (v/v) 1-butanol. After every 3-6 parallel transfers, cultures of highest cell density were transferred into fresh medium in which the 1-butanol concentration was increased by 0.05%. The OD_{600} of cultures transferred to medium with increased 1-butanol concentration is summarized in Figure 4.1. The end point cell density decreased with increasing 1-butanol concentration during the first three transfers. However, at 0.3% 1-butanol, a portion of the cultures were able to grow to similar OD_{600} of that at 0.15% 1-butanol, suggesting critical genetic mutations related to 1-butanol tolerance may occur in these cultures. A single colony was separated from this culture and denoted as BHBT3, which was used for the following enrichment experiments. After a total number of 40 transfers, a mutant that is able to grow at 0.5% 1-butanol was isolated and denoted as BHBT5. The sizes of BHBT3 and BHBT5 colonies on agar plates were identical with that of wild type, but appeared to be white instead of pink. Although attempts to select even more resistant strains are being continued, it has been difficult to obtain stable cultures with more than 0.5% 1-butanol. Therefore, the following studies focus on evaluation of the 1-butanol resistance of BHBT3 and BHBT5.

4.3.2 Influence of 1-butanol on growth of *M. extorquens* AM1

To study 1-butanol tolerance of BHBT3 and BHBT5, growth of wild type, BHBT3 and BHBT5 in hypho methanol medium with different amounts of 1-butanol was investigated. No significant disparities were observed between growth rates of the three strains in medium without

1-butanol (Figure 4.2 A). However, BHBT3 and BHBT5 were more tolerant to 0.15% 1-butanol than wild type despite growth inhibition of all three strains (Figure 4.2 B). The growth rate of wild type was reduced by 40% with the addition of 0.15% 1-butanol while the growth rates of BHBT3 and BHBT5 were only reduced by 20% (Figure 4.3 B). In the presence of 0.5% 1-butanol, only BHBT5 was able to grow with a reduced growth rate compared to no 1-butanol (50%) but similar final OD_{600} compared with that in normal hypho medium (Figure 4.2 C, Figure 4.3 B). Both wild type and BHBT3 did not grow after 72h incubation. Cell counting results are consistent with OD_{600} measurements (Figure 4.3 A). The cell counts of BHBT3 and BHBT5 are 4- and 7-fold higher than that of wild type respectively after 24h of incubation in the presence of 0.15% 1-butanol, while there were only 2-fold more viable cells in BHBT3 and BHBT5 cultures than wild type culture in the medium without 1-butanol. Despite the low OD_{600} of both wild type and BHBT3 incubated in 0.5% 1-butanol medium, the cell count of BHBT3 is 3 times higher than that of wild type. The number of viable BHBT5 cells is 2 orders of magnitude higher than WT and BHBT3. These results suggest that two strains of *M. extorquens* AM1 with different levels of 1-butanol tolerance were successfully isolated through the enrichment experiments.

The survival rate of *M. extorquens* AM1 strains during exposure to a high concentration of 1-butanol was investigated by exposing wild type, BHBT3 and BHBT5 to 50 g/L1-butanol for 30 min. The survival rate of both BHBT3 and BHBT5 were above 80%, almost 4 times higher than that of wild type (23%, Figure 4.4). This result shows the evolved strains are more robust to high concentration of 1-butanol.

4.3.3 1-butanol production of BHBT5

To assess whether the genetic mutations of BHBT5 would improve 1-butanol production, a plasmid harboring the 1-butanol synthetic pathway reported in Chapter 3 was introduced into

BHBT5 by bacterial conjugation. 1-butanol production of the new strain, designated as BHBT10, was investigated in hypho medium using ethylamine as the carbon source. Compared with the previous construct, both cell density and 1-butanol production of BHBT10 were increased (Figure 4.5). After 72h incubation, BHBT10 was able to produce a maximum of 25.5 mg/L 1-butanol, representing 67% more than the original strain BHB9. OD_{600}-calibrated 1-butanol production of BHBT10 was also 30% higher than that of BHB9, suggesting the improvement of 1-butanol production is ascribed to the combination of optimized cell growth and enhanced flux toward 1-butanol pathway.

4.3.4 Whole genome sequencing of BHBT3 and BHBT5

In order to identify specific mutations in BHBT3 and BHBT5 responsible for 1-butanol tolerance, the genomes of BHBT3 and BHBT5 were sequenced via the Illumina Miseq platform. The sequenced reads were de novo assembled by mapping to the reference genome which was performed by David Beck, a research assistant profession in University of Washington. The coverage of reads across the genome allows us to identify structural variations on the genome including single-nucleotide polymorphisms (SNPs), indels, and duplications. A comprehensive analysis of sequencing data is still ongoing, but the preliminary sequencing results are summarized in Table 4.1.

The majority of genotypic differences between wild type and butanol-tolerance mutants occur at uncharacterized protein coding regions, which is partially ascribed to the limited genomic information of *M. extorquens* AM1. All but one mutation occurring in BHBT3 is also present in BHBT5, while 5 unique SNPs and 1 indel are present only in BHBT5, which may contribute to the phenotypic difference between BHBT3 and BHBT5. Among the mutated genes with annotated functions, a single-nucleotide polymorphism (a T-G transition) in the intergenic

region between *depB* and Meta1_4598, annotated as coding for PHB depolymerase and succinate-semialdehyde dehydrogenase respectively, was revealed in both genome sequences of BHBT3 and BHBT5. A single-nucleotide polymorphism (an A-C transition (L171R)) was identified in the potassium/proton antiporter-coding region (*kefB*) of BHBT5, which may affect the proton gradient across the membrane. These mutations would be targeted for further analysis.

4.4 Discussion

1-butanol toxicity to microorganisms is one of the important factors that limit industrial production potential of this next-generation biofuels. Due to the inherent complexity of physiological changes caused by 1-butanol toxicity, it is hard to predict and design an effective targeted approach for tolerance improvement [116]. This is particularly true in the case of *M. extorquens* AM1 since mechanisms of solvent stress response have never been studied. In this work, we demonstrated the use of an adaptive laboratory evolution approach for evolving a 1-butanol resistant strain by stepwise increase of 1-butanol concentration as a selective pressure towards 1-butanol tolerance. In comparison to the wild type, the isolated mutants BHBT3 and BHBT5 showed less growth inhibition by 0.15% 1-butanol and exhibited increased survival rate during exposure to 20 g/L 1-butanol. Furthermore, BHBT5 is able to maintain 50% of the normal growth rate in 0.5% (v/v) 1-butanol, a level that can severely damage viability of many industrial microorganisms such as *P. putida*, *E.coli* and *B. subtilis* [41]. Based on previous studies, strain fitness during enrichment experiments typically rises rapidly during the first 100-500 generations and slows down considerably during the course of ALE [104]. Therefore, prolonged selection that exceeds the first rapid evolutionary adaptation phase will not necessarily lead to significantly improved phenotypes. A typical ALE experiment for solvent tolerance takes a few weeks up to a few months across 100 to 1000 generations of targeted microorganism [98,106,117].

This general principle is well applied to the time span of the serial transfer experiments in this study, which was performed for about 200 generations.

Preliminary analysis of the genome sequence of BHBT3 and BHBT5 revealed several genetic changes in the mutated strains compared to wild type, most of which are SNPs. Previous genome resequencing of adapted isobutanol-tolerant *E. coli* suggested that the majority of mutations contributing to the phenotype are insertion sequence elements contained in the coding regions [106]. Given the high frequency of genome rearrangement through mobile elements in *M. extorquens* AM1 [115], further interpretation of the resequenced genome is expected to uncover more insertions of IS elements that affect the function of targeted genes. A point mutation was detected in *kefB* in BHBT5. In *Escherichia coli*, KefB is a glutathione-gated potassium channel that protects cells during electrophilic attack via the modulation of the cellular pH [118]. It has been shown that mutated *C. beijerinckii* with stable transmembrane ΔpH was found to be significantly more tolerant of added butanol than the wild-type [119]. There may be a correlation between KefB-affiliated cellular pH maintenance and 1-butanol tolerance in *M. extorquens* AM1. Since butanol tolerance is an essential microbial trait for industrial scale production of butanol, the butanol-tolerant strains obtained via adaptive laboratory evolution are a better platform than wild type *M. extorquens* AM1. By incorporating the genetic data with other system biology approaches such as transcriptome analysis, detailed mechanisms for the response to butanol stress are expected to be uncovered. This would open the door for rational design of a butanol-tolerant strain in the future.

4.5 Tables and Figures

Table 4.1: Summary of genome resequencing of BHBT3 and BHBT5

	BHBT3	BHBT5
Total number of paired-end reads	8,342,206	9,517,254
Genome coverage rate	99.6%	99.5%
Average coverage	280±79	324±69
SNPs (synonymous)	5	7
SNPs	1 (intergenic depB/Meta1_4598)	3 (intergenic depB/Meta1_4598, gpmA, kefB)
Indels (synonymous)	0	1
IS elements (synonymous)	2	2

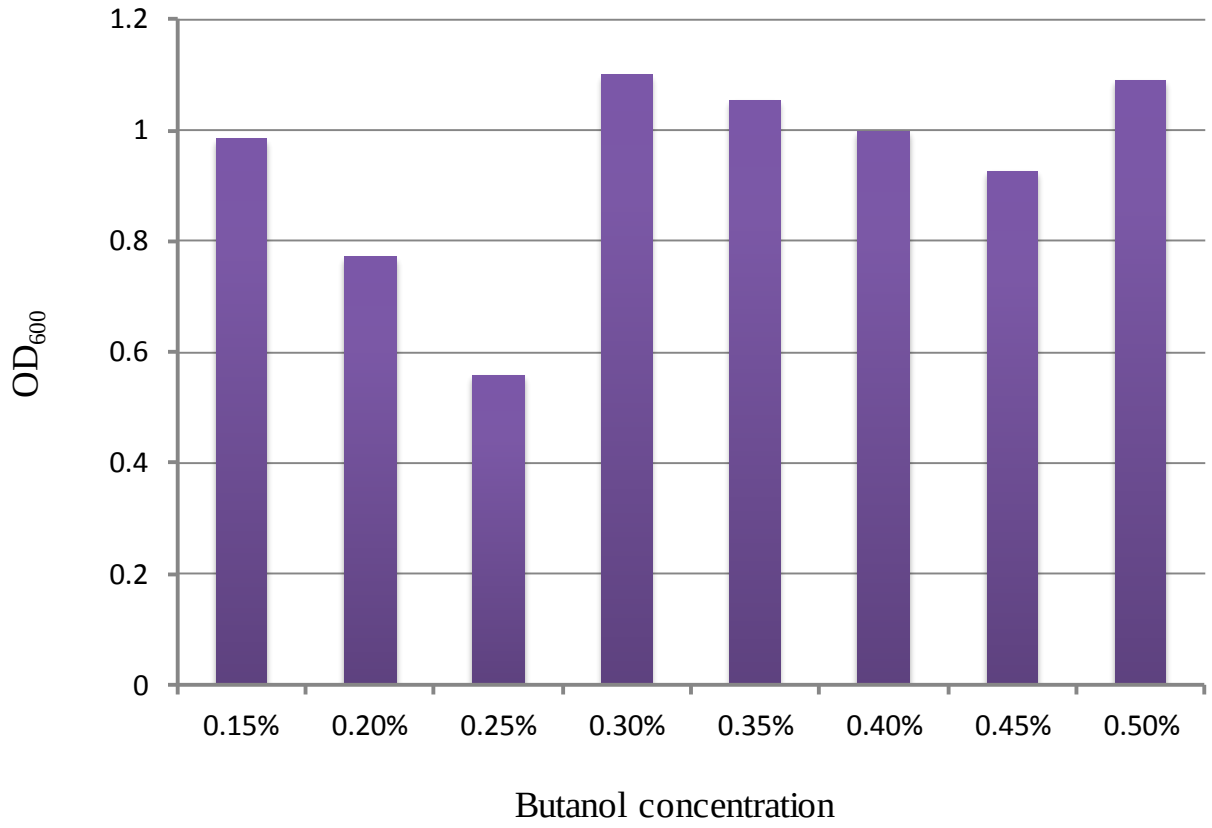

Figure 4.1: Adaptive evolution of *M. extorquens* AM1 for butanol tolerance. Cells were inoculated in 5ml hypho methanol medium at 30 ^{o}C for 72 h. The butanol concentration was increased by 0.05% after 3-5 parallel transfers at the same butanol level. OD_{600} reflects the final optical density of the culture used for the next increase in butanol concentration.

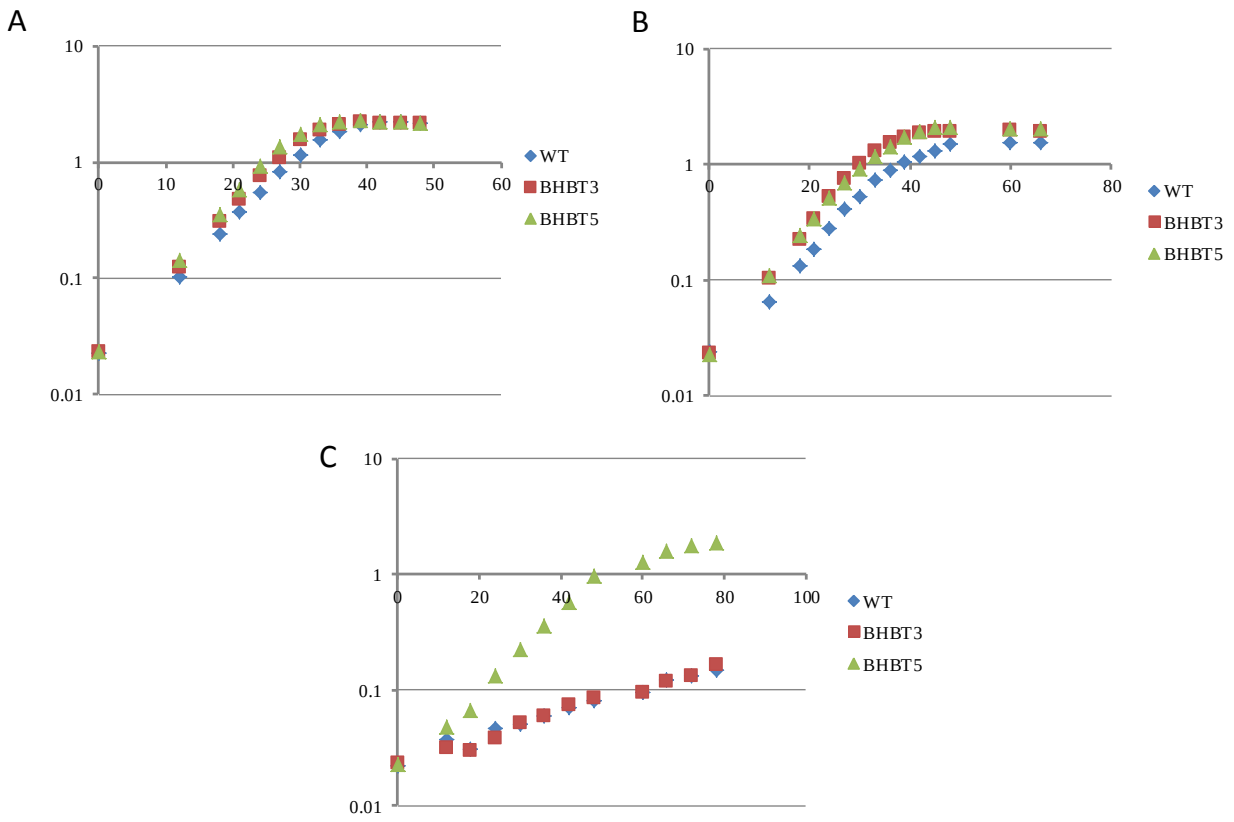

Figure 4.2: Time course for the growth of wild type (diamonds), BHBT3 (Squares) and BHBT5 (Triangles) in the presence of 0% (A), 0.15% (B), 0.5% (C) 1-butanol.

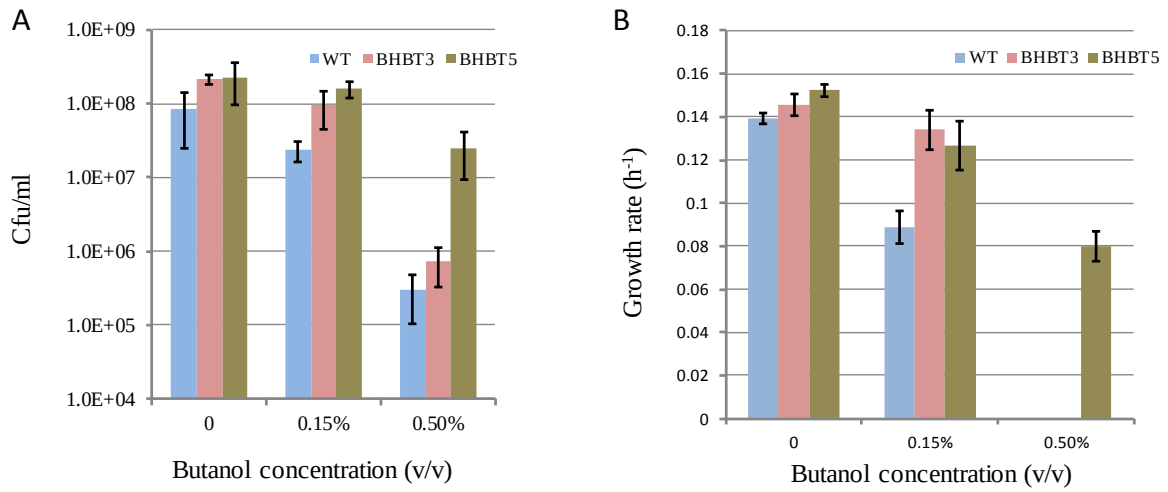

Figure 4.3: Growth inhibition of 1-butanol for wild type (Blue), BHBT3 (Pink) and BHBT5 (Brown). A) Plate cell counts of cultures grown with different amounts of butanol for 24h. B) Growth rates of cultures grown with different amounts of butanol. Cells were inoculated in 50 ml of hypho methanol medium at 30 ^{o}C. Growth rates of wild type and BHBT3 at 0.5% butanol were not calculated because of the very low cell density. All experiments were carried out in triplicate.

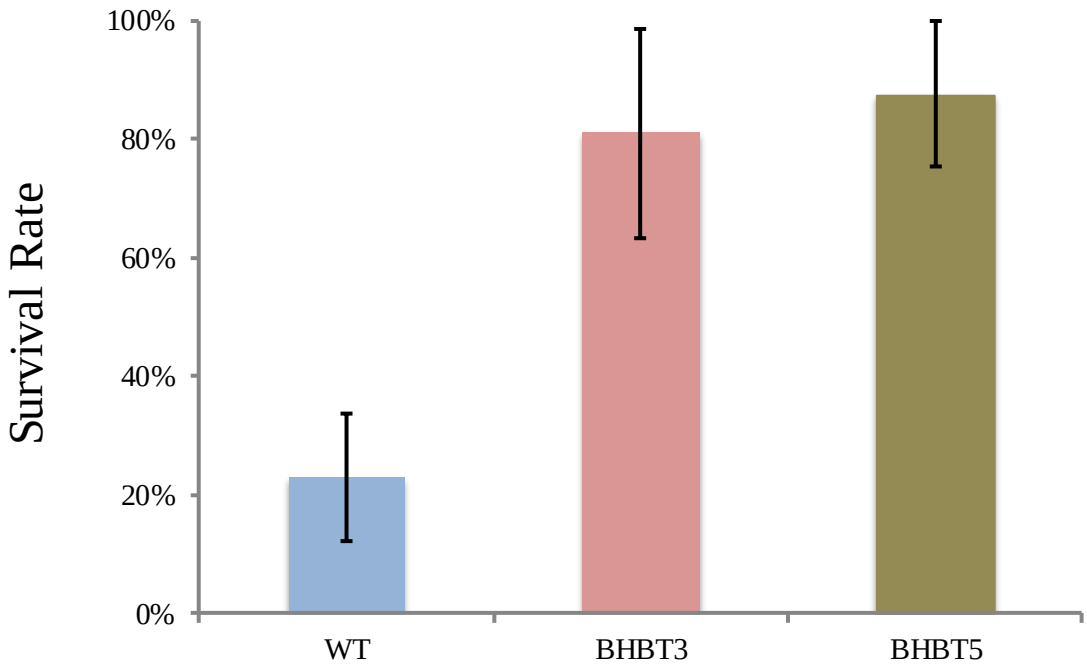

Figure 4.4: The ratio of viable cells exposed to 0 g/L and 50 g/L (5% w/v) 1-butanol. The cultures were incubated with 0 g/L and 50 g/L butanol for 30 min and the cell survival rate were calculated by counting viable cells on the plates. All experiments were performed in triplicates.

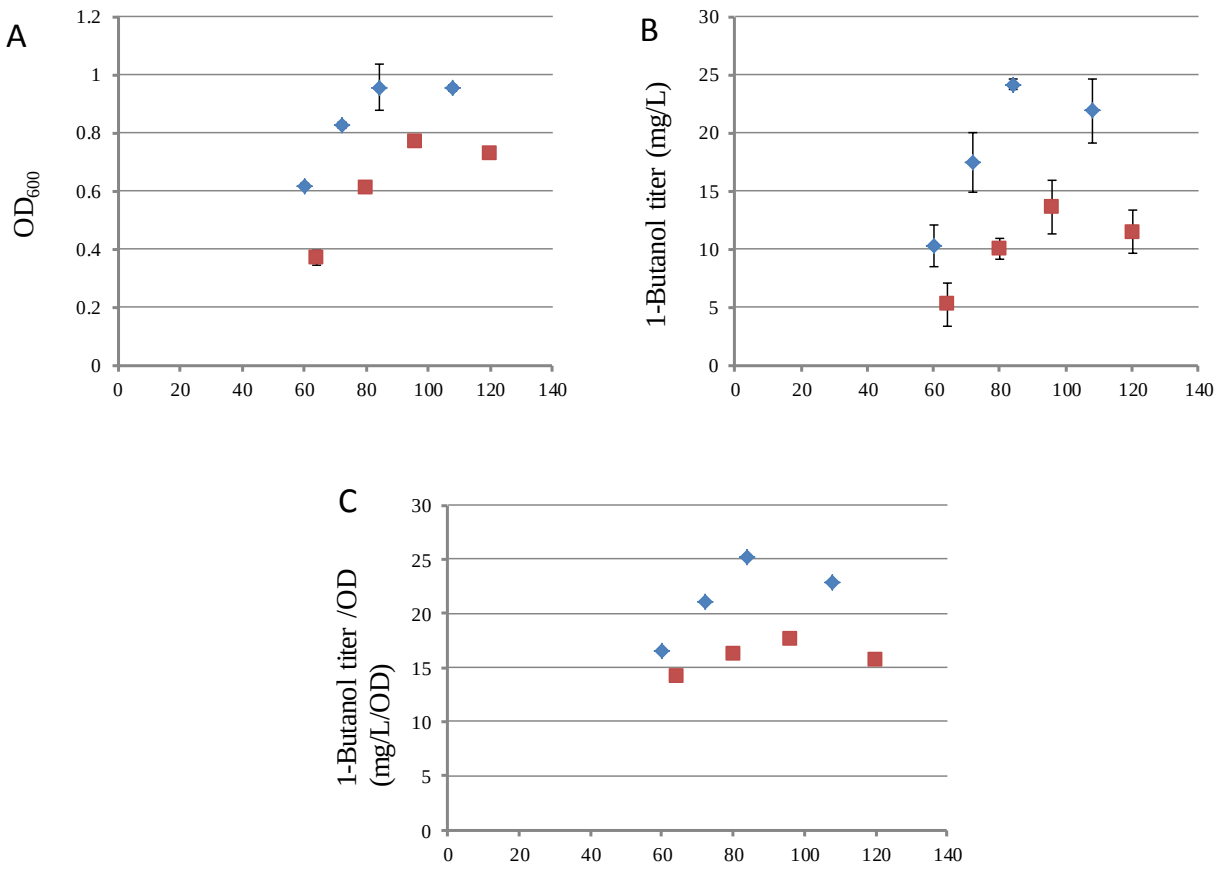

Figure 4.5: 1-Butanol production of BHB9 (red square) and BHB10 (blue diamond) on ethylamine. A) Growth curve of BHB9 and BHB10. B) 1-Butanol titer of BHB9 and BHB10. C) OD_{600} calibrated 1-butanol titer of BHB9 and BHB10. All experiments were performed in triplicates.

Chapter 5 : Summary and Future directions

5.1 Summary

In recent years, *M. extorquens* AM1 has gained interest as an industrial microorganism due to the important role of methanol as a future alternative carbon feedstock. With the development of metabolic engineering tools and enriched understanding of metabolic pathways in *M. extorquens* AM1, it is practical to rationally engineer this microorganism for biotechnological purposes. However, potential application of this organism faces several roadblocks including insufficient knowledge of regulatory mechanisms and a lack of examples of manipulating metabolism to produce biochemical. This thesis covers a set of initial efforts to address the above issues with regard to manipulation of flux through the EMC pathway, a key target for biotechnological applications of *M. extorquens* AM1.

We first addressed regulation of the EMC pathway, by assessing a TetR-type regulator (CcrR) (Chapter 2). CcrR was found to positively regulate the expression of *ccr*, a critical gene of the EMC pathway, by binding to a palindromic sequence upstream of the *katA-ccr* operon. *M. extorquens* AM1 mutants deficient in CcrR showed a reduced growth rate and final cell density compared with wild type during growth on C_1 and C_2 compounds and the enzymatic activities of Ccr decreased by 50% in *ccr* mutant compared with that in wild type. This work is the first example of a regulatory mechanism for the EMC pathway, and sets the stage for further elucidation of regulatory mechanism of key pathways in *M. extorquens* AM1, as well as future development of unique metabolic pathways in *M. extorquens* AM1 for biofuel production.

In order to demonstrate the potential of *M. extorquens* AM1 as a future industrial microorganism, we chose as a proof of principle example the generation of 1-butanol from EMC

pathway intermediates. A 1-butanol synthesis pathway was established in *M. extorquens* AM1 by diverting part of the native crotonyl-CoA flux to 1-butanol production (Chapter 3). Engineered strains demonstrated different 1-butanol production using ethylamine as a substrate. By using metabolomics strategies such as metabolic profiling and isotopic tracing as a tool for bottleneck identification, an optimized strain overexpressing the *Treponema denticola* trans-enoyl-CoA reductase, *Clostridium acetobutylicum* alcohol dehydrogenase and native crotonase was obtained that produced the highest amount of 1-butanol (15.2 mg/L). This will not only establish the biotechnological potential of ethylmalonyl-CoA pathway, but also set *M. extorquens* AM1 up as a potential platform to produce value-added chemicals.

Finally, as a next step towards development of *M. extorquens* AM1 as an industrial platform, adaptive laboratory evolution was used as a tool to develop *M. extorquens* AM1 for high 1-butanol tolerance. We applied a serial transfer method to isolate two mutants (Chapter 4), BHBT3 and BHBT5, both of which demonstrated 50% increase of fitness compared to the parent strain at 0.15% 1-butanol despite the fact that only BHBT5 could survive at 0.5% 1-butanol. In the absence of 1-butanol, BHBT3 and BHBT5 showed similar growth patterns compared to the wild type with methanol as the substrate but much improved growth rate and final cell density with ethylamine. This trait contributed to increased 1-butanol production after introducing the 1-butanol synthetic pathway into BHBT5. Whole genome sequencing of BHBT3 and BHBT5 identified mutations responsible for the observed phenotype. The collected information from this research will be useful for uncovering the cellular response of *M. extorquens* AM1 to solvent stress, and in addition will also provide the genetic blueprint for the rational design of a strain of *M. extorquens* AM1 with increased 1-butanol-tolerance in the future.

Combined together, the results demonstrated in this work represent the first attempt to integrate the principles of metabolic engineering and the knowledge of assimilatory pathways in *M. extorquens* AM1 to produce valuable chemicals. Our success in producing 1-butanol from the engineered *M. extorquens* AM1 opens the possibility for using methylotrophs for bulk chemical production. In addition, the genetic information and engineering experience obtained from this study would provide useful guidance for similar research in the future.

5.2 Future Directions

To take the next steps in moving *M. extorquens* AM1 forward as a commercial platform to generate 1-butanol, future work must be applied to several aspects including a detailed understanding of flux regulation mechanisms related to the 1-butanol synthesis pathway, strain improvement for higher 1-butanol titer and tolerance, and trouble-shooting of 1-butanol production from methanol. A long-term goal would be to investigate enzymatic reactions and regulatory mechanisms involved in acetyl-CoA synthesis in *M. extorquens* AM1 in order to rationally modify the *M. extorquens* AM1 genome and heterologous pathway enzymes for increased product titers [120]. Short-term approaches such as random mutagenesis followed by high-throughput screening or selection can be employed as preliminary efforts towards strain development of *M. extorquens* AM1.

Although experimental evolution has been applied to improve host tolerance to toxic products, it has been rarely used to screen for strains with increased production of desired chemicals because only a small group of targeted compounds can be readily screened using standard assay techniques. Methods based on chromatography or spectrometry have been used as the primary way of detection for such products [121]. Although they have demonstrated good sensitivity and selectivity in the detection and quantification of small-molecules, these assays are

inherently low throughput which significantly limits the capacity of library screening [122]. In addition, it is difficult to apply enrichment experiments to screen for phenotypes overproducing small molecules that do not have a spectral signature. Therefore, it remains a challenge to convert the production of small molecules into detectable traits such as growth rates. Small molecule-based biosensors have just begun to be explored to solve this issue. These biosensors often form as *in vivo* biosynthetic pathways with undetectable substrate inputs and detectable product outputs, which could be quantitatively transferred via the activity of biosensors [123,124]. Recently, Jay Keasling's lab at UC-Berkeley developed a biosensor composed of a 1-butanol-responsive transcription factor-promoter pair and a tetracycline resistance reporter protein, to couple the small-molecule product (including 1-butanol) concentration to host growth rate for strain screening [125]. This system involves a putative σ^{54}-transcriptional activator (BmoR) from *Pseudomonas butanovora*, which can bind to a σ^{54}-dependent, alcohol-regulated promoter (P_{BMO}) in the presence of medium chain alcohols (C_4-C_7) to initiate transcription [126]. Since multiple ORFs coding for sigma factors have been identified in the genome of *M. extorquens* AM1, we hypothesize that this biosensor should be able to accept alcohol signals once transferred into *M. extorquens* AM1. We then would seek to apply this device for selection of *M. extorquens* AM1 strains with high 1-butanol productivity.

Preliminary work has been carried out to assess the feasibility of this approach. The biosensor cassette encoding BmoR, P_{BMO} and the tetracycline/proton antiporter (tetA) were integrated into the chromosome of wild type *M. extorquens* AM1, and tetracycline resistance in the presence of incremental 1-butanol was assessed. The final cell densities of engineered *M. extorquens* AM1 were measured in hypho methanol medium containing various concentrations of tetracycline (1mg, 5mg, 10mg) and 1-butanol (0mM, 5mM, 15mM). Cells were first

inoculated in fresh hypho methanol medium to a cell density of OD_{600} 0.5. Then the culture was incubated with 1-butanol for 2 h to induce the synthesis of tetracycline antiporter. Following addition of 1-butanol, cultures were incubated for 24 h (30 °C, 250 rpm). Cell densities measured at 0 h, 8 h, 16 h, 24 h after the addition of 1-butanol are summarized in Figure 5.1. In the absence of 1-butanol, no measurable growth of culture was observed in the presence of tetracycline at any of the tested concentrations. Cultures supplemented with 5 mM 1-butanol, in contrast, were able to grow up to OD_{600} 0.72 in the presence of 1 mg/L tetracycline. Interestingly, cultures with a supplement of 15mM 1-butanol did not grow as well, presumably due to the sensitivity of *M. extorquens* AM1 to high levels of 1-butanol as reported in Chapter 4. All cultures were unable to grow with 5 mg and 10 mg of tetracycline even when the biosensor was fully activated; suggesting tetracycline concentration has exceeded limits of the biosensor capability. In general, the biosensor was able to discriminate between differences in wild type and engineered strains in the presence of 5 mM 1-butanol and 1 mg/L tetracycline. However, high concentrations of 1-butanol could not rescue the biosensor strain from tetracycline inhibition, likely due to the toxicity of 1-butanol itself. Additional optimization of the screening parameters must be carried out by altering the time between addition of 1-butanol and tetracycline to the culture medium as well as the concentration of 1-butanol and tetracycline in order to obtain a larger linear detection range of biosensors.

To demonstrate the possibility of utilizing this biosensor to screen for phenotypes with improved 1-butanol production, we tested the sensitivity of the 1-butanol biosensor under conditions of concomitant *in vivo* alcohol production and synthetic selection. Previously constructed plasmids containing the 1-butanol production pathway (pBHB8 and pBHB9) were transformed into the engineered strain with chromosomal 1-butanol biosensors to construct

strains BHB11 and BHB12, respectively. The *M. extorquens* AM1 biosensor strain containing an empty vector without the 1-butanol pathway was used as a control. All strains were cultivated in hypho ethylamine medium. After the addition of tetracycline at mid-exponential phase, cultures were incubated for another 36 h. The cell densities of the culture were monitored during the time course (Figure 5.2). In keeping with the results from the biosensor characterization assays, a slight fitness difference between production and non-production phenotypes was observed during growth in medium with 1 mg/L tetracycline. Although BHB12 was able to produce 50% more 1-butanol than BHB11 under this condition (Figure 5.3), the fitness difference between BHB11 and BHB12 was not obvious, suggesting the correlation between 1-butanol production and final cell culture density is out of the linear range of biosensor. Furthermore, the selective pressure must be adjusted to not exceed the available level of induced biosensor because both BHB11 and BHB12 could barely grow with the presence of 1 mg/L tetracycline, and 10 mg/L tetracycline resulted in no growth. To amplify the fitness difference between strains with different 1-butanol-producing capacity, the concentration of tetracycline was manipulated between 0 and 1 mg/L to explore appropriate selective pressure for strain screening. At lower tetracycline levels, the control culture was able to grow, presumably due to the leaky expression of the biosensor. However, the fitness difference maximized at 0.75 mg/L tetracycline, which can be used for strain screening in the future. These results indicate that BmoR-P_{BMO} can be used to construct a synthetic selection for a 1-butanol production phenotype; however, because fold-enrichment is intrinsically linked to the fitness differences between strains, further improvements of biosensor function are necessary in order to isolate strains with higher 1-butanol production.

Here we showed the potential feasibility of utilizing a biosensor-based selection method as an approach for *M. extorquens* AM1 strain improvement. The preliminary results suggest that

it is possible to isolate strains with higher 1-butanol production via biosensor selection, whose sensitivity relies on key parameters such as the level of selective pressure. Compared to the native 1-butanol producers clostridia or the engineered *E. coli* strains, significant future optimization is required to move this system from proof of principle to a viable industrial strain. However, previous studies of metabolic engineering have shown such magnitude of increases, providing optimism that such increases can be achieved.

In the future, the same types of approaches can be used to modify the metabolism in *M. extorquens* AM1 to produce other chemicals. Although clearly more work needs to be done to position this bacterium for commercial production of 1-butanol or other endproducts, the work presented in this thesis represents an important step forward in that direction.

5.3 Tables and Figures

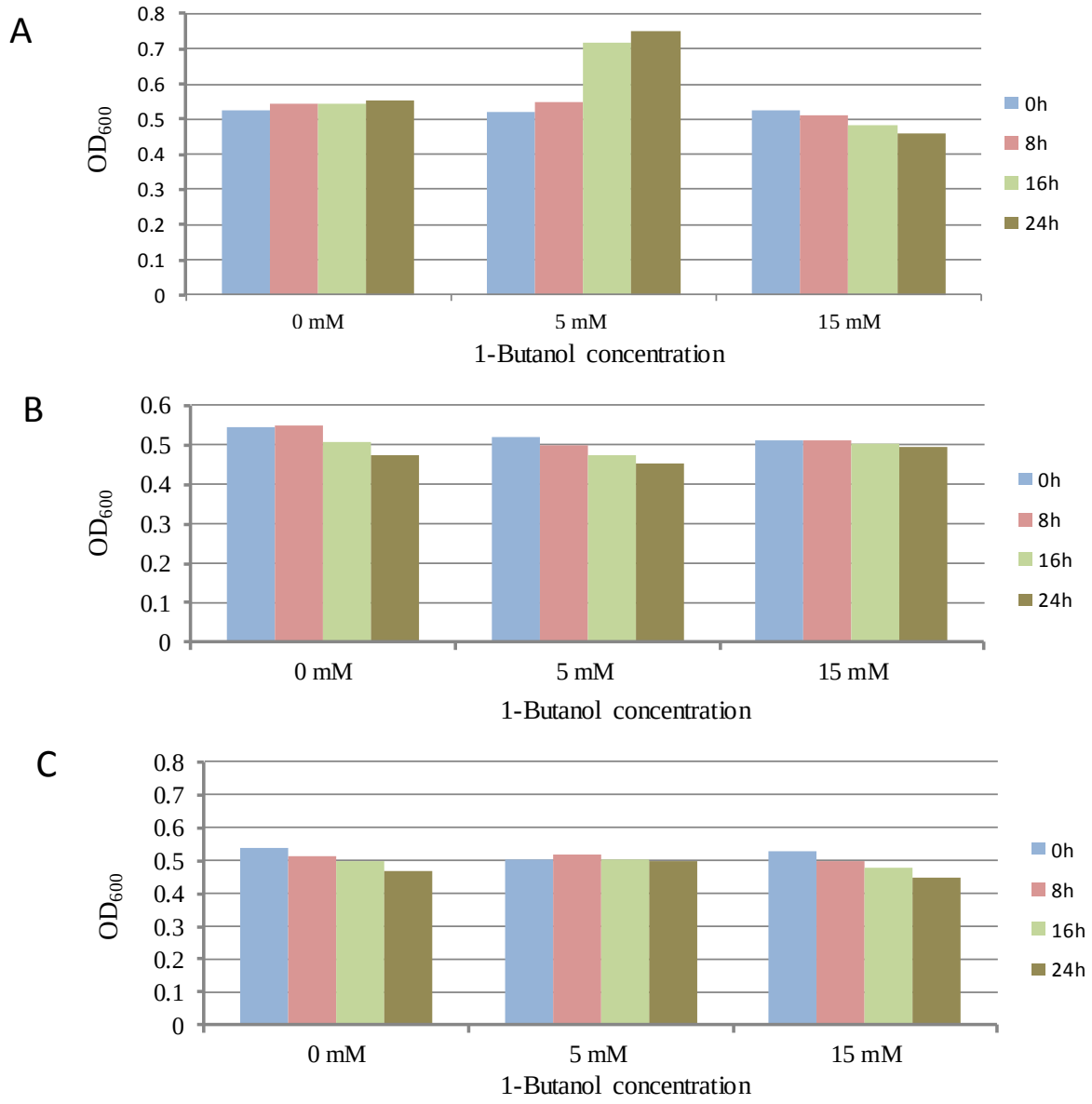

Figure 5.1: Tetracycline resistance of biosensor-containing *M. extorquens* AM1 induced by exogenous butanol. Cells were inoculated to mid-exponential phase and incubated with appropriate amounts of 1-butanol for 2h, then the cultures were supplied with different amounts of tetracycline: 1 mg/L (A), 5 mg/L (B), 10 mg/L (C). Each individual experiment was performed in duplicate.

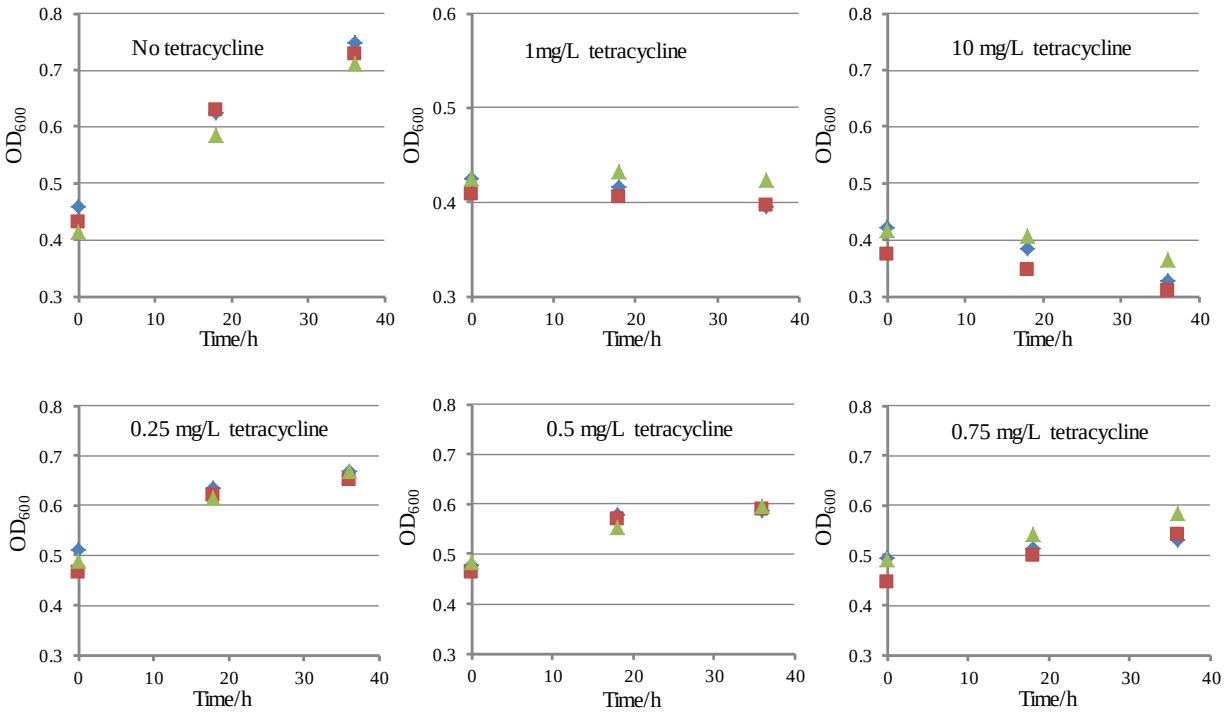

Figure 5.2: Tetracycline resistance of empty vector (diamond), BHB11 (square), BHB12 (triangles). Tetracycline was added at mid-exponential phase. Each individual experiment was performed in triplicate.

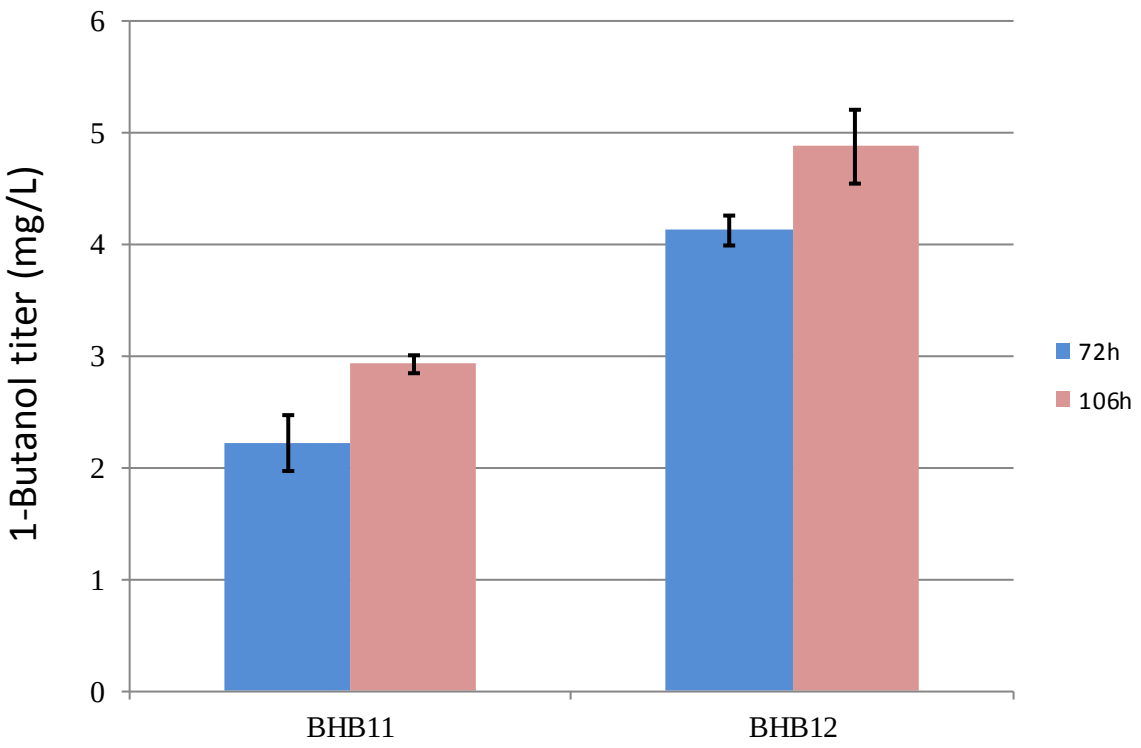

Figure 5.3: 1-Butanol titer of BHB11 (blue bar) and BHB12 (red bar) at 72h and 106h. Cells were grown with 1mg/L tetracycline.

References:

1. Anthony, C. The biochemistry of methylotrophs. *Comp. Biochem. Physiol. Part A Physiol.* **75,** 497 (1983).

2. Chistoserdova, L., Kalyuzhnaya, M. G. & Lidstrom, M. E. The expanding world of methylotrophic metabolism. *Annu. Rev. Microbiol.* **63,** 477–499 (2009).

3. Quayle, J. R. & Cell, C. Microbial Growth on C_1 Compounds. *Biochem. J.* 465–469 (1961).

4. Nemecek-marshall, M., Macdonald, R. C., Franzen, J. J., Wojciechowski, C. & Fall, R. Methanol Emission from Leaves. *plant phsiology* **108**: 1359-1368 (1995).

5. Schrader, J. *et al.* Methanol-based industrial biotechnology: current status and future perspectives of methylotrophic bacteria. *Trends Biotechnol.* **27,** 107–115 (2009).

6. Chistoserdova, L., Chen, S., Lapidus, A. & Lidstrom, M. E. MINIREVIEW Methylotrophy in *Methylobacterium extorquens* AM1 from a Genomic Point of View. **185,** 2980–2987 (2003).

7. Skovran, E., Crowther, G. J., Guo, X., Yang, S. & Lidstrom, M. E. A systems biology approach uncovers cellular strategies used by *Methylobacterium extorquens* AM1 during the switch from multi- to single-carbon growth. *PLoS One* **5,** e14091 (2010).

8. Anthony, C. & Williams, P. The structure and mechanism of methanol dehydrogenase. *Biochim. Biophys. Acta - Proteins Proteomics* **1647,** 18–23 (2003).

9. Keltjens, J. T., Pol, A., Reimann, J. & Op den Camp, H. J. M. PQQ-dependent methanol dehydrogenases: rare-earth elements make a difference. *Appl. Microbiol. Biotechnol.* **98**, 6163-6183 (2014).

10. Skovran, E., Palmer, A. D., Rountree, A. M., Good, N. M. & Lidstrom, M. E. XoxF is required for expression of methanol dehydrogenase in *Methylobacterium extorquens* AM1. *J. Bacteriol.* **193,** 6032–6038 (2011).

11. Nakagawa, T. *et al.* A catalytic role of XoxF1 as La^{3+}-dependent methanol dehydrogenase in *Methylobacterium extorquens* strain AM1. *PLoS One* **7,** e50480 (2012).

12. Chistoserdova, L. C_1 Transfer Enzymes and Coenzymes Linking Methylotrophic Bacteria and Methanogenic Archaea. *Science.* **281,** 99–102 (1998).

13. Crowther, G. J., Kosály, G. & Lidstrom, M. E. Formate as the main branch point for methylotrophic metabolism in *Methylobacterium extorquens* AM1. *J. Bacteriol.* **190,** 5057–5062 (2008).

14. Chistoserdova, L. *et al.* Identification of a fourth formate dehydrogenase in *Methylobacterium extorquens* AM1 and confirmation of the essential role of formate oxidation in methylotrophy. *J. Bacteriol.* **189,** 9076–9081 (2007).

15. Martinez-Gomez, N. C., Nguyen, S. & Lidstrom, M. E. Elucidation of the role of the methylene-tetrahydromethanopterin dehydrogenase MtdA in the tetrahydromethanopterin-dependent oxidation pathway in *Methylobacterium extorquens* AM1. *J. Bacteriol.* **195,** 2359–2367 (2013).

16. Peyraud, R. *et al.* Genome-scale reconstruction and system level investigation of the metabolic network of *Methylobacterium extorquens* AM1. *BMC Syst. Biol.* **5,** 189 (2011).

17. Peyraud, R. *et al.* Demonstration of the ethylmalonyl-CoA pathway by using ^{13}C metabolomics. *Proc. Natl. Acad. Sci. U. S. A.* **106,** 4846–4851 (2009).

18. Van Dien, S. J. Reconstruction of C_3 and C_4 metabolism in *Methylobacterium extorquens* AM1 using transposon mutagenesis. *Microbiology* **149,** 601–609 (2003).

19. Schneider, K. *et al.* The ethylmalonyl-CoA pathway is used in place of the glyoxylate cycle by *Methylobacterium extorquens* AM1 during growth on acetate. *J. Biol. Chem.* **287,** 757–766 (2012).

20. Okubo, Y., Yang, S., Chistoserdova, L. & Lidstrom, M. E. Alternative route for glyoxylate consumption during growth on two-carbon compounds by *Methylobacterium extorquens* AM1. *J. Bacteriol.* **192,** 1813–1823 (2010).

21. Korotkova, N., Chistoserdova, L., Kuksa, V. & Lidstrom, M. E. Glyoxylate Regeneration Pathway in the Methylotroph *Methylobacterium extorquens* AM1 †. **184,** 1750–1758 (2002).

22. Guo, X. & Lidstrom, M. E. Physiological analysis of *Methylobacterium extorquens* AM1 grown in continuous and batch cultures. *Arch. Microbiol.* **186,** 139–149 (2006).

23. Smejkalová, H., Erb, T. J. & Fuchs, G. Methanol assimilation in *Methylobacterium extorquens* AM1: demonstration of all enzymes and their regulation. *PLoS One* **5,** e13001 (2010).

24. Schneider, K. *et al.* The Ethylmalonyl-CoA pathway is used in place of the glyoxylate cycle by *Methylobacterium extorquens* AM1 during growth on acetate *J. Biol Chem.* **287,** 757–766 (2012).

25. Alber, B. E. Biotechnological potential of the ethylmalonyl-CoA pathway. *Appl. Microbiol. Biotechnol.* **89,** 17–25 (2011).

26. Sonntag, F., Buchhaupt, M. & Schrader, J. Thioesterases for ethylmalonyl-CoA pathway derived dicarboxylic acid production in *Methylobacterium extorquens* AM1. *Appl. Microbiol. Biotechnol.* **1,** (2014).

27. Yolande A. Chana, Angela M. Podevelsa, Brian M. Kevanya, and M. G. T. Biosynthesis of polyketide synthase extender units. *Nat Prod Rep* **26,** 90–114 (2009).

28. Dürre, P. Biobutanol: an attractive biofuel. *Biotechnol. J.* **2,** 1525–1534 (2007).

29. Saavalainen, P. & Keiski, R. L. Biobutanol as a Potential Sustainable Biofuel - Assessment of Lignocellulosic and Waste-based Feedstocks. *JSDEWES* **1,** 58–77 (2013).

30. Dürre, P. Fermentative butanol production: bulk chemical and biofuel. *Ann. N. Y. Acad. Sci.* **1125,** 353–362 (2008).

31. Lee, S. Y. *et al.* Fermentative butanol production by Clostridia. *Biotechnol. Bioeng.* **101,** 209–228 (2008).

32. Andersch, W., Bahl, H. & Gottschalk, G. Microbiology and biotechnology level of enzymes involved in acetate , butyrate , acetone and butanol formation by *Clostridium acetobutylicum*. **3,** 327–332 (1983).

33. Tomas, C. A. *et al.* DNA array-based transcriptional analysis of asporogenous , Nonsolventogenic *Clostridium acetobutylicum* strains SKO1 and M5. **185,** 4539–4547 (2003).

34. Paredes, C. J. *et al.* A general framework for designing and validating oligomer-based DNA microarrays and its application to *Clostridium acetobutylicum*. *Appl. Environ. Microbiol.* **73,** 4631–4638 (2007).

35. Sullivan, L. & Bennett, G. N. Proteome analysis and comparison of *Clostridium acetobutylicum* ATCC 824 and Spo0A strain variants. *J. Ind. Microbiol. Biotechnol.* **33,** 298–308 (2006).

36. Heap, J. T., Pennington, O. J., Cartman, S. T., Carter, G. P. & Minton, N. P. The ClosTron: a universal gene knock-out system for the genus Clostridium. *J. Microbiol. Methods* **70,** 452–464 (2007).

37. Al-Hinai, M. a, Fast, A. G. & Papoutsakis, E. T. Novel system for efficient isolation of Clostridium double-crossover allelic exchange mutants enabling markerless chromosomal gene deletions and DNA integration. *Appl. Environ. Microbiol.* **78,** 8112–8121 (2012).

38. Atsumi, S. *et al.* Metabolic engineering of *Escherichia coli* for 1-butanol production. *Metab. Eng.* **10,** 305–311 (2008).

39. Steen, E. J. *et al.* Metabolic engineering of *Saccharomyces cerevisiae* for the production of n-butanol. *Microb. Cell Fact.* **7,** 36 (2008).

40. Lan, E. I. & Liao, J. C. Metabolic engineering of cyanobacteria for 1-butanol production from carbon dioxide. *Metab. Eng.* **13,** 353–363 (2011).

41. Nielsen, D. R. *et al.* Engineering alternative butanol production platforms in heterologous bacteria. *Metab. Eng.* **11,** 262–273 (2009).

42. Shen, C. R. *et al.* Driving forces enable high-titer anaerobic 1-butanol synthesis in *Escherichia coli*. *Appl. Environ. Microbiol.* **77,** 2905–2915 (2011).

43. Atsumi, S., Hanai, T. & Liao, J. C. Non-fermentative pathways for synthesis of branched-chain higher alcohols as biofuels. *Nature* **451,** 86–89 (2008).

44. Clomburg, J. M., Vick, J. E., Blankschien, M. D., Rodríguez-Moyá, M. & Gonzalez, R. A synthetic biology approach to engineer a functional reversal of the β-oxidation cycle. *ACS Synth. Biol.* **1,** 541–554 (2012).

45. Dellomonaco, C., Clomburg, J. M., Miller, E. N. & Gonzalez, R. Engineered reversal of the β-oxidation cycle for the synthesis of fuels and chemicals. *Nature* **476,** 355–359 (2011).

46. Peyraud, R. *et al.* Demonstration of the ethylmalonyl-CoA pathway by using ^{13}C metabolomics. *Proc. Natl. Acad. Sci. U. S. A.* **106,** 4846–4851 (2009).

47. Vuilleumier, S. *et al.* Methylobacterium genome sequences: a reference blueprint to investigate microbial metabolism of C_1 compounds from natural and industrial sources. *PLoS One* **4,** e5584 (2009).

48. Korotkova, N., Chistoserdova, L., Kuksa, V. & Lidstrom, M. E. Glyoxylate regeneration pathway in the methylotroph *Methylobacterium extorquens* AM1 †. *J. Bacteriol.* **184,** 1750–1758 (2002).

49. Okubo, Y., Skovran, E., Guo, X., Sivam, D. & Lidstrom, M. E. Implementation of microarrays for *Methylobacterium extorquens* AM1. *OMICS* **11,** 325–340 (2007).

50. Marx, C. J. & Lidstrom, M. E. Development of improved versatile broad-host-range vectors for use in methylotrophs and other Gram-negative bacteria. *Microbiology* **147,** 2065–2075 (2001).

51. Marx, C. J. & Lidstrom, M. E. Broad-host-range cre-lox system for antibiotic marker recycling in gram-negative bacteria. *Biotechniques* **33,** 1062–1067 (2002).

52. Helinski, D. R. Replication of an origin-containing derivative of plasmid RK2 dependent. **76,** 1648–1652 (1979).

53. Erb, T. J. *et al.* Synthesis of C5-dicarboxylic acids from C_2-units involving crotonyl-CoA carboxylase/reductase: the ethylmalonyl-CoA pathway. *Proc. Natl. Acad. Sci. U. S. A.* **104,** 10631–10636 (2007).

54. Ali, H. & Murrell, J. C. Development and validation of promoter-probe vectors for the study of methane monooxygenase gene expression in *Methylococcus capsulatus* Bath. *Microbiology* **155,** 761–771 (2009).

55. Chistoserdova, L. V & Lidstrom, M. E. Molecular characterization of a chromosomal region involved in the oxidation of acetyl-CoA to glyoxylate in the isocitrate-lyase-negative methylotroph *Methylobacterium extorquens* AM1. *Microbiology* **142,** 1459–68 (1996).

56. Ramos, J. L. *et al.* The TetR Family of Transcriptional Repressors. **69,** 326–356 (2005).

57. Chatterjee, A., Cui, Y., Hasegawa, H. & Chatterjee, A. K. PsrA, the Pseudomonas sigma regulator, controls regulators of epiphytic fitness, quorum-sensing signals, and plant interactions in *Pseudomonas syringae pv.* tomato strain DC3000. *Appl. Environ. Microbiol.* **73,** 3684–3694 (2007).

58. Pompeani, A. J. *et al.* The Vibrio harveyi master quorum-sensing regulator, LuxR, a TetR-type protein is both an activator and a repressor: DNA recognition and binding specificity at target promoters. *Mol. Microbiol.* **70,** 76–88 (2008).

59. Alatoom, A. A., Aburto, R., Hamood, A. N. & Colmer-Hamood, J. A. VceR negatively regulates the *vceCAB* MDR efflux operon and positively regulates its own synthesis in *Vibrio cholerae* 569B. *Can. J. Microbiol.* **53,** 888–900 (2007).

60. Hirano, S., Tanaka, K., Ohnishi, Y. & Horinouchi, S. Conditionally positive effect of the TetR-family transcriptional regulator AtrA on streptomycin production by *Streptomyces griseus*. *Microbiology* **154,** 905–914 (2008).

61. Horinouchi, S. & Beppu, T. Autoregulatory factors of secondary metabolism and morphogenesis in actinomycetes. *Crit. Rev. Biotechnol.* **10,** 191–204 (1990).

62. Delany, I., Ieva, R., Alaimo, C., Rappuoli, R. & Scarlato, V. The iron-responsive regulator fur is transcriptionally autoregulated and not essential in *Neisseria meningitidis*. *J. Bacteriol.* **185,** 6032–6041 (2003).

63. Aramaki, H., Sagara, Y., Hosoi, M. & Horiuchi, T. Evidence for autoregulation of camR, which encodes a repressor for the cytochrome P-450cam hydroxylase operon on the *Pseudomonas putida* CAM plasmid. *J. Bacteriol.* **175,** 7828–7833 (1993).

64. Lütke-Eversloh, T. Application of new metabolic engineering tools for *Clostridium acetobutylicum*. *Appl. Microbiol. Biotechnol.* **98,** 5823–5837 (2014).

65. Kuehne, S. a & Minton, N. P. ClosTron-mediated engineering of Clostridium. *Bioengineered* **3,** 247–254 (2012).

66. Branduardi, P., de Ferra, F., Longo, V. & Porro, D. Microbial n -butanol production from Clostridia to non-Clostridial hosts. *Eng. Life Sci.* **14,** 16–26 (2014).

67. Berezina, O. V *et al.* Reconstructing the clostridial n-butanol metabolic pathway in *Lactobacillus brevis*. *Appl. Microbiol. Biotechnol.* **87,** 635–646 (2010).

68. Conrado, R. J. & Gonzalez, R. Envisioning the Bioconversion of Methane to Liquid Fuels. *Science.* **343,** 621–623 (2014).

69. Peyraud, R., Kiefer, P., Christen, P., Portais, J.C. & Vorholt, J.A. Co-consumption of methanol and succinate by *Methylobacterium extorquens* AM1. *PLoS One* **7,** e48271 (2012).

70. Delaney, N. F. *et al.* Development of an optimized medium, strain and high-throughput culturing methods for *Methylobacterium extorquens*. *PLoS One* **8,** e62957 (2013).

71. Zhang, M., FitzGerald, K. a & Lidstrom, M. E. Identification of an upstream regulatory sequence that mediates the transcription of *mox* genes in *Methylobacterium extorquens* AM1. *Microbiology* **151,** 3723–3728 (2005).

72. Lee, M.-C., Chou, H.-H. & Marx, C. J. Asymmetric, bimodal trade-offs during adaptation of Methylobacterium to distinct growth substrates. *Evolution* **63,** 2816–2830 (2009).

73. Bond-watts, B. B., Bellerose, R. J. & Chang, M. C. Y. Enzyme mechanism as a kinetic control element for designing synthetic biofuel pathways. *Nat. Chem. Biol.* **537,** 3–8 (2011).

74. Hartmanis, M. G. & Gatenbeck, S. Intermediary metabolism in *Clostridium acetobutylicum*: Levels of enzymes involved in the formation of acetate and butyrate. *Appl. Environ. Microbiol.* **47,** 1277–1283 (1984).

75. Yang, S., Sadilek, M., Synovec, R. E. & Lidstrom, M. E. Liquid chromatography-tandem quadrupole mass spectrometry and comprehensive two-dimensional gas chromatography-time-of-flight mass spectrometry measurement of targeted metabolites of *Methylobacterium extorquens* AM1 grown on two different carbon sources. *J. Chromatogr. A* **1216,** 3280–9 (2009).

76. Boynton, Z. L., Bennett, G. N. & Rudolph, F. B. Cloning , sequencing , and expression of clustered genes encoding beta-hydroxybutyryl-coenzyme A (CoA) dehydrogenase , crotonase , and butyryl-CoA dehydrogenase from *Clostridium acetobutylicum* ATCC 824. *J. Bacteriol.* **178,** 3015–3024 (1996).

77. Tucci, S. & Martin, W. A novel prokaryotic trans-2-enoyl-CoA reductase from the spirochete *Treponema denticola*. *FEBS Lett.* **581,** 1561–1566 (2007).

78. Papoutsakis, E. T. Engineering solventogenic clostridia. *Curr. Opin. Biotechnol.* **19,** 420–429 (2008).

79. Fontaine, L. *et al.* Molecular characterization and transcriptional analysis of *adhE2* , the gene encoding the NADH-dependent aldehyde / alcohol dehydrogenase responsible for butanol production in alcohologenic cultures of *Clostridium acetobutylicum* ATCC 824. *J. Bacteriol.* **184,** 821–830 (2002).

80. Page, M. D. & Anthony, C. Regulation of formaldehyde oxidation by the methanol dehydrogenase modifier proteins of methylophilus *methylotrophus* and *Pseudomonas* AM1. *Microbiology* **132,** 1553–1563 (1986).

81. Morris, C. J. & Lidstrom, M. E. Cloning of a methanol-inducible *moxF* promoter and its analysis in *moxB* mutants of *Methylobacterium extorquens* AM1^{rif}. *J. Bacteriol.* **174,** 4444–4449 (1992).

82. Erb, T. J., Brecht, V., Fuchs, G., Müller, M. & Alber, B. E. Carboxylation mechanism and stereochemistry of crotonyl-CoA carboxylase/reductase, a carboxylating enoyl-thioester reductase. *Proc. Natl. Acad. Sci. U. S. A.* **106,** 8871–8876 (2009).

83. Zhang, K., Sawaya, M. R., Eisenberg, D. S. & Liao, J. C. Expanding metabolism for biosynthesis of nonnatural alcohols. *Proc. Natl. Acad. Sci. U. S. A.* **105,** 20653–20658 (2008).

84. Hu, B. & Lidstrom, M. CcrR, a TetR family transcriptional regulator, activates the transcription of a gene of the Ethylmalonyl coenzyme A pathway in *Methylobacterium extorquens* AM1. *J. Bacteriol.* **194,** 2802–2808 (2012).

85. Bond-Watts, B. B., Bellerose, R. J. & Chang, M. C. Y. Enzyme mechanism as a kinetic control element for designing synthetic biofuel pathways. *Nat. Chem. Biol.* **7,** 222–227 (2011).

86. Tucci, S. & Martin, W. A novel prokaryotic trans-2-enoyl-CoA reductase from the spirochete *Treponema denticola*. *FEBS Lett.* **581,** 1561–1566 (2007).

87. Dien, S. J. Van & Lidstrom, M. E. Stoichiometric model for evaluating the metabolic capabilities of the facultative methylotroph *Methylobacterium extorquens* AM1 , with application to reconstruction of C_3 and C_4 metabolism. *Biotechnol. Bioeng.* **78,** 296–312 (2002).

88. Lan, E. I., Ro, S. Y. & Liao, J. C. Oxygen-tolerant coenzyme A-acylating aldehyde dehydrogenase facilitates efficient photosynthetic n-butanol biosynthesis in cyanobacteria. *Energy Environ. Sci.* **6,** 2672–2681 (2013).

89. Marx, C. J. Recovering from a bad start: rapid adaptation and tradeoffs to growth below a threshold density. *BMC Evol. Biol.* **12,** 109 (2012).

90. Kung, Y., Runguphan, W. & Keasling, J. D. From fields to fuels: Recent advances in the microbial production of biofuels. *ACS Synth. Biol.* **1,** 498–513 (2012).

91. Bowles, L. K. & Ellefson, W. L. Effects of butanol on *Clostridium acetobutylicum*. *Appl. Environ. Microbiol.* **50,** 1165–1170 (1985).

92. Ramos, J. L. *et al.* Mechanisms of solvent tolerance in gram-negative bacteria. *Annu. Rev. Microbiol.* **56,** 743–768 (2002).

93. Nicolaou, S. a, Gaida, S. M. & Papoutsakis, E. T. A comparative view of metabolite and substrate stress and tolerance in microbial bioprocessing: From biofuels and chemicals, to biocatalysis and bioremediation. *Metab. Eng.* **12,** 307–331 (2010).

94. Brynildsen, M. P. & Liao, J. C. An integrated network approach identifies the isobutanol response network of *Escherichia coli*. *Mol. Syst. Biol.* **5,** 277 (2009).

95. Rutherford, B. J. *et al.* Functional genomic study of exogenous n-butanol stress in *Escherichia coli*. *Appl. Environ. Microbiol.* **76,** 1935–1945 (2010).

96. Liu, S. & Qureshi, N. How microbes tolerate ethanol and butanol. *N. Biotechnol.* **26,** 117–121 (2009).

97. Reyes, L. H., Almario, M. P. & Kao, K. C. Genomic library screens for genes involved in n-butanol tolerance in *Escherichia coli*. *PLoS One* **6,** e17678 (2011).

98. Reyes, L. H., Almario, M. P., Winkler, J., Orozco, M. M. & Kao, K. C. Visualizing evolution in real time to determine the molecular mechanisms of n-butanol tolerance in *Escherichia coli*. *Metab. Eng.* **14,** 579–590 (2012).

99. Portnoy, V. a, Bezdan, D. & Zengler, K. Adaptive laboratory evolution--harnessing the power of biology for metabolic engineering. *Curr. Opin. Biotechnol.* **22,** 590–594 (2011).

100. Barrick, J. E. *et al.* Genome evolution and adaptation in a long-term experiment with *Escherichia coli*. *Nature* **461,** 1243–1247 (2009).

101. Dettman, J. R. *et al.* Evolutionary insight from whole-genome sequencing of experimentally evolved microbes. *Mol. Ecol.* **21,** 2058–2077 (2012).

102. Conrad, T. M., Lewis, N. E. & Palsson, B. Ø. Microbial laboratory evolution in the era of genome-scale science. *Mol. Syst. Biol.* **7,** 509 (2011).

103. Mozhayskiy, V. & Tagkopoulos, I. Microbial evolution in vivo and in silico: methods and applications. *Integr. Biol. (Camb).* **5,** 262–277 (2013).

104. Dragosits, M. & Mattanovich, D. Adaptive laboratory evolution -- principles and applications for biotechnology. *Microb. Cell Fact.* **12,** 64 (2013).

105. Reyes, L. H., Almario, M. P., Winkler, J., Orozco, M. M. & Kao, K. C. Visualizing evolution in real time to determine the molecular mechanisms of n-butanol tolerance in *Escherichia coli*. *Metab. Eng.* **14,** 579–590 (2012).

106. Atsumi, S. *et al.* Evolution, genomic analysis, and reconstruction of isobutanol tolerance in *Escherichia coli*. *Mol. Syst. Biol.* **6,** 449 (2010).

107. Gourion, B., Francez-Charlot, A. & Vorholt, J.A. PhyR is involved in the general stress response of *Methylobacterium extorquens* AM1. *J. Bacteriol.* **190,** 1027–1035 (2008).

108. Yomano, L. P., York, S. W. & Ingram, L. O. Isolation and characterization of ethanol-tolerant mutants of *Escherichia coli* KO11 for fuel ethanol production. *J. Ind. Microbiol. Biotechnol.* **20,** 132–138 (1998).

109. Moore, E., Arnscheidt, A. & Mau, M. Simplified protocols for the preparation of genomic DNA from bacterial cultures. 3–18 (2004).

110. Deatherage, S.E., Barrick, J. E. Identification of mutations in laboratory-evolved microbes from next-generation sequencing data using breseq. *Methods Mol. Biol.* **1151,** 165–188 (2014).

111. Nurk, S. & Bankevich, A. Assembling single-cell genomes and mini-metagenomes from chimeric MDA products. *J. Mol. Biol.* **20,** 714–737 (2013).

112. Altschul, S. F., Gish, W., Miller, W., Myers, E. W. & Lipman, D. J. Basic local alignment search tool. *J. Mol. Biol.* **215,** 403–410 (1990).

113. Li, H. & Durbin, R. Fast and accurate long-read alignment with Burrows-Wheeler transform. *Bioinformatics* **26,** 589–595 (2010).

114. Li, H. *et al.* The Sequence Alignment/Map format and SAMtools. *Bioinformatics* **25,** 2078–2079 (2009).

115. Carroll, S. M., Xue, K. S. & Marx, C. J. Laboratory divergence of *Methylobacterium extorquens* AM1 through unintended domestication and past selection for antibiotic resistance. *BMC Microbiol.* **14,** 2 (2014).

116. Dunlop, M. J. Engineering microbes for tolerance to next-generation biofuels. *Biotechnol. Biofuels* **4,** 32 (2011).

117. Minty, J. J. *et al.* Evolution combined with genomic study elucidates genetic bases of isobutanol tolerance in *Escherichia coli*. *Microb. Cell Fact.* **10,** 18 (2011).

118. Healy, J. *et al.* Understanding the structural requirements for activators of the Kef bacterial potassium efflux system. *Biochemistry* **53,** 1982–1992 (2014).

119. Wang, F., Kashket, S. & Kashket, E. R. Maintenance of DeltapH by a butanol-tolerant mutant of *Clostridium beijerinckii*. *Microbiology* **151,** 607–613 (2005).

120. Prather, K. L. J. & Martin, C. H. De novo biosynthetic pathways: rational design of microbial chemical factories. *Curr. Opin. Biotechnol.* **19,** 468–474 (2008).

121. Finehout, E. J. & Lee, K. H. An introduction to mass spectrometry applications in biological research. *Biochem. Mol. Biol. Educ.* **32,** 93–100 (2004).

122. Dietrich, J. A, McKee, A. E. & Keasling, J. D. High-throughput metabolic engineering: advances in small-molecule screening and selection. *Annu. Rev. Biochem.* **79,** 563–590 (2010).

123. Santos, C. N. S. & Stephanopoulos, G. Melanin-based high-throughput screen for L-tyrosine production in *Escherichia coli*. *Appl. Environ. Microbiol.* **74,** 1190–1197 (2008).

124. Bernhardt, P., McCoy, E. & O'Connor, S. E. Rapid identification of enzyme variants for reengineered alkaloid biosynthesis in periwinkle. *Chem. Biol.* **14,** 888–897 (2007).

125. Dietrich, J. A, Shis, D. L., Alikhani, A. & Keasling, J. D. Transcription factor-based screens and synthetic selections for microbial small-molecule biosynthesis. *ACS Synth. Biol.* **2,** 47–58 (2013).

126. Kurth, E. G., Doughty, D. M., Bottomley, P. J., Arp, D. J. & Sayavedra-Soto, L. A. Involvement of BmoR and BmoG in n-alkane metabolism in "*Pseudomonas butanovora*". *Microbiology* **154,** 139–147 (2008).